Integrated Masters in Bioengineering

Detection of synthetic musk fragrances in aqueous matrices by ultrasound-assisted dispersive liquid-liquid microextraction followed by GC-MS

Master's Thesis

of

Alice Maria de Araújo Alves

Developed within the discipline of Dissertation

conducted at

Laboratory for Process Engineering, Environment, Biotechnology and Energy

Faculty of Engineering, University of Porto

FEUP Advisor: **Dr. Lúcia Santos**

FEUP Co-Advisor: **Dr. Vera Homem**

Department of Chemical Engineering

July 2014

Acknowledgments

Firstly, I wish to thank LEPABE (Laboratory for Process Engineering, Environment, Biotechnology and Energy) and the Department of Chemical Engineering for providing the materials, equipment and facilities.

This work was funded by FEDER funds through the Operational Programme for Competitiveness Factors – COMPETE, ON.2 - O Novo Norte - North Portugal Regional Operational Programme and National Funds through FCT - Foundation for Science and Technology under the projects: PEst-C/EQB/UI0511, NORTE-07-0124-FEDER-000025 - RL2_ Environment&Health.

I would like to express my gratitude to my advisor, Dr. Lúcia Santos, for the encouragement, support and trust that were given to me since the beginning of the project.

My sincere thanks also goes to my co-advisor, Dr. Vera Homem, for always being patient, understanding and always being there for any and all doubts I ever had during this thesis and for all the hard work and time invested in order to help me.

I would also like to thank the group from the laboratory MIA 201 for the animation and enthusiasm, allowing for a relaxed and excellent environment to work with.

To my friends from Biological Engineering, I offer my thanks for the companionship, making every work day a little brighter, with special mention of Rita Silva, Mafalda Andrade, Maria Fachada and Lígia Rocha.

Lastly, for the support and because well spent leisure time is essential to go through this stage of the academic life in good spirits, I thank my parents, Manuela Araújo and Rui Alves, my sister and brother, Sofia Alves and Carlos Alves, and my friends Catarina Oliveira and Inês Carvalho.

Abstract

Synthetic musks are organic compounds used in a wide variety of personal care products as a fragrance and as a fixative. They have a pleasant odour and can be divided in four different musk classes: nitro, polycyclic, macrocyclic and alicyclic musks. Due to their widespread use, these synthetic compounds have been found in environmental matrices, such as water, sediments, biota and air. For this reason, these compounds are interesting targets for future research, for the study of their occurrence in the environment and their toxicity.

In this study, an ultrasound-assisted dispersive liquid-liquid microextraction method coupled to gas chromatography-mass spectrometry to detected and quantify synthetic musks was successfully developed. Twelve synthetic musks, including three classes of synthetic musks (five nitro, five polycyclic and two macrocyclic musks) were studied. Design of experiments was used for the optimization of this methodology. The influence of seven factors (volume of the extraction solvent, volume of the disperser solvent, sample volume, extraction time, ionic strength, extraction solvent and disperser solvent) was investigated. The optimal conditions achieved were 80 μL of chloroform (as extraction solvent), 880 μL of acetonitrile (as disperser solvent), 6 mL of sample volume, 3.5% (m/m) of NaCl and 2 minutes of extraction time (defined as the time the sample underwent ultrasonic treatment).

The limits of detection and quantification obtained for galaxolide were 0.004 $ng \cdot L^{-1}$ and 0.01 $ng \cdot L^{-1}$, respectively, being much lower than any values reported in the literature for the detection of synthetic musks in water samples. The rest of the compounds presented limits of detection ranging from 2 to 83 $ng \cdot L^{-1}$.

Five types of water samples (tap, sea, river water, effluent and influent wastewater) were analysed. In general, satisfactory precision and accuracy values were obtained. Wastewaters exhibited the highest concentrations of synthetic musks (5735 and 14369 $ng \cdot L^{-1}$ of total musks concentration for effluent and influent, respectively). Tap water had the least amount of synthetic musks (228 $ng \cdot L^{-1}$ of ethylene brassylate). Sea and river water presented 643 $ng \cdot L^{-1}$ and 1401 $ng \cdot L^{-1}$ of total synthetic musks, respectively. The most detected musk was galaxolide, followed by tonalide, exaltolide, cashmeran and ethylene brassylate. Besides the detection musk ketone in effluent water, no other nitro musks were found in any water matrix.

Keywords: synthetic musks; ultrasound-assisted dispersive liquid–liquid microextraction; gas chromatography–mass spectrometry; aqueous matrices; design of experiments

Resumo

Os musks sintéticos são compostos orgânicos usados numa grande variedade de produtos de higiene e cuidado pessoais como fragrâncias e fixativos. Têm um odor agradável e podem ser divididos em quatro classes: nitro musks, musks policíclicos, macrocíclicos e alicíclicos. Devido à sua ampla utilização, estes compostos sintéticos têm vindo a ser encontrados em matrizes ambientais, como água, sedimentos, biota e ar. Por esta razão, estes compostos são alvos interessantes para a investigação futura, para o estudo da sua ocorrência no meio ambiente e a sua toxicidade.

Neste estudo, um método de microextração líquido-líquido dispersiva assistida por ultrassons, acoplada a cromatografia gasosa-espectrometria de massa para detetar e quantificar musks sintéticos foi desenvolvido com sucesso. Doze musks sintéticos, incluindo três classes de musks sintéticos (cinco nitro musks, cinco musks policíclicos e dois macrocíclicos) foram estudados. Foi utilizado o desenho experimental para a otimização desta metodologia. A influência de sete fatores (volume de solvente de extração, volume de solvente de dispersão, volume de amostra, força iónica, solvente de extração e solvente de dispersão) foi investigada. As condições ótimas obtidas foram 80 µL de clorofórmio, 880 µL de acetonitrilo, 6 mL de volume de amostra, 3,5% (m/m) de NaCl e 2 minutos de tempo de extração (definido como o tempo que a amostra foi submetida a ultrassons).

Os limites de deteção e quantificação obtidos para o galaxolide foram de 0,004 $ng \cdot L^{-1}$ e 0,01 $ng \cdot L^{-1}$, respetivamente, sendo muito menores que quaisquer valores obtidos na literatura para a deteção de musks sintéticos em amostras aquosas. Os restantes compostos apresentaram limites de deteção entre 2 e 83 $ng \cdot L^{-1}$.

Cinco tipos de amostras aquosas reais (água de torneira, mar, rio, efluente e influente) foram analisados. Em geral, foram obtidos valores satisfatórios de precisão e exatidão. As águas residuais apresentaram as concentrações mais elevadas de musks sintéticos (5735 e 14369 $ng \cdot L^{-1}$ de concentração total de musks para efluente e afluente, respetivamente). A água de torneira exibiu a menor quantidade de musks sintéticos (228 $ng \cdot L^{-1}$ de *ethylene brassylate*). As águas de mar e de rio apresentaram concentrações totais de musks de 643 $ng \cdot L^{-1}$ e 1401 $ng \cdot L^{-1}$, respetivamente. O musk mais detetado foi o *galaxolide*, seguido do *tonalide, exaltolide, cashmeran* e *ethylene brassylate*. Para além da deteção de *musk ketone* em águas de efluente, nenhum outro nitro musk foi encontrado em qualquer uma das matrizes.

Palavras-chave: musks sintéticos; microextração líquido-líquido dispersiva assistida por ultrassons; cromatografia gasosa-espectrometria de massa; matrizes aquosas; desenho experimental

Contents

List of Figures

List of Tables

Notation and Glossary

R	Correlation coefficient
R^2	Coefficient of determination
S_D	Disperser solvent
S_E	Extraction solvent
t_E; X_3	Extraction time
V_D; X_2	Volume of disperser solvent
V_E	Volume of extraction solvent
V_S; X_1	Sample volume
X_4	Percentage of sodium chloride

List of Acronyms

Acet	Acetone
ACN	Acetonitrile
ADBI	Celestolide
AHMI	Phantolide
AHTN	Tonalide
ATD	Automated thermal desorption
ATII	Traseolide
C	Concentration
CB	Chlorobenzene
CCD	Central composite design
CF	Chloroform
CI	Chemical ionization
DCM	Dichloromethane
DI	Direct immersion
DLLME	Dispersive liquid-liquid microextraction
DOE	Design of experiments
DPMI	Cashmeran
DVB	Divinylbenzene
D-μ-SPE	Dispersive micro-solid phase extraction
EB	Ethylene brassylate
EI	Electron ionization
EtAc	Ethyl acetate
EtOH	Ethanol
EXA	Exaltolide
GC	Gas chromatography
GLC	Gas-liquid chromatography
GSC	Gas-solid chromatography
Hex	Hexane
HHCB	Galaxolide
HHCB-lactone	Galaxolidone
HLB	Hydrophilic-lipophilic balance copolymer
HS	Headspace
IPA	Isopropyl alcohol
LD	Liquid desorption
LDPE	Low-density polyethylene
LLE	Liquid-liquid extraction
LOD	Limit of detection
LOF	Lack of fit
LOQ	Limit of quantification
LVI	Large volume injection
MA	Musk ambrette

MALLE	Membrane assisted liquid-liquid extraction
MASE	Membrane assisted solvent extraction
MDL	Method detection limit
MeOH	Methanol
MEPS	Microextraction by packed sorbent
MK	Musk ketone
MM	Musk moskene
MQL	Method quantification limit
MS	Mass spectrometry
MT	Musk tibetene
MWA	Microwave-assisted
MX	Musk xylene
PCP	Personal care product
PDMS	Polydimethylsiloxane
PPCP	Pharmaceutical and personal care product
PPL	A modified styrene-divinylbenzene polymer
PTV	Programmed temperature vaporiser
Rec	Recovery
RSD	Relative standard deviation
RTL	Retention time locking
SBSE	Stir-bar sorptive extraction
SCOT	Support-coated open tubular
SIC	Single ion chromatogram
SIS	Selected ion storage
SPE	Solid-phase extraction
SPME	Solid-phase microextraction
TD	Thermal desorption
TCC	Carbon tetrachloride
TCE	Tetrachloroethylene
TIC	Total ion chromatogram
UA	Ultrasound-assisted
USAEME	Ultrasound-assisted emulsification-microextraction
WCOT	Wall-coated open tubular
WWTP	Wastewater treatment plant

1 Introduction

1.1 Background and Presentation of the Project

By the end of the last century, the focus of chemical pollution was mostly directed to the conventional "priority pollutants", those compounds that display persistence in the environment, especially acutely toxic/carcinogenic pesticides and industrial intermediates. However, these compounds represent only a part in the entire picture of risk assessment. As the risk associated with previously unknown, unrecognized, or unsuspected chemical pollutants in the environment became a growing concern, research has nowadays been extended to substances referred to as "emerging contaminants". Even though emerging contaminants have long been present in the environment, it was only recently that they have aroused attention and, therefore, they are generally not included in the environmental legislation. This recent attention happened due to the introduction of new and more sensitive analytical equipment, which enable the detection of these emerging contaminants (Wille et al., 2012; Arbulu et al., 2011; Daughton and Ternes, 1999). Due to their recent discovery as potential pollutants, their environmental and human health impact is still unknown. Emerging contaminants are, therefore, new substances, or substances newly discovered in the environment or only recently categorized as contaminants, without regulatory status and whose effects on environment and human health are unknown (Lapworth et al., 2012; Thomaidis et al., 2012; Deblonde et al., 2011). They include a wide array of substances (as well as metabolites and transformation products) including pharmaceuticals and personal care products (PPCPs), illicit drugs and drug of abuse, hormones, steroids, polar pesticides, veterinary products, industrial compounds/by-products, food additives as well as engineered nanomaterials (Lapworth et al., 2012; Thomaidis et al., 2012).

This work focuses on the determination of synthetic musks, which are comprised within the category of emerging contaminants as a personal care product in environmental aqueous matrices. Musk compounds are a class of fragrant substances used as base notes in perfumery. Due to their widespread use in consumer products such as detergents, cosmetics and others, it is of interest to study their occurrence in the environment. This work aims to optimize a relatively novel extraction technique, dispersive liquid-liquid microextraction (DLLME), for the detection of synthetic musks in real water samples.

1.2 Personal Care Products

Personal care products (PCPs) are chemical products used in daily human life that are released continuously to the environment mainly through urban wastewater effluents, that come mainly from individual households, after showering and bathing. They comprise different groups of compounds that are currently used as additives in cosmetic, household, food and pharmaceutical products, among others. These additives include chemicals such as synthetic musk fragrances, antimicrobials, UV-filters, antioxidants, insect repellents and parabens (Posada-Ureta et al., 2012; Ramírez et al., 2012; Arbulu et al., 2011). Most of these compounds are lipophilic and tend to accumulate in the environment having adverse effects on aquatic ecosystems, and therefore are considered as emerging contaminants (Arbulu et al., 2011). In recent years, several PCPs have been found in environmental matrices, such as water, sediments, biota and air (Bester, 2009; Matamoros et al., 2009; Peck, 2006). Together with various pharmaceuticals (e.g. antibiotics, analgesics, anti-inflammatories, lipid regulators, psychiatric drugs, ß-blocking agents, etc) they constitute the class of pharmaceuticals and personal care products (PPCPs) that include a wide variety of important emerging contaminants in everyday urban activities. Following the precautionary principle, some PPCPs have been identified as future emerging priority candidates for monitoring and regulation, underlining the need of reliable analytical methods (Posada-Ureta et al., 2012; Pietrogrande and Basaglia, 2007).

As mentioned before, within the PCPs considered as emerging contaminants are the synthetic musks. These compounds are incorporated in a wide range of consumer products such as detergents, cosmetics and other personal care products both as a fragrance and as a fixative. Their intensive and widespread use, and its lipophilic nature, made these compounds interesting targets for future research, for the study of their occurrence in the environment and their toxicity (Ramírez et al., 2012; Breitholtz et al., 2003).

1.2.1 Natural musks

Musk originally designated a gland secretion produced by the male musk deer (*Moschus moschiferus*), which has been used as a fragrance material for centuries. Nowadays, the term is also applied to a whole class of fragrant substances used as base notes in perfumery, which are different in their chemical structure, but exhibit a common, distinct and typical flavour (Milojević, 2013; Sommer, 2004).

The use and importance of musk odour date back to ancient times. Musk fragrances were firstly used in religious ceremonies, and have also been applied as pharmaceutical ingredients and odorants (Ravi, et al., 2001). Until the end of the nineteenth century, these fragrances were only obtained from natural sources (Sommer, 2004). In the musk

deer, these substances were obtained from the exocrine odour glands, also called pods, which are located in the skin of the abdomen in the proximity of the male genitalia. These substances were highly valued due to its fixative and scent properties that enhance and harmonize perfume compositions. Musks can also be obtained from other animal sources, as the American musk rat (*Ondarta zibethicus rivalicius*), the civet cat (*Civetticitis civetta*), the musk ox (*Vibus moschatus*), etc, and plants, as angelica root (*Angelica archangelica*) and ambrette seeds (*Abelmoschus moschatus, Hibiscus abelmoschus*) (Yang et al., 2003; Ravi et al., 2001; Mookherjee and Wilson, 1982).

The high cost, uncertainty of supply and obvious ethical issues related to the killing of endangered animals to remove their odour glands, lead the fragrance industry to replace natural musks by chemically synthesised musk compounds (López-Nogueroles et al., 2011).

1.2.2 Synthetic musks

Nowadays, synthesised compounds are almost exclusively used, comparatively to musk compounds from natural sources (Sommer, 2004). Synthetic musks are man-made chemicals, components of fragrance compositions, produced in large quantities and extensively in a wide variety of PCPs such as perfume, cosmetics, detergents, soaps and cleaning products (Tanabe, 2005).

Synthetic musks mainly include four categories of compounds: nitro, polycyclic, macrocyclic and alicyclic musks (Posada-Ureta et al., 2012; Arbulu et al., 2011).

1.2.2.1 Nitro musks

The nitro class of musks was first discovered by Baur at the end of the nineteenth century, in 1891. These compounds consist of dinitro- and trinitro- substituted benzene derivatives, and although they are structurally completely different from the naturally occurring musks, they exhibit similar fragrance properties (Schmeiser et al., 2001). The best known nitro musks are listed in Table 1, where their chemical structure and some of their properties are presented.

For many years, they were the most produced musk compounds, mainly because of their low prices and easy preparation (Sommer, 2004; Schmeiser et al., 2001). However, the use in cosmetic products of musk ambrette (MA), musk tibetene (MT) and musk moskene (MM) is banned in the European Union, according to directive 76/768/EEC, the first one since 1995, and the other two since 1998, while the use of musk xylene (MX) and musk ketone (MK) is limited to around 1%, since 2004. Nevertheless, its use is permitted in North America (Posada-Ureta et al., 2012; López-Nogueroles et al., 2011). As a result,

among this group of musks, MX and MK are, by far, the most relevant compounds, nowadays.

Observing the properties presented in Table 1, it is noticeable that all nitro musks have values of log K_{ow} superior to 4, which indicates a lipophilic nature. MT and MM have the highest water solubility. All boiling points are between 350 °C and 400 °C, MX and MT have the highest boiling point and MM the lowest.

Table 1 - Chemical structure and physicochemical properties of the nitro musks class.

Compound Cas No. Chemical Formula	Chemical Structure	Molecular weight ($g \cdot mol^{-1}$)	Boiling point (°C) (at 760 mmHg) [a]	Log K_{ow}	Water solubility ($mg \cdot L^{-1}$)	Vapour Pressure (Pa)
Musk ambrette (MA) 83-66-9 $C_{12}H_{16}N_2O_5$	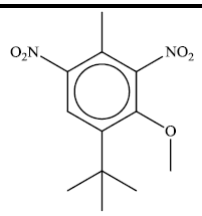	268.3	369	5.7[b]	2.10[e]	1.8×10^{-3} [e]
Musk ketone (MK) 81-14-1 $C_{14}H_{18}N_2O_5$	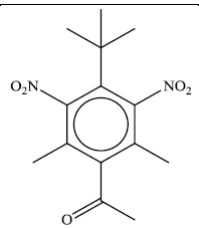	294.3	369	4.3[b,d] 3.8[c]	1.90[d] 0.46[c]	4.0×10^{-5} [d]
Musk moskene (MM) 116-66-5 $C_{14}H_{18}N_2O_4$	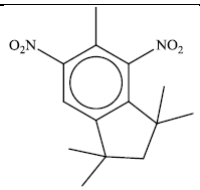	278.3	351	5.8[b]	12.40[e]	1.2×10^{-11} [e]
Musk tibetene (MT) 145-39-1 $C_{13}H_{18}N_2O_4$	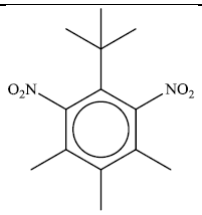	266.3	391	5.9[b]	22.00[e]	2.7×10^{-11} [e]
Musk xylene (MX) 81-15-2 $C_{12}H_{15}N_3O_6$	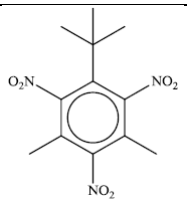	297.2	392	4.8[b] 4.9[d]	0.49[d]	3.0×10^{-5} [d]

[a]Royal Society of Chemistry, 2014 - predicted using the ACD/Labs' ACD/PhysChem Suite; [b]Osemwengi and Steinberg, 2001; [c]Wollenberger et al., 2003; [d]Chase et al., 2012; [e]Royal Society of Chemistry, 2014 - predicted using the US Environmental Protection Agency's EPISuite™

1.2.2.2 Polycyclic musks

In the 1990s, the use of nitro musks declined significantly and the polycyclic musks emerged (Roosens et al., 2007). These compounds were not discovered until the 1950s.

They are nitro-free alkylated tetralin or indane derivatives (Zeng et al., 2007; Herren and Berset, 2000). Like the nitro musks, they are chemically different from the natural musks, but exhibit musk-like odour (Heberer, 2002). The low cost synthesis, compared to the macrocyclic compounds, and increased resistance to light and alkali, compared to the nitro musks, are the main reasons for their extensive use (Roosens et al., 2007; Sommer, 2004). Galaxolide (HHCB) and tonalide (AHTN) are the most widely used polycyclic musks and they represent about 95% of the European market and 90% of the United States market for all polycyclic musks (Reiner et al., 2007a).

The most important representatives of polycyclic musks are listed in Table 2, along with their chemical structure and some of their physicochemical properties.

Table 2 - Chemical structure and physicochemical properties of the polycyclic musks class.

Compound Cas No. Chemical Formula	Chemical Structure	Molecular weight ($g \cdot mol^{-1}$)	Boiling point (°C) (at 760 mmHg) [a]	Log K_{ow}	Water solubility ($mg \cdot L^{-1}$)	Vapor Pressure (Pa)
Cashmeran (DPMI) 33704-61-9 $C_{14}H_{22}O$	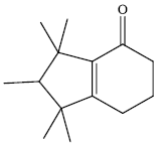	206.3	286	4.9	0.17	5.2×10^{0}
Celestolide (ADBI) 13171-00-1 $C_{17}H_{24}O$	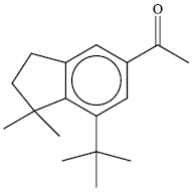	244.4	309	6.6 5.4[c]	0.02	2.0×10^{-2}
Galaxolide (HHCB) 1222-05-5 $C_{18}H_{26}O$	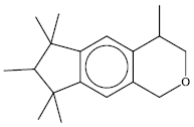	258.4	326	5.9	1.75	7.3×10^{-2}
Phantolide (AHMI) 15323-35-0 $C_{17}H_{24}O$	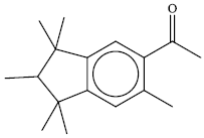	244.4	337	6.7	0.03	2.4×10^{-2}
Tonalide (AHTN) 1506-02-1 $C_{18}H_{26}O$	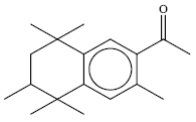	258.4	357	5.7	1.25	6.8×10^{-2}
Traseolide (ATII) 68140-48-7 $C_{18}H_{26}O$	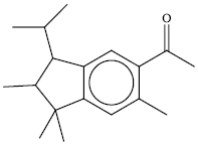	258.4	350	8.1	0.09	1.2×10^{0}

[a]Royal Society of Chemistry, 2014 - predicted using the ACD/Labs' ACD/PhysChem Suite; [b]Chase et al., 2012; [c]Wollenberger et al., 2003

Traseolide (ATII) seems to be the most lipophilic polycyclic compound, having the highest log K_{ow} of 8.1 and low water solubility. They have lower boiling points than the

nitro musks, all of which are below 360 °C. Tonalide (AHTN) has the highest boiling point (357 °C) and cashmeran (DPMI) the lowest (286 °C). Polycyclic compounds are more volatile than nitro musks, as they present, not only lower boiling points, but also higher vapour pressures.

1.2.2.3 Macrocyclic musks

Macrocyclic musks, more recently introduced to the market, are large ringed (10-15 carbons) ketones or lactones, and they are chemically similar to natural occurring musks (Sumner et al., 2010). Due to their outstanding stability, fixation properties and high quality odour, they are highly regarded by the industry. However, because of their expensive production, they represent only a small part of the musks on the market (3-4%) and are almost exclusively used in perfumes (Roosens et al., 2007; Abramsson-Zetterberg and Slanina, 2002). Some of the most prominent macrocyclic musks are listed in Table 3.

Table 3 - Chemical structure and physicochemical properties of the macrocyclic musks class.

Compound Cas No. Chemical Formula	Chemical Structure	Molecular weight ($g \cdot mol^{-1}$)	Boiling point (°C) (at 760 mmHg) [a]	Log K_{ow} [b]	Water solubility ($mg \cdot L^{-1}$) [b]	Vapor Pressure (Pa) [b]
Ambrettolide 123-69-3 $C_{16}H_{28}O_2$	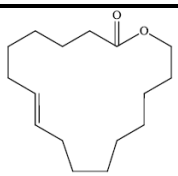	252.4	379[a]	5.4[a]	0.59[a]	3.0×10^{-3} [a]
Civetone 542-46-1 $C_{17}H_{30}O$	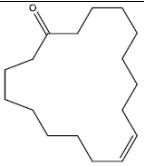	250.4	344[b]	6.3[b]	0.10[b]	4.5×10^{-2} [b]
Ethylene brassylate 105-95-3 $C_{15}H_{26}O_4$	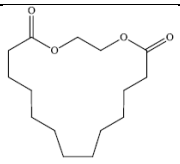	270.4	434[c]	4.7[c]	1.72[c]	6×10^{-5} [c]
Exaltolide (Thibetolide) 106-02-5 $C_{15}H_{28}O_2$	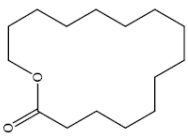	240.4	364[d]	6.0[d]	0.15[d]	6.9×10^{-3} [d]
Globalide (Habanolide) 111879-80-2 $C_{15}H_{26}O_2$	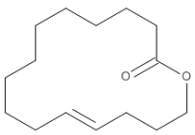	238.4	283-331[e] (at 710 mmHg)	6.2[e]	0.96[e]	1.6×10^{-1} [e]
Muscone 541-91-3 $C_{16}H_{30}O$	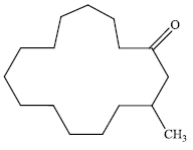	238.4	322[f] (at 730 mmHg)	6.0[f]	0.22[f]	6.3×10^{-2} [f]

[a]McGinty et al., 2011a; [b]McGinty et al., 2011b; [c]McGinty et al., 2011c; [d]McGinty et al., 2011d; [e]McGinty et al., 2011e; [f]McGinty et al., 2011f

Similar to the other classes, these compounds exhibit lipophilic properties, with high log K_{ow} values and low water solubility values. Ethylene brassylate is the most soluble in water, having also the lowest log K_{ow} (4.7), while civetone is the most lipophilic compound, having the highest log K_{ow} (6.3), and lowest water solubility. Ethylene brassylate has the highest boiling point (434 °C), while the rest of the compounds have boiling points below 400 °C.

1.2.2.4 Alicyclic musks

Alicyclic musks, also known as linear musks, are a relatively novel class of musk compounds. They are completely different in structure from the other musk classes as they are modified akyl esters (Table 4). They were first introduced in 1975, with the discovery of Cyclomusk, but it was only in 1990 that a compound of this class made it to production scale with the discovery and introduction of Helvetolide. Romandolide, the most important alicyclic musk along with Helvetolide, was introduced ten years later (Kraft, 2004; Eh, 2004).

Table 4 - Chemical structure and physicochemical properties of the alicyclic musks class.

Compound Cas No. Chemical Formula	Chemical Structure	Molecular weight ($g \cdot mol^{-1}$)	Boiling point (°C) (at 760 mmHg) [a]	Log K_{ow} [b]	Water solubility ($mg \cdot L^{-1}$) [b]	Vapor Pressure (Pa) [b]
Cyclomusk 84012-64-6 $C_{17}H_{28}O_2$	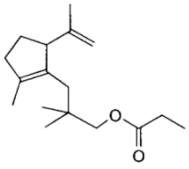	264.4	337	6.8	0.03	5.5×10^{-2}
Helvetolide 141773-73-1 $C_{17}H_{32}O_3$	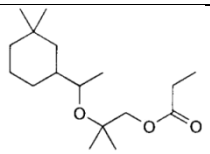	284.4	346	5.5	0.30	4.4×10^{-2}
Romandolide 236391-76-7 $C_{15}H_{26}O_4$	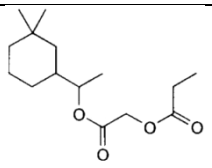	270.4	335	4.5	2.86	3.6×10^{-1}

[a]Royal Society of Chemistry, 2014 - predicted using the ACD/Labs' ACD/PhysChem Suite; [b]Royal Society of Chemistry, 2014 - predicted using the US Environmental Protection Agency's EPISuite™

As the other classes of musks, alicyclic musk compounds are lipophilic, having high values of log K_{ow} (superior to 4). Cyclomusk is the most lipophilic, having the highest log K_{ow} (6.8) and the lower water solubility, while Romandolide has the lowest log K_{ow} (4.5)

and the highest water solubility. Their boiling points do not differ very much, being between 335 °C and 350 °C for the three compounds.

1.3 Synthetic musks in the environment

As it has been observed, synthetic musks have a lipophilic nature, causing them to have a tendency to bioaccumulate, namely in lipid-rich tissues (Ramírez et al., 2011; Reiner et al., 2007b). These compounds, more specifically nitro musks, were first detected in the environment in 1981 in Japan (Yamagishi et al., 1981). Currently, synthetic musks have been detected in several environmental samples, including air (Xie et al., 2007; Peck and Hornbuckle, 2006), freshwater, seawater (Lee et al., 2010; Silva and Nogueira, 2010), sediments (Chase et al., 2012; Wu and Ding, 2010), biota such as fish, mussel and crustacean (Nakata et al., 2007; Rüdel et al., 2006) and even in human samples, such as adipose tissue (Schiavone et al., 2010; Kannan et al., 2005), breast milk (Raab, et al., 2008; Reiner et al., 2007a), serum from umbilical cords (Kang et al., 2010) and blood (Hutter et al., 2009). The concentration of musks in air samples were in the range of $pg \cdot m^{-3}$ (varying from low values to thousands). In water samples, freshwater usually contained values bellow the medium hundreds of $ng \cdot L^{-1}$, while seawater contained lower values (below the thousands of $pg \cdot L^{-1}$) and wastewaters presented the highest values, reaching the low $\mu g \cdot L^{-1}$. For sediments, the range of concentrations obtained were bellow the medium hundreds of $ng \cdot g^{-1}$, including values bellow 10 $ng \cdot g^{-1}$. Biota and human samples presented values usually between the low $ng \cdot g^{-1}$ (1-5) and one thousand $ng \cdot g^{-1}$ (human blood: up to 820 $ng \cdot L^{-1}$). In almost every case, for all matrices, HHCB was the synthetic musk found in higher concentrations, followed by AHTN.

Since synthetic musks are used in consumer products, due to their regular use, they continuously enter the wastewaters through down-the-drain practices, making wastewater effluents the main source of these compounds into the environment (Chase et al., 2012; Ramírez et al., 2012; Arbulu et al., 2011). This is indicated by high concentrations found in wastewaters effluents and its occurrence in surface water and groundwater located near wastewater discharge areas, with peak environmental concentrations occurring near effluent discharge points (Chase et al., 2012; Nakata et al., 2007).

Synthetic musks are only partially biodegradable, so they are not completely eliminated by wastewater treatment plants (WWTPs). Their removal has been reported from 50 to more than 90% in WWTPs, mainly by means of their sorption onto sludge particles (Ramírez et al., 2012). For this reason, the disposal of sludge to terrestrial environment through landfill or agricultural application also contributes to the release of synthetic musks into the environment (Horii et al., 2007). In fact, due to the efficient adsorption of synthetic musks to particles, high concentrations of these compounds have

been found in sewage sludge (Chen et al., 2007, Yang and Metcalfe, 2006). The incineration of sludge efficiently reduces the discharge of synthetic musks to terrestrial environment (Horii et al., 2007). The elimination of synthetic musks during treatment is highly dependent on WWTP size, WWTP type/processes of waste treatment, type of waste (municipal vs. industrial), and populations served (rural vs. highly urbanized) by the WWTP. The factors that affect their concentrations after release from a WWTP are dilution factors, removal rates during treatment and amount released during WWTPs bypasses (Chase et al., 2012). In addition, some degradation products of these compounds can also be formed during wastewater treatment, which are usually more oxidized and less lipophilic substances, making them more easily found in aquatic environments (Ramírez et al., 2012). Galaxolidone (HHCB-lactone) is an oxidation product of the polycyclic musk galaxolide and it has been indentified in natural waters and wastewaters (Bester, 2004; Bester, 2005), and due to its cycle in nature, it has even been detected in human milk (Reiner et al., 2007a). Its biotranformation tends to occur in WWTP operating with activated sludge (Bester, 2005). For nitro musks, in some cases, they can be transformed into amino derivates, which may be more dangerous than original compounds (López-Nogueroles et al., 2011).

Due to their presence in cosmetic products, synthetic musks can also directly reach the aquatic environment from swimming activities in seas, rivers and lakes (López-Nogueroles et al., 2011). Runoff from agricultural fields irrigated with treated effluent has also been detected to have synthetic musks (Pedersen et al., 2005), which indicates potential for non-point source pollution from these compounds. Moreover, synthetic musks also occur in rainwater due to atmospheric deposition (Peters et al., 2008). Nevertheless, there are several potential elimination pathways, once synthetic musks are transported to surface waters, such as water–air exchange (volatilization), photolysis, biodegradation, and sorption. To date, regulatory limits have not been set for these compounds and their discharge from WWTPs (Chase et al., 2012).

As mentioned before, due to the lipophilic nature of synthetic musks, they tend to partition onto sludge solids during wastewater treatment. When the sludge is applied to agricultural soil, the compounds may remain in the soil for months to years because of their sorption to organic, mineral, and amorphous phases of soil and slow rates of biodegradation (Stevens et al., 2003). Their presence in soils leads to these compounds potentially being taken up by plants and animals and, therefore, accumulating in the terrestrial food chain. Consequently, the animals at the top of the food chain, including humans, are often subjected to high concentrations of these compounds (Kallenborn and Rimkus, 1999).

Synthetic musks have also been found in remote non-anthropogenic areas such as the Great Lakes (Peck and Hornbuckle, 2006; Peck and Hornbuckle, 2004) and Arctic waters (Xie et al., 2007). This is caused by the long-range transport and persistence of synthetic musks, as well as their exchange between air and water matrices, highlighting the importance of atmospheric transport in dispersing these fragrances throughout the global environment. Synthetic musks have been suggested to be used as chemical markers of anthropogenic pollution, because of their widespread use and their detection in natural waters (Arbulu et al., 2011; Ramírez et al., 2011).

The purpose of this work is to detect and quantify synthetic musks in aqueous environmental matrices. As mentioned, these compounds are only partially biodegradable and their main route of exposure into the environment is through wastewater effluents, impacting the aquatic environment. For this reason it is important to determine their occurrence in wastewaters and in natural water samples. Since synthetic musks mostly occur in very low concentrations, knowledge in analytical and extraction methods is fundamental.

1.4 Analytical methods for the determination of synthetic musks in aqueous matrices

In the last decades, numerous analytical methodologies have been applied for the determination of musks in aqueous matrices, most of them based on gas chromatography-mass spectrometry (GC-MS) analysis. However, the samples cannot be analyzed by GC-MS without any preparation. Therefore, sample preparation to remove compounds that may interfere with the detection of the musks and also to allow pre-concentration, since musks occur in the environment at very low concentrations, is required. Hence, extraction techniques are applied.

1.4.1 Extraction techniques

In this section, a brief explanation of the most used extraction techniques for the determination of musks in aqueous matrices will be addressed. The technique used in this work, dispersive liquid-liquid microextraction (DLLME), will be explained more thoroughly.

1.4.1.1 Liquid-liquid extraction (LLE)

Liquid–liquid extraction is the most classical approach for the extraction of compounds from aqueous samples. LLE is based on the principles of mass transfer, where a liquid sample contacts an immiscible solvent in which the analyte of interest is more readily soluble. Therefore, the separation occurs between two immiscible liquids or phases

in which the compound has different solubilities (Müller et al., 2000). Usually, one phase is aqueous and the other phase is an organic solvent. The basis of the extraction process is that the more non-polar hydrophobic compounds will migrate to the organic solvent, while the more polar hydrophilic compounds stay in the aqueous (polar) phase (Dean, 2009).

1.4.1.2 Solid phase extraction (SPE)

Solid phase extraction is also a popular sample preparation method used for the extraction of components of interest from aqueous samples. In SPE the liquid sample is brought into contact with a solid phase or sorbent whereby the compound is selectively adsorbed onto the surface. The solid phase may be in the form of cartridges, columns or discs (Rodríguez et al., 2013). The target analytes distribute between the liquid sample and the solid surface either by simple adsorption to the surface or through penetration of the outer layer of molecules on that surface. The analyte of interest is eluted from the sorbent by the passing of a solvent suitable for its desorption (it should provide a more desirable environment for the analyte than the solid phase). Undesirable compounds can be washed from the sorbent using an appropriate solvent between retention and elution, for it is likely that some co-retained compounds will be eluted with the compound of interest (Simpson, 2000).

1.4.1.3 Solid phase microextraction (SPME)

Solid phase microextraction is a method of pre-concentration whereby a compound of interest is adsorbed onto the surface of a coated-silica fibre. The sorbent must have a strong affinity for the target compound, so that pre-concentration can occur from either dilute aqueous samples or the gas phase. The most reported stationary phase for SPME is polydimethylsiloxane (PDMS), which is a non-polar phase that can be used for the extraction of a range of non-polar compounds (Prosen and Zupančič-Kralj, 1999). The adsorption may be done by having the SPME fibre placed directly into the aqueous sample, which is called direct immersion SPME (DI-SPME) or by a headspace approach (HS-SPME), provided that the compounds are volatile (Pawliszyn, 2002). After the step of adsorption, the fibre is transferred to the injector of the gas chromatograph, where heat is provided for a thermal desorption. Alternatively, desorption can also be done via solvent, mostly when applied to liquid chromatography (Dean, 2009).

1.4.1.4 Stir-bar sorptive extraction (SBSE)

Stir-bar sorptive extraction uses a magnetic stir bar coated with a sorbent (e.g. PDMS), which is placed and stirred in an aqueous sample. This technique is based on similar principles as the SPME, whereby a compound of interest is adsorbed to the sorbent. Like in the SPME, thermal or liquid desorption follow the process of adsorption. However

for thermal desorption, a special instrument, usually coupled on-line to capillary gas chromatography is used (David and Sandra, 2007; Baltussen et al., 1999).

1.4.1.5 Dispersive liquid-liquid microextraction (DLLME)

Dispersive liquid-liquid microextraction is a relatively novel extraction and pre-concentration technique that was developed in 2006 (Rezaee et al., 2006). It uses an extraction solvent, immiscible in the aqueous phase, and a disperser solvent, miscible in both the extraction solvent (organic phase) and in the sample (aqueous phase) (Zgoła-Grześkowiak and Grześkowiak, 2011; Rezaee et al., 2006). The mixture of solvents is rapidly injected in the sample in a tube with conic bottom by the use of a syringe, where the disperser solvent promotes the dispersion of the organic phase (extraction solvent) in the form of microdroplets, as can be seen in Figure 1 (Rodríguez et al., 2013; Panagiotou et al., 2009). This creates an infinitely large superficial area between the two phases, which allows a quicker transference of the analytes from the aqueous phase to the organic phase, so the equilibrium is attained rapidly (Etxebarria et al., 2012; López-Nogueroles et al., 2011). The cloudy mixture is then centrifuged and depending on the density of the extraction solvent, it either sediments at the bottom of the test tube or floats at the top of the solution (Rodríguez et al., 2013). Finally, the organic phase is tranferred to a microvial for the analysis of the analytes. The steps of DLLME are represented in Figure 2.

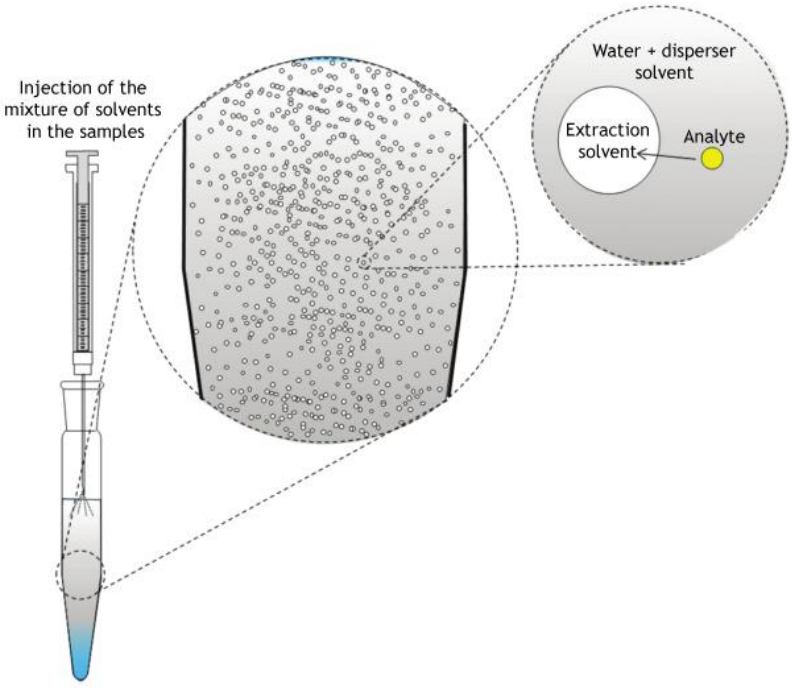

Figure 1 – Simplified diagram demonstrating the first step of DLLME (adapted from Martins et al.,2012).

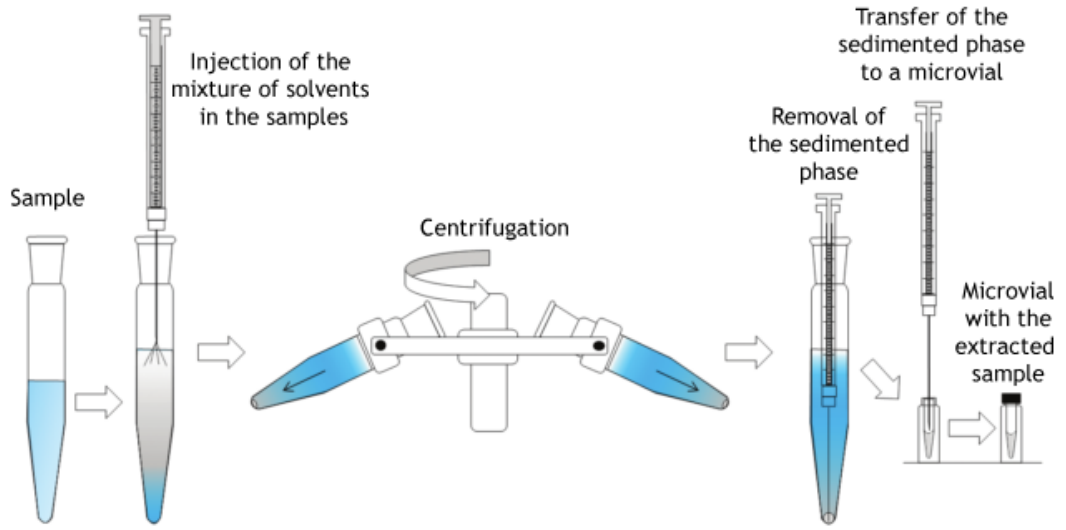

Figure 2 – Simplified diagram demonstrating the main steps of DLLME (adapted from Martins et al.,2012).

The main factors that affect the extraction efficiency in DLLME are the type and volume of the extraction and disperser solvents (Martins et al., 2012; Zgoła-Grześkowiak and Grześkowiak, 2011). A key parameter for the extraction solvent is, of course, its extraction capacity for the analytes of interest, and its low solubility in water is obviously another fundamental parameter. Usually the density of the extraction solvent is higher than the one of the water, so it can sediment during the centrifugation (Yang and Ding, 2012; López-Nogueroles et al., 2011; Rezaee et al., 2006). However, as mentioned before, extraction solvents with lower density than water can also be used (Martins et al., 2012). If gas chromatography is used, the boiling point of the extraction solvent is also important (Martins et al., 2012), and it should have a good chromatographic behaviour (López-Nogueroles et al., 2011; Rezaee et al., 2006). The solvents most commonly used as extractants are halogenated hydrocarbons such as chloroform, carbon tetrachloride, trichloroethane, tetrachloroethylene, chlorobenzene, etc (Etxebarria et al., 2012; Yang and Ding, 2012). For the disperser solvent, the fundamental parameter is its solubility in both the organic and aqueous phase. The most commonly used disperser solvents are acetone, acetonitrile, methanol and ethanol (Yang and Ding, 2012; López-Nogueroles et al., 2011; Zgoła-Grześkowiak and Grześkowiak, 2011). Both solvents, disperser and extraction, should have relatively low vapour pressure and relatively high boiling points to avoid significant losses during the extraction process (Martins et al., 2012). The volume of extraction solvent determines the pre-concentration factor of the method; the more volume is used, the lower is the pre-concentration factor. The optimal volume should ensure a high pre-concentration factor, while enough volume of the sedimented phase for the necessary analysis is obtained (Etxebarria et al., 2012; Rezaee et al., 2006). The volume of the sedimented phase depends on the solubility of the extraction solvent in

water, on the volume and characteristics of the sample and on the volume of both the extraction and disperser solvents. The appropriate volume of disperser solvent for a good formation of microdroplets depends on both the volume of the aqueous phase and the volume of extraction solvent (Etxebarria et al., 2012; Martins et al., 2012).

Though in DLLME the equilibrium is attained quickly, the extraction time, usually defined as the interval between the injection of the mixture of solvents in the sample and the centrifugation, should also be optimized. Other factors that should also be considered are the ionic strength and the pH (Martins et al., 2012; López-Nogueroles et al., 2011; Zgoła-Grześkowiak and Grześkowiak, 2011).

1.4.2 Gas chromatography-mass spectrometry (GC-MS)

In the last decades, GC-MS has been chosen for the analysis of synthetic musks by almost every author. For semi-volatile compounds like synthetic musks, GC is a preferable choice, in contrast with liquid chromatographic analysis, which is more appropriate for non-volatile compounds(Pietrogrande and Basaglia, 2007). Coupled with MS, a more precise analysis is granted, as it allows to distinguish and quantify compounds that are co-eluted.

Chromatography is a physical method of separation of substances, in which the separation of the components to be analyzed is based on differential partitioning between a mobile phase and a stationary phase held in a column. In gas chromatography, the mobile phase is gaseous and the stationary phase is either liquid – gas-liquid chromatography (GLC) - or solid – gas-solid chromatography (GSC). GLC is more commonly used and its name is usually shortened to gas chromatography (GC) (Skoog et al., 2007). The mobile phase in GC is called the carrier gas and it must be chemically inert. In contrast to most other types of chromatography, the mobile phase does not interact with the molecules of the analyte, as its only function is to transport the analyte through the column. The most common gas carrier used is helium, although argon, nitrogen and hydrogen can also be used (Skoog et al., 2007).

When coupled with mass spectrometry (GC-MS), this analytical method allows, not only the separation of the components of a mixture, but also the characterization of those components. Figure 3 shows a scheme of a typical GC-MS system.

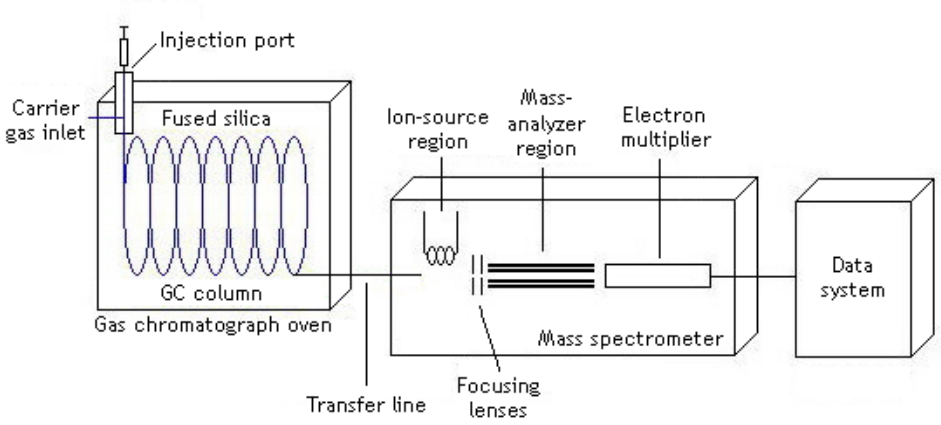

Figure 3 - Schematic of a typical GC-MS system (adapted from Skoog et al., 2007).

A chromatographic analysis starts with the introduction of the sample onto the column, and the device that allows this is called the injector. The sample may be introduced in liquid state or adsorbed into a support (SPME fibres). The samples are injected into the interior of an evaporation tube (liner), where the solvent and the dissolved sample evaporate and mix with the carrier gas. The temperature in this tube should allow a rapid volatilization of the sample (and in case of SPME fibres it allows the thermal desorption as well), so usually it is set 50 °C above the boiling temperature of the least volatile component of the sample (Hübschmann, 2009; Skoog et al., 2007). The liquid samples are injected with calibrated microsyringes through a rubber or silicone diaphragm or septum. Most higher-end gas chromatographs use automatic injectors (autosampler) instead of manual syringe injections, for the better precision of the injected volume (McMaster, 2008; Skoog et al., 2007). The most common type of injector is the split/splitless injector. In split mode injection, the sample/carrier gas stream is divided and only a small portion passes on to the column, while the rest is rejected. In splitless mode, the sample is transferred to the column in its totality (Hübschmann, 2009).

There are two types of columns used in GC, packed and open tubular, also called capillary. Nowadays, capillary columns are more commonly used because of their efficiency. The column is placed inside a thermostatted oven, so that the temperature can be controlled, since it is an important variable. The optimal columns temperature is defined by the boiling point of the analytes and solvent and the degree of separation required. Usually, when the sample contains analytes with a wide boiling range, a program of temperatures is employed (Skoog et al., 2007). The choice of the most suitable stationary phase is essential for a good separation of the different analytes in a sample. The stationary phase should exhibit affinity for the analytes, otherwise there will be no retention and the compounds leave the column in the dead time. Therefore, the polarity

of the stationary phase should correspond to the polarity of the sample components (Hübschmann, 2009).

Several detectors have been used with GC separations and mass spectrometer is one of the most powerful detectors. It aims to measure the ratio of mass/charge (m/z) of ions produced by the sample molecules (Skoog et al., 2007).

The sample is first ionized and fragmented, usually by an ion source. There are two types of ion sources: hard and soft sources. Hard ionization sources, such as electron ionization (EI), transfer enough energy to leave the analyte molecules in a highly energy state which then leads to the breaking of bonds, producing fragment ions. Soft ionization sources, such as chemical ionization (CI), use less energy, producing little fragmentation. In this work, electron ionization is used, in which a beam of energetic electrons interacts with the sample molecules, and ionizes the molecules, causing them to lose an electron due to electrostatic repulsion. Electrons are emitted from a heated tungsten or rhenium filament and accelerated by applying 70 eV between the filament and the anode (Skoog et al., 2007). The produced ions reach then the mass analyzer.

The most common mass analyzers are quadrupoles and ion traps. In this work, an ion trap is used. It is composed of a central ring electrode and two end-cap electrodes, as it is shown in Figure 4. Ions produced by the ion source enter through the upper end cap. The function of an ion trap is to change the electric and magnetic field inside the device, so that the trajectories of ions captured of consecutive mass/charge ratio become sequentially unstable and the ions have to leave the ion trap in order of their ratio mass/charge. On output the ions reach a transducer, such as the electron multiplier, providing a signal (McMaster, 2008; March, 2000). As the positive ions strike the lead oxide glass cathode surface of the electron multiplier, electrons are released from it inner surface. These bounce down the inner walls, releasing a cascade of electrons on each contact. The electrons reach the anode cup and send a signal to the data system (McMaster, 2008).

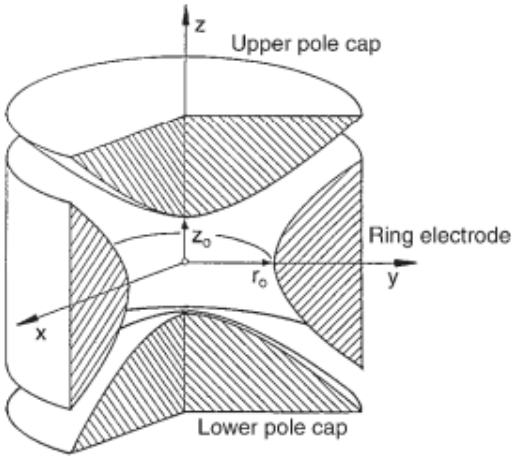

Figure 4 - Diagram of an ion trap analyzer (adapted from Hübschmann,2009).

Mass spectrometer data is stored as a tree-dimensional block with three axis: time, intensity and mass/charge ratio (m/z) (McMaster, 2008). Two two-dimensional representations are obtained by the end of an analysis: the chromatogram, which represents intensity vs. time, and the mass spectrum, which represents intensity vs. m/z.

The acquisition of data can be done in full-scan or selected ion storage (SIS). A full-scan ion chromatogram is a summation of the intensities of all mass fragments at a given time, while in SIS mode, only the selected m/z ranges are detected by the instrument during the analysis. This operation mode usually increases the sensibility of the method for the selected ions, leading to lower detection limits. However, it provides limited qualitative information, because the characteristic mass spectrum of the compounds is not created (Hübschmann, 2009; Fountain, 2002). Mass spectrometry can be used for obtaining information even when the compounds are not completely separated. The nature of MS detector allows the quantification of more than one compound even if co-eluted, as long as the ions have different mass/charge.

2 State of the Art

In the last years, several analytical methods have been developed for the determination of synthetic musks in aqueous matrices, most of them based on GC–MS analysis. The nature of the matrix (surface water, groundwater, wastewater, etc.) may determine the extraction methodology applied, due to the existence of substances which may interfere in the analysis, such as organic matter, surfactants, inorganic salts, etc. However some authors have applied the same method to different kinds of aqueous matrices. Table 5 summarizes the methods used in studies since 2006.

Two of the most commonly used extraction techniques for the determination of synthetic musks in water samples are the more classical approaches, such as liquid-liquid extraction (LLE) and solid-phase extraction (SPE). In LLE, hexane (Hex) and dichloromethane (DCM) have been the extraction solvents used for both surface waters and wastewaters, usually in sequence (Reiner and Kannan, 2010; Lee et al., 2010; Horii et al., 2007; Reiner et al., 2007b). Hex and DCM are non and low-polar solvents, respectively, so they have good affinity with low-polar compounds, such as synthetic musks.

For SPE, different sorbents have been successfully used, being the most common C_{18} discs (Guo et al., 2013; Chase et al., 2012; Hu et al., 2011; Zhang et al., 2008; Chen et al., 2007; Zeng, et al. 2007). However, other sorbents have also been used, such as HLB (hydrophilic-lipophilic balance copolymer) cartridges (Villa et al., 2012; Sumner et al., 2010) and sorbents based-on polystyrene-divinylbenzene (Ren et al., 2013; Quednow and Püttmann, 2008), sorbents of more broad use, being appropriate for both polar and non-polar compounds (Agilent Technologies, 2011; Bonna-Agela Technologies, 2011; Waters Corporation, 1998). Most of these sorbents have been used for more than one type of aqueous matrix. Different eluents have also been used, such as Hex/DCM (Zhang et al., 2008; Chen et al., 2007), Hex and Hex/DCM in sequence (Guo et al., 2013; Hu et al., 2011; Zeng, et al. 2007), acetone (Acet)/Hex (Chase et al., 2012), Hex and ethyl acetate (EtAc) in sequence (Villa et al., 2012), EtAc/DCM/methanol (MeOH) (Sumner et al., 2010), acetonitrile (ACN)/MeOH (Quednow and Püttmann, 2008) and ACN/DCM (Moldovan, 2006; Ren et al., 2013). Once again, due to the low polarity of synthetic musks, non-polar or low polar solvents are the most used.

One problem particular to wastewaters is that they contain a high amount of surfactants and particles, which may interfere with the analysis. This is especially problematic if SPE is utilized, but it may be overcome by filtration, centrifugation or by using larger amount of extraction materials or extraction devices with higher diameter to decrease clogging (extraction discs instead of cartridges). LLE has the advantage on this matter, because surfactants and particles usually do not influence the extraction very much (Bester, 2009). This is particularly beneficial for the extraction of synthetic musks, because the

concentration of these compounds in aqueous samples can be influenced by the quantity of particles present, since lipophilic compounds such as synthetic compounds tend to adsorb on suspended particles (Horii et al., 2007). So, filtration and/or centrifugation of samples prior to the extraction may cause the lost of the analytes. From the studies that used LLE, only one proceeded to sample filtration before extraction (Yang and Metcalfe, 2006). On the contrary, two studies of SPE did not filter their samples before extraction (Guo et al., 2013; Hu et al., 2011). In both cases, surface water was being analysed (it does not have so many suspended particles as wastewater) using extraction discs, which, as mentioned before, due to its larger diameter prevents clogging. In some studies, in which filtration/centrifugation was used, the authors also analysed the suspended solids (Villa et al., 2012; Sumner et al., 2010; Zhang et al., 2008; Chen et al., 2007). The major advantage of SPE over LLE is that it uses a considerable smaller amount of solvent than LLE; however it can be relatively expensive due to the need of cartridges. These two techniques have also the disadvantage of being time-consuming (Chung et al., 2013; Regueiro et al., 2008).

As can be seen in Table 5, LLE was one of the extraction techniques that had consistently high recoveries, with values above 80%. However, when using SPE, some lower recoveries values were reached (57–107%). The lower recovery values were in general associated to wastewaters (Chen et al., 2007; Zeng et al., 2007; Zhang et al., 2008), while most studies that analyzed surface waters obtained recoveries above 78% (Guo et al., 2013; Villa et al., 2012; Hu et al., 2011; Moldovan, 2006). This implies that the type of matrix, as mentioned before, affects the recovery values of SPE more than it does for LLE.

Due to the need of lower solvent consumptions and faster sample preparations, miniaturization in analytical chemistry has become of interest (Regueiro et al., 2008). Two of the most common miniaturizations of SPE are solid-phase microextraction (SPME) and stir-bar sorptive extraction (SBSE). Besides reducing the time of sample preparation, they also require low to no solvent consumption. When coupled to thermal desorption (TD), they also reduce the risk of background contamination, since the use of organic solvents is avoided and minimal manipulation of the sample is required (Ramírez et al., 2012). Since synthetic musks are low-polar compounds, they present a high affinity for the polydimethylsiloxane (PDMS) used in both SPME fibres and commercial stir bars (Ramírez et al., 2012). SPME has been successfully used for the determination of synthetic musks in surface waters (Liu et al., 2010) and wastewaters (Wang and Ding, 2009), but in recent years, SBSE has been more applied. SBSE is considered a more powerful technique because of its higher pre-concentration capacity, since the amount of sorbent is 50–250-fold higher than in SPME fibre (Ramírez et al., 2011). Most studies using SPME or SBSE applied TD at 270-300 °C. Nevertheless, liquid desorption was also used, using Hex (Silva and Nogueira, 2010) or Acet/Hex (Chase et al., 2012) as extraction solvents. TD has the advantage of not using solvent; however, to apply

this technique to SBSE, a specific thermal desorption system is required, which may explain the reason why some authors opted for liquid desorption. The main disadvantages of these two techniques are the price, due to the limited lifetime of extracting fibres and stir-bars (they begin to degrade with multiple uses) and the carryover problems, which requires time-consuming clean-up procedures of the extraction devices (Chung et al., 2013; Yang and Ding, 2012; Regueiro et al., 2008).

SBSE was another extraction technique, along with LLE, that had consistently high recoveries, with values above 80%, with no matrix effects observed (Ramírez et al., 2012; Ramírez et al., 2011; Silva and Nogueira, 2010). When SPME was used, some lower values of recoveries were reached (64 - 117%), depending on the synthetic musk analysed for either wastewaters (Wang and Ding, 2009) or surface waters (Liu et al., 2010).

Other two miniaturizations of SPE used for the determination of synthetic musks in aqueous matrices are microextraction by packed sorbent (MEPS) used for surface waters and wastewaters (Moeder et al., 2010), and dispersive micro-solid phase extraction (D-μ-SPE), used for surface waters (Chung et al., 2013). For MEPS, 1 mg of sorbent, C_8 for surface waters and C_{18} for wastewaters, in cartridge was used and the elution was carried with two portions of 25 μL of EtAc. Compared to SPE, this method requires shorter extraction times and small amount of sample and solvent volumes, making the MEPS technique attractive also from the economical and ecological points of view. The technique was applied to two polycyclic musks, HHCB and AHTN and four UV-filters, and both sorbents were reported as recommended for the extraction of these compounds from water samples (due to their low polarity). For the most lipophilic compounds, carryover was observed and, therefore, a proper clean-up was required (Moeder et al., 2010). Recoveries below 78% and going as low as 57% were obtained when C_8 was used as sorbent (applied to surface waters), however recoveries above 78% were obtained when C_{18} was used (applied to wastewaters) (Moeder et al., 2010).

D-μ-SPE involved immersing of the C_{18} adsorbent in the water sample and after vigorous shaking the adsorbents were collected on a filter and dried. The adsorbent were then subjected to TD-GC–MS analysis (Chung et al., 2013). TD provides high sensitivity, time efficiency, low cost and is eco-friendly. D-μ-SPE allows the advantages of TD, without the disadvantages of SBSE and SPME (high cost, fragile devices and carryover problems). Recoveries between 74 and 90% were obtained for surface waters (Chung et al., 2013).

As an alternative to traditional LLE, two studies used membrane-assisted solvent extraction (MASE), also called membrane-assisted liquid–liquid extraction (MALLE) (Posada-Ureta et al., 2012; Einsle et al., 2006). Membrane based techniques are simple liquid–liquid extraction between the aqueous sample (donor phase) and a microvolume of acceptor phase, protected by a membrane that avoids the mixture of the two phases and acts as a selective barrier in terms of analyte permeation through the membrane. Both studies used a non-

porous LDPE (low-density polyethylene) membrane and as extraction solvent, Hex (Posada-Ureta et al., 2012) and chloroform (Einsle et al., 2006) were used. This technique requires low volumes of organic solvents (400-1000 µL) and medium sample volumes (10-150 mL). Both groups of authors affirmed that this technique is suitable for the determination of synthetic musks in water samples, and the method was deemed to be simple, reliable and economic. MASE is advantageous for its low solvent consumption and a selective permeation of the membrane, but its main drawback is that it is time-consuming, as it may even require a longer time than traditional LLE, where time was already a disadvantage.

This extraction technique's recoveries were between 47 and 138%, having the lowest minimum recovery among all techniques (Posada-Ureta et al., 2012; Einsle et al., 2006). Posada-Ureta et al. (2012) analyzed wastewaters and surface waters, and the recoveries obtained for wastewaters (47 – 126%) were in general lower than for surfaces waters (64 – 138%).

Dispersive liquid-liquid microextraction (DLLME) is a miniaturization technique that has already been used by few authors for the determination of synthetic musks in aqueous matrices, such as surface water, sea waters and wastewaters (Yang and Ding, 2012; López-Nogueroles et al., 2011; Panagiotou et al., 2009). This technique uses a very small volume of extraction solvent and the contact surface between phases is infinitely large, leading to high enrichment factors and low extraction times. Rapidity, simplicity, low cost, high enrichment factors, and being effective and eco-friendly are the main advantages of this technique.

Yang and Ding (2012) analysed six polycyclic musks using the previously mentioned technique. They tested three extraction solvents (carbon tetrachloride, tetrachloroethylene and chlorobenzene) and five dispersants (MeOH), ethanol (EtOH), isopropyl alcohol (IPA), Acet, and ACN and concluded that carbon tetrachloride and IPA were the best extracting solvent and dispersant, respectively. The authors also studied the effect of the dispersant and verify that when the amount of IPA was increased the extraction efficiency (indirectly measured by the peak abundances) also increases. This can be explained due to the fact that a larger amount of dispersant allows more homogenous cloudy solutions, allowing the extraction solvent to be more efficiently dispersed in the aqueous solution. However, the amounts of the sedimented phases were decreased with increasing amounts of IPA. López-Nogueroles and co-workers (2011) analysed five nitro musks using this technique. They tested two extraction solvents, DCM, which did not form a cloudy solution with none of the disperser solvents tested, and chloroform, which did not form a cloudy solution with EtOH, but positive and similar results were obtained with Acet or ACN as disperser solvents. Acet was chosen because of its low toxicity and cost. Panagiotou and co-workers (2009) analysed five polycyclic musks using carbon tetrachloride and methanol as extraction and disperser solvents, respectively.

The effect of ionic strength was studied by the three groups of authors, although different conclusions were reached. In this technique, the addition of salt has two effects: it decreases the solubility of the extraction solvent in water, leading to a greater volume of sedimented phase, and the salting out effect that favours the extraction. López-Nogueroles and co-workers (2011) observed that the first effect was stronger and the volume of sedimented phase increased considerably with the ionic strength. Greater volumes lead to less concentration of the target analytes and, therefore, reduced signal. For this reason, no salt was added. On the other hand, Yang and Ding (2012) realized that the abundances increased when the added NaCl was increased from 0.3 to 0.5 g, but decreased for larger amounts, so 0.5 g of NaCl was added. Panagiotou and co-workers (2009) simply stated that NaCl had no significant impact on the extraction yield. They also stated that extraction time had no significant impact on the extraction yield, and López-Nogueroles and co-workers (2011) mentioned that they did not study its effect, because it was not expected for it to affect the results. Yang and Ding (2012) used ultrasound-assisted DLLME (UA-DLLME), where the dispersion was ultrasonicated to accelerate the extraction of the analytes into the droplets.

DLLME mostly presented good recovery values: Panagiotou et al. (2009) obtained recoveries above 77%, and López-Nogueroles et al. (2011) obtained recoveries above 87%. Yang and Ding (2012) obtained some lower values of 70 and 73% for DPMI and ATII, respectively, for surface water, and 75 and 77% for the same compounds for wastewater. However, the remaining four polycyclic musks analyzed had recoveries above 82% for both matrices.

The major drawbacks of DLLME are that it is difficult to automate and the necessity of using a third component, disperser solvent, which usually decreases the partition coefficient of analytes into the extraction solvent (Regueiro et al., 2008). Aiming to overcome some of these disadvantages, another method has been used, the ultrasound-assisted emulsification-microextraction (USAEME), where the fragmentation of one of the phases to form emulsions is propelled by ultrasounds (Regueiro et al., 2008). In this work, chloroform was used as extraction solvent and, contrary to DLLME, the extraction time had significant effect on the extraction. This technique gathers most of the advantages of DLLME, simple, non-expensive, low organic solvent consumption, and it overcomes the drawbacks of DLLME, as it is easy to automate and does not use a third component. However, although it is rapid when compared with other techniques, when compared to DLLME, it seems to take longer, as the extraction time is a more significant parameter than for DLLME. Good recoveries percentages, above 80%, were obtained with USAEME.

Regarding the LOD values of the studies presented in this work, ranges from 0.02-0.20 $ng \cdot L^{-1}$ to 60-120 $ng \cdot L^{-1}$ were obtained. The highest LOD values were obtained with

SPE (Chen et al., 2007), but the rest of the studies that used this extraction technique attained lower LOD values (0.05-20 ng·L^{-1}). The lowest LOD values were obtained when SBSE with thermal desorption was used (Ramírez et al., 2012). When liquid desorption was used, this technique lead to higher LOD values (12-67 ng·L^{-1}) (Chase et al., 2012; Silva and Nogueira, 2010). Studies that used LLE reported LOD values between 5 and 10 ng·L^{-1}, though LOQ values of 0.4-4.0 ng·L^{-1} were also reported in studies that didn't report an LOD values (Reiner and Kannan, 2010; Yang and Metcalfe, 2006). SPME lead to relatively low LOD values, in a similar range as LLE and SPE (0.05-9.6 ng·L^{-1}), and D-μ-SPE also achieved low LOD values (0.5-1.0 ng·L^{-1}) (Chung et al., 2013). When MASE was used, slightly higher LOD values were reported (8-20 ng·L^{-1}). MEPS reported high LOD values (37-54 ng·L^{-1}). DLLME and USAEME led to average-high LOD values in the ranges of 4-63 ng·L^{-1} (López-Nogueroles et al., 2011; Panagiotou et al., 2009) and 6-29 ng·L^{-1} (Regueiro et al., 2008), respectively. However, the most recent DLLME study, that was ultrasound assisted, was able to achieve a much lower LOD value, 0.2 ng·L^{-1} (Yang and Ding, 2012).

To the author's best knowledge, all studies in recent years have used GC-MS for the determination of synthetic musks in water samples, regardless of the extraction method. Synthetic musks' semi-volatile nature makes GC a more appropriate choice, compared to LC. Furthermore, for GC-MS, the identification is not based solely on retention time, allowing the differentiation between compounds that might possess the same retention time, but a different mass spectrum (McMaster, 2008).

Regarding the concentration levels of synthetic musks in the aqueous matrices, as expected, wastewaters generally presented much higher levels than surface waters (Chase et al., 2012; Ramírez et al., 2012; Reiner and Kannan, 2010; Sumner et al., 2010). The two older classes of synthetic musks (nitro and polycyclic musks) have been the target group of most studies. In general, polycyclic musks have been detected in higher concentrations (up to 595 μg·L^{-1} in wastewater influents, up to 32 μg·L^{-1} in wastewater effluents and up to 14 μg·L^{-1} in surface waters) and more often than the other musk classes. HHCB was the most detected musk in these matrices and, in almost every case, in higher concentration levels (wastewaters: up to 595 μg·L^{-1} and surface water: up to 14 μg·L^{-1}). AHTN was the second most detected synthetic musk, being detected in a range up to 68 μg·L^{-1} in wastewaters and up to 520 ng·L^{-1} in surface waters. Other synthetic musks were detected in lower levels, usually below 1 μg·L^{-1}. The most detected nitro musk was MK, followed by MX. The maximum concentrations of MK were 1010 ng·L^{-1} in wastewaters and 420 ng·L^{-1} in surface waters, while for MX, the maximum concentrations were 91 ng·L^{-1} in wastewaters and only 0.58 ng·L^{-1} for surface waters. The rest of the nitro musks were only detected occasionally and in very low levels. Macrocyclic and alicyclic musks were only analysed in one study (Arbulu et al., 2011).

Thibetolide, a macrocyclic musk, was the most abundant musk among the five synthetic musks detected in river waters, with a maximum concentration of 2544 $ng \cdot L^{-1}$, however it was not detected in wastewaters, and neither were any other macrocyclic musks. Romandolide, an alicyclic musk, was occasionally detected in river waters (73-306 $ng \cdot L^{-1}$) and in wastewaters (45-56 $ng \cdot L^{-1}$), while Helvetolide was only detected in wastewaters (21-70 $ng \cdot L^{-1}$).

As expected, the most extreme levels were detected in the wastewaters from a cosmetic plant, 550 $\mu g \cdot L^{-1}$ in the influent and 32 $\mu g \cdot L^{-1}$ in the effluent for HHCB and the remnant five polycyclic analysed were detected from concentrations of 3.7 to 68 $\mu g \cdot L^{-1}$ in the influent and from not detected to 6 $\mu g \cdot L^{-1}$ in the effluent (Chen et al., 2007). In other wastewaters, HHCB and AHTN were detected usually between the hundreds of $ng \cdot L^{-1}$ and 1 to 3 $\mu g \cdot L^{-1}$, though concentrations up to 13 $\mu g \cdot L^{-1}$ were reached, while others synthetic musks were detected with lower levels, or not even detected.

The concentrations obtained in surface waters were usually bellow the medium hundreds of $ng \cdot L^{-1}$, including values bellow 50 $ng \cdot L^{-1}$, which were common. However there were some exceptions, such as concentrations of HHCB up to 14 $\mu g \cdot L^{-1}$ and of AHTN and MK up to 2.8 $\mu g \cdot L^{-1}$ in river waters (Lee et al., 2010), and concentrations up to 2.5 $\mu g \cdot L^{-1}$ in other river waters (Arbulu et al., 2011). Cases of musks that were not detected were more common in surface waters than in wastewaters.

Only few studies analyzed seawater, but synthetic musks were mostly not detected, except for HHCB in one study, with a concentration of 64 $ng \cdot L^{-1}$ (Silva and Nogueira, 2010). Groundwaters were analysed more rarely, one study reporting concentrations up to 72 $ng \cdot L^{-1}$ (Chase et al., 2012), and another study reporting concentrations up to 530 $ng \cdot L^{-1}$ (Arbulu et al., 2011).

Many extraction techniques have been successfully applied to the determination of musks in aqueous matrices, being DLLME a promising one. Its rapidity, low solvent consumption and low cost make DLLME a very attractive option. Only few studies have focused on the musks' determination using this technique. However, the recoveries obtained in those studies were good, for different aqueous matrices (surface waters, sea waters and wastewaters) and when ultrasound-assisted DLLME was applied, the LOD values were some of the lowest among all the studies reported in this study. To the author’s best knowledge, DLLME was never applied to different classes of musks in the same study and was only applied to polycyclic or nitro musks. Therefore, the aim of this study is to apply US-DLLME to different types of water matrices (river, sea, wastewaters and drinking waters) for the determination of twelve musks within three classes of musks (five polycyclic musks, five nitro musks and two macrocyclic musks), and optimize the methodology using a design of experiments approach.

Table 5 - Overview on analytical methods for determination of synthetic musks in aqueous matrices.

Matrix	Analytes	Extraction method	Analysis method	%Rec	LOD ($ng \cdot L^{-1}$)	LOQ ($ng \cdot L^{-1}$)	C ($ng \cdot L^{-1}$)	References
Surface water (river)	HHCB, AHTN, MK, MX	LLE (DCM, Hex)	GC-MS	82-92	5	10	HHCB: 100-13920 AHTN,MK: BQ-2800 MX: ND	(Lee et al., 2010)
Surface water (river)	HHCB, AHTN	LLE (Hex, DCM)	GC-MS	85-98	NA	1	3.95-25.1	(Reiner and Kannan, 2010)
Surface water (river)	HHCB, AHTN, ADBI	SPE (500 mg HLB; Hex, EtAc)	GC-MS	>80 (ADBI: 50)	0.05-0.25	NA	ND-1141	(Villa et al., 2012)
Surface water	HHCB, AHTN, AHMI, ADBI, MX, MK	SPE (500 mg HLB; EtAc/DCM/MeOH 2:2:1)	LVI-PTV-GC-MS	59-100	0.3-1.2	NA	HHCB,AHTN: ND-28 remnant: ND	(Sumner et al., 2010)
Surface water (lake)	HHCB, AHTN, MK, MX	SPE (C_{18} disc; Hex, Hex/DCM 1:1)	GC-MS	79-85	NA	NA	0.12-212	(Guo et al., 2013)
Surface water (river)	HHCB, AHTN, ATII, ADBI, AHMI, MX, MK	SPE (C_{18} disc; Hex, Hex/DCM 1:1)	GC-MS	78-106	1.0-1.2	NA	Individual: ND-34.6 Total: 5.9-120.6	(Hu et al., 2011)
Surface water (river)	HHCB, AHTN	SPE (100 mg PPL; ACN/MeOH 1:1)	GC-MS	NA	3-5	NA	ND-678	(Quednow and Püttmann, 2008)
Surface water (river)	HHCB, AHTN	SPE (60 mg Oasis; ACN/DCM 1:1, DCM)	GC-MS	87-91	NA	30	81-314	(Moldovan, 2006)
Surface water (lake and river)	HHCB, AHTN	SPE (C_{18} disc; Acet/Hex 1:1) SBSE (PDMS; Acet/Hex 1:1 x 1 h[b])	GC-MS	NA	SPE: MDL: 1 SBSE: MDL: 66.7	SPE: MQL: 5 SBSE: MQL: 333	Lake: ND-83 River: 56-794	(Chase et al., 2012)
Surface water (river)	DPMI, ADBI, AHMI, ATII, HHCB, AHTN, MX, MM, MK	SBSE (PDMS; RT x 4 h[a]; 300 °C x 15 min[b])	TD-GC-MS	82-100	MDL: 0.02-0.2	MQL: 0.1-0.5	ND-16	(Ramírez et al., 2012)

Table 5 – Overview on analytical methods for determination of synthetic musks in aqueous matrices (cont.)

Matrix	Analytes	Extraction method	Analysis method	%Rec	LOD ($ng \cdot L^{-1}$)	LOQ ($ng \cdot L^{-1}$)	C ($ng \cdot L^{-1}$)	References
Surface water (river)	ADBI, AHMI, AHTN, ATII, DPMI, HHCB, MA, MK, MM, MX, MT, Helv, Glob, Rom, Thib, Musc, Amb and EB	SBSE-ATD (PDMS; 30 °C x 4 h[a]; 290 °C x 5 min[b])	RTL-GC-MS	NA	NA	5-80	ND-2544	(Arbulu et al., 2011)
Surface water (river)	DPMI, ADBI, AHMI, ATII, HHCB, AHTN, MX, MM, MK	SBSE (PDMS; 25 °C x 4 h[a]; 300 °C x 15 min[b])	TD-GC-MS	82-95	MDL: 0.2-0.3	MQL: 0.1-1.0	ND-26.2	(Ramírez et al., 2011)
Surface water (river) Sea water	ADBI, HHCB, AHTN, MK	SBSE-LD (PDMS, 25 °C x 4 h[a]; Hex x 30 min[b])	LVI-PTV-GC-MS	83-108	12-19	41-62	River: ND-236 Sea: ND-64	(Silva and Nogueira, 2010)
Surface water (river)	ADBI, AHMI, ATII, HHCB, AHTN	SPME (PMDS; RT x 90 min[a] 280 °C x 7 min[b])	GC-MS	64-117	0.4-9.6	1.3-32.0	ND-520	(Liu et al., 2010)
Surface water (river)	ADBI, AHMI, ATII, HHCB, AHTN	D-μ-SPE (3.2 mg ENVI-18; 337 °C x 4 min[b])	TD-GC-MS	74-90	0.5-1.0	1.2-3.0	HHCB,AHTN: 11-140 remnant: ND	(Chung et al., 2013)
Surface water (lake)	HHCB, AHTN	MEPS (1 mg C_8; EtAc)	LVI-PTV-GC-MS	57-78	45-54	NA	10-22	(Moeder et al., 2010)
Surface water (river)	HHCB, AHTN	MASE (LDPE; $CHCl_3$)	GC-MS	54-93	20	NA	HHCB: 50-350 AHTN: <25	(Einsle et al., 2006)
Surface water (estuary)	ADBI, AHMI, AHTN, ATII, DPMI, HHCB, MA, MK, MM, MX	MASE (LDPE; Hex)	LVI-PTV-GC-MS	64-138	3-8 MDL: 4-25	NA	HHCB: 41±7 remnant: NA	(Posada-Ureta et al., 2012)
Surface water (creek)	DPMI, ADBI, AHMI, ATII, HHCB, AHTN	UA-DLLME (ES: TCC; DS: IPA; US: 1 min)	GC-MS	70-95	0.2	0.6	ND-5.5	(Yang and Ding, 2012)
Surface water	MA, MX, MM, MT, MK	DLLME (ES: CF; DS: Acet)	GC-MS	87-93	4-33	14-109	NA	(López-Nogueroles et al., 2011)

Table 5 – Overview on analytical methods for determination of synthetic musks in aqueous matrices (cont.)

Matrix	Analytes	Extraction method	Analysis method	%Rec	LOD ($ng \cdot L^{-1}$)	LOQ ($ng \cdot L^{-1}$)	C ($ng \cdot L^{-1}$)	References
Surface water (river, lake) Sea water	ADBI, AHMI, ATII, HHCB, AHTN	DLLME (ES: TCC; DS: MeOH)	GC-MS	77-93	28-63	90-227	NA	(Panagiotou et al., 2009)
Surface water (river) Sea water Other (swimming pool)	DPMI, ADBI, AHMI, ATII, HHCB, AHTN, MX, MM, MK	USAEME (CF; 40 kHz, 100 W x 10 min)	GC-MS	80-103	6.0-29	20-97	River and sea water: ND Swimming pool water: HHCB,AHTN: 119-274 remnant: ND	(Regueiro et al., 2008)
Ground water	HHCB, AHTN	SPE (C_{18} disc; Acet/Hex 1:1) SBSE (PDMS; Acet/Hex 1:1 x 1 h[b])	GC-MS	NA	SPE: MDL: 1 SBSE: MDL: 66.7	SPE: MQL: 5 SBSE: MQL: 333	ND-72	(Chase et al., 2012)
Ground water	ADBI, AHMI, AHTN, ATII, DPMI, HHCB, MA, MK, MM, MX, MT, Helv, Glob, Rom, Thib, Musc, Amb and EB	SBSE-ATD (PDMS; 30 °C x 4 h[a]; 290 °C x 5 min[b])	RTL-GC-MS	NA	NA	5-80	ND-530	(Arbulu et al., 2011)
Wastewater	HHCB, AHTN, MK, MX	LLE (DCM, Hex)	GC-MS	82-92	10	20	HHCB: 2560-4520 (I) AHTN: 550-1210 (I) Total: 3690-7330 (I) 960-2690 (E)	(Lee et al., 2010)
Wastewater	HHCB, AHTN	LLE (Hex, DCM)	GC-MS	85-87	NA	10	HHCB: 1780-12700 (I) 2360-3730 (E) AHTN: 304-2590 (I) 495-807 (E)	(Reiner et al., 2007b)
Wastewater	HHCB, AHTN	LLE (Hex, DCM)	GC-MS	85-87	NA	10	43-7022 (I) 10-225 (E)	(Horii et al., 2007)

Table 5 – Overview on analytical methods for determination of synthetic musks in aqueous matrices (cont.)

Matrix	Analytes	Extraction method	Analysis method	%Rec	LOD ($ng \cdot L^{-1}$)	LOQ ($ng \cdot L^{-1}$)	C ($ng \cdot L^{-1}$)	References
Wastewater	DPMI, ADBI, AHMI, ATII, HHCB, AHTN, MA, MK, MM, MT, MX	LLE (Hex)	GC-MS	>80 (DPMI: 70%)	NA	0.4-4.0	ND-568 (I) ND-234 (E)	(Yang and Metcalfe, 2006)
Wastewater	HHCB, AHTN	SPE (PEP; ACN/DCM 1:1, DCM)	GC-MS	79-83	1	3.3	HHCB: 22.6-182.5 (I) AHTN: 2.2-19.3 (I)	(Ren et al., 2013)
Wastewater	HHCB, AHTN, AHMI, ADBI, MX, MK	SPE (500 mg HLB; EtAc/DCM/MeOH 2:2:1)	LVI-PTV-GC-MS	59-100	1.1-8.0	NA	HHCB: 987-2098 (E) AHTN: 55-159 (E) remnant: ND-20 (E)	(Sumner et al., 2010)
Wastewater	DPMI, ADBI, AHMI, ATII, HHCB, AHTN, MK, MX	SPE (C_{18} disc; Hex/DCM 1:1)	GC-MS	62-83	1-2	2-4	HHCB: 1467-3430 (I) 233-336 (E) AHTN,MK: 418-1043 (I) 43-101 (E) MX: BQ remnant: ND	(Zhang et al., 2008)
Wastewater (cosmetic plant)	DPMI, ADBI, AHMI, ATII, HHCB, AHTN	SPE (C_{18} disc; Hex/DCM 1:1)	GC-MS	57-107	60-120	NA	HHCB: 549680 (I) 32060 (E) remnant: 3730-68120 (I) ND-5970 (E)	(Chen et al., 2007)
Wastewater	DPMI, ADBI, AHMI, ATII, HHCB, AHTN	SPE (C_{18} disc; Hex, Hex/DCM 1:1)	GC-MS	60-84	10-20	NA	HHCB: 1010-3080 (I) 950-2050 (E) remnant: ND-340 (I) ND-140 (E)	(Zeng et al., 2007)
Wastewater	HHCB, AHTN, DPMI, ADBI, AHMI, ATII, MX, MK	SPE (C_{18} disc; Acet/Hex 1:1) SBSE (PDMS; Acet/Hex 1:1 x 1 h[b])	GC-MS	NA	SPE: MDL: 4 SBSE: MDL: 66.7	SPE: MQL: 40 SBSE: MQL: 333	HHCB: 4772-13399 (I) 2960-10525 (E) AHTN: 627-2337 (I) BQ-1754 (E) remnant: ND-950 (I) ND-421 (E)	(Chase et al., 2012)

Table 5 – Overview on analytical methods for determination of synthetic musks in aqueous matrices (cont.)

Matrix	Analytes	Extraction method	Analysis method	%Rec	LOD ($ng \cdot L^{-1}$)	LOQ ($ng \cdot L^{-1}$)	C ($ng \cdot L^{-1}$)	References
Wastewater	DPMI, ADBI, AHMI, ATII, HHCB, AHTN, MX, MM, MK	SBSE (PDMS; RT x 4 h[a]; 300 °C x 15 min[b])	TD-GC-MS	82-100	MDL: 0.02-0.2	MQL: 0.1-0.5	ND-2219 (I) ND-954 (E)	(Ramírez et al., 2012)
Wastewater	ADBI, AHMI, AHTN, ATII, DPMI, HHCB, MA, MK, MM, MX, MT, Helv, Glob, Rom, Thib, Musc, Amb and EB	SBSE-ATD (PDMS; 30 °C x 4 h[a]; 290 °C x 5 min[b])	RTL-GC-MS	NA	NA	5-80	HHCB: 900-3568 (I) 689-3021 (E) DPMI: 70-530 (I) 100-400 (E) remnant: ND-91 (I) ND-80 (E)	(Arbulu et al., 2011)
Wastewater	DPMI, ADBI, AHMI, ATII, HHCB, AHTN, MX, MM, MK	SBSE (PDMS; 25 °C x 4 h[a]; 300 °C x 15 min[b])	TD-GC-MS	82-95	MDL: 0.2-0.3	MQL: 0.1-1.0	HHCB: 476-2069 (I) 233-1432 (E) remnant: ND-87.7 (I) ND-126 (E)	(Ramírez et al., 2011)
Wastewater	ADBI, HHCB, AHTN, MK	SBSE-LD (PDMS; 25 °C x 4 h[a]; Hex x 30 min[b])	LVI-PTV-GC-MS	83-108	12-19	41-62	HHCB: 4670 (I); 1270 (E) ATHN: 1290 (I); 259 (E) remnant: ND	(Silva and Nogueira, 2010)
Wastewater	DPMI, ADBI, AHMI, ATII, HHCB, AHTN	MWA-HS-SPME (PDMS-DVB; 180 W x 4 min[a]; 270 °C x 2 min[b])	GC-MS	64-89	0.05-0.1	0.2-0.25	ND-37.3 (E)	(Wang and Ding, 2009)
Wastewater	HHCB, AHTN	MEPS (1 mg C_{18}; EtAc)	LVI-PTV-GC-MS	78-109	37-42	NA	110-1374 (E)	(Moeder et al., 2010)
Wastewater	ADBI, AHMI, AHTN, ATII, DPMI, HHCB, MA, MK, MM, MX	MASE (LDPE; Hex)	LVI-PTV-GC-MS	47-126	3-8 MDL: 4-25	NA	24-295 (I) 82-259 (E)	(Posada-Ureta et al., 2012)
Wastewater	DPMI, ADBI, AHMI, ATII, HHCB, AHTN	UA-DLLME (ES: TCC; DS: IPA; US: 1 min)	GC-MS	75-90	0.2	0.6	ND-42	(Yang and Ding, 2012)
Wastewater	MA, MX, MM, MT, MK	DLLME (ES: CF; DS: acet)	GC-MS	87-93	4-33	93-116	NA	(López-Nogueroles et al., 2011)

Table 5 – Overview on analytical methods for determination of synthetic musks in aqueous matrices (cont.)

Matrix	Analytes	Extraction method	Analysis method	%Rec	LOD ($ng \cdot L^{-1}$)	LOQ ($ng \cdot L^{-1}$)	C ($ng \cdot L^{-1}$)	References
Wastewater	DPMI, ADBI, AHMI, ATII, HHCB, AHTN, MX, MM, MK	USAEME (CF; 40 kHz, 100 W x 10 min)	GC-MS	81-114	6.0-29	20-97	HHCB: 2893 (I); 718 (E) AHTN: 334 (I); 99 (E) remnant: ND-113 (I) ND-31 (E)	(Regueiro et al., 2008)

NA – not available; ND – not detected; BQ – below quantification limit; MDL – method detection limit; MQL – method quantification limit;
ATD - automated thermal desorption; LD – liquid desorption; UA – ultrasound-assisted; MWA – microwave-assisted;
LVI – large volume injection; PTV – programmed temperature vaporiser; TD – thermal desorption; RTL - retention time locking;
ES - extraction solvent; DS - disperser solvent; [a] - adsorption; [b] – desorption; I – influent; E – effluent; RT – room temperature
Helv – Helvetolide; Glob – Globalide; Rom – Romandolide; Thib – Thibetolide; Musc – Muscone; Amb – Ambrettolide; EB - Ethylene brassylate
Solvent abbreviations: Acet - acetone; Hex - hexane; IPA – isopropyl alcohol; TCC – carbon tetrachloride; CF – chloroform; EtAc - ethyl acetate; DCM – dichloromethane; MeOH – methanol; ACN – acetonitrile

3 Technical Description

3.1 Reagents and materials

Twelve musks (five nitro, five polycyclic, and two macrocyclic) were included in this study. Solid standards of synthetic polycyclic musks cashmeran, celestolide, galaxolide, phantolide, and tonalide were obtained from LGC Standards (Barcelona, Spain) with 99% purity, except for galaxolide, which contains approximately 25% of diethyl phthalate. Musk tibetene and musk moskene were also purchased as 10 $mg \cdot L^{-1}$ solution in cyclohexane from LGC Standards. Musk ambrette and musk ketone were purchased as solid standards from Dr. Ehrenstorfer (Augsburg, Germany) with 99 and 98% purity, respectively. Musk xylene was obtained from Sigma-Aldrich (St. Louis, MO, USA) as 100 $mg \cdot L^{-1}$ solution in ACN and with ≥95% purity. Exaltolide and ethylene brassylate were also purchased from Sigma-Aldrich with ≥99% and ≥95% purity, respectively. Surrogate standards musk xylene-d_{15} and tonalide-d_3 were purchased from Dr. Ehrenstorfer (Augsburg, Germany) as 100 $mg \cdot L^{-1}$ solutions in acetone and iso-octane, respectively.

Acetone, acetonitrile, methanol, chlorobenzene, chloroform, tetrachloroethylene and dichloromethane were purchased from VWR BDH Prolabo (Fontenay-sous-Bois, France), carbon tetrachloride was obtained from Riedel-de Haën (Seelze-Hannover, Germany) and ethanol (96% v/v) was obtained from Panreac (Barcelona, Spain). Acetone, ethanol, chlorobenzene and chloroform were analytical grade, while acetonitrile and methanol were HPLC grade, tetrachloroethylene and carbon tetrachloride were spectroscopy grade and dichloromethane was pesticide residue analysis grade. Analytical grade sodium chloride, used to adjust the ionic strength, was purchased from Merck (Darmstadt, Germany).

3.2 Standards preparation

For each polycyclic musk, individual stock solutions were prepared in cyclohexane at 15 $g \cdot L^{-1}$. Individual stock solutions of exaltolide and ethylene brassylate were prepared at 10 $g \cdot L^{-1}$ in cyclohexane. Musk ambrette and musk ketone were prepared at 10 $g \cdot L^{-1}$ each, also in cyclohexane. A 10 $mg \cdot L^{-1}$ intermediate stock solution containing all polycyclic and macrocyclic musks, and musk ambrette and ketone was prepared by diluting appropriate amounts in ACN. The final mixed stock solution at 4 $mg \cdot L^{-1}$ was prepared by first evaporating an appropriate amount of musk tibetene and moskene solutions under a gentle stream of nitrogen. This step was followed by the addition of the necessary amounts of the

former stock solution and of the musk xylene standard and makeup with ACN. A mixed solution of surrogate standards musk xylene-d_{15} and tonalide-d_3 was prepared at 10 mg·L^{-1}, from which a 222 µg·L^{-1} solution was prepared. All solutions were stored and preserved at −20 °C, protected from the light.

3.3 Samples

To evaluate the accuracy and applicability of the proposed method, the extraction of musks was performed in different water samples (tap, river and sea waters and wastewaters). Sea water was collected from Matosinhos and river water was collected from river Leça (Matosinhos). Influent and effluent wastewater was collected from a WWTP (Parada, Maia) and each was composed of various samples taken out during a 24 hours period. All samples except for tap water were store in the dark at -20 °C until they were processed. Tap water samples were taken from our laboratory.

3.4 Sample extraction

A 6 mL aqueous sample was placed in a 15 mL screw-capped polyethylene centrifuge tube with conical bottom containing 0.22 g of sodium chloride (3.5% m/m) and 20 µL of a 222 µg·L^{-1} solution of musk xylene-d_{15} and tonalide-d_3 (as surrogate standards) were added (final concentration of 0.75 µg·L^{-1}). A mixture of 880 µL of ACN (as disperser solvent) and 80 µL of chloroform (as extraction solvent) was rapidly injected into the water sample with a syringe. A cloudy suspension was formed and the dispersion was ultrasonicated for 2 min in an ultrasonic bath J.P. Selecta (Barcelona, Spain). Phase separation was then performed by centrifugation at 4000 rpm for 10 min, and the sedimented phase (65±6 µL) was collected with a 100 µL syringe and transferred into a 100 µL insert placed inside a 1.5 mL amber vial, which was then analysed by GC-MS.

3.5 Instrumental analysis

The sedimented phase was analyzed using a Varian Ion Trap GC–MS system (Walnut Creek, CA, USA), equipped with a 450-GC gas chromatograph, a 240-MS ion trap mass spectrometer, a CP-1177 split/splitless injector, a waveboard for multiple MS analysis (MS^n) and an autosampler model CP-8410. The mass spectrometer was operated in the electron ionization (EI) mode (70 eV) and the system was controlled by Varian MS workstation v. 6.9.3 software. The separation was obtained at a constant flow of 1.0 mL·min^{-1} of helium with a purity of 99.999%, in a Varian CP-Sil 8 CB capillary column (50 m × 0.25 mm

id, 0.12 µm). The oven temperature was programmed as follows: 60 °C hold for 1 min, raised at 6 °C·min^{-1} to 150°C (hold for 10 min), then 6 °C·min^{-1} to 225 °C and finally 20 °C·min^{-1} to 300 °C (hold for 2.5 min). Injection (1 µL) was in splitless mode, with the split valve closed for 5 min. Temperatures of manifold, ion trap, injector and transfer line were maintained at 50, 250, 250 and 250 °C, respectively. The filament emission current was 50 µA. For quantitative analysis of target compounds, selected ion storage (SIS) mode was applied. Table 6 shows the retention times and the quantifier and qualifier ions used for the SIS detection.

Table 6 - Quantification and qualifier ions of each individual compound studied in the GC-MS and respective retention times.

Compound	Retention time (min)	Quantifier Ion (m/z)	Qualifier Ion (m/z)
Cashmeran (DPMI)	19.850	191	135, 163
Celestolide (ADBI)	29.212	229	173, 244
Phantolide (AHMI)	30.675	229	173, 187
Exaltolide (EXA)	32.765	67	55, 83
Musk ambrette (MA)	32.926	253	91, 77
Musk xylene-d_{15}	33.284	294	122, 154
Galaxolide (HHCB)	33.400	243	157, 213
Musk xylene (MX)	33.657	282	115, 128
Musk tonalide-d_3	33.689	246	128, 160
Tonalide (AHTN)	33.751	243	128, 159
Musk moskene (MM)	34.296	263	115, 128
Musk tibetene (MT)	35.464	251	115, 128
Musk ketone (MK)	36.512	279	128, 160
Ethylene Brassylate (EB)	37.128	227	98, 125

4 Results and Discussion

In order to evaluate the main factors affecting the efficiency of DLLME method, and to obtain the optimum experimental extraction conditions a design of experiments (Appendix 1) with two steps (screening and optimization) was used. For this purpose JMP 11.1.1 (SAS Institute Inc., Cary, USA) statistical software was used to generate the experimental matrix and to evaluate the results.

4.1 Screening Design

Several factors can affect the DLLME extraction and screening design's objective is to determine the main factors affecting the extraction. Seven factors were selected: volume of the extraction solvent (V_E), volume of the disperser solvent (V_D), sample volume (V_S), extraction time (t_E), ionic strength (% NaCl), extraction solvent (S_E) and disperser solvent (S_D). The extractions were tested using a concentration of each musk of 1 $\mu g \cdot L^{-1}$.

The investigated values for each factor are shown in Table 7. In this work, the extraction time was defined as the time the sample underwent ultrasonic treatment. The solvents were selected based on the properties that an extraction or disperser solvent should have, as discussed in the previous sections. Carbon tetrachloride (TCC), tetrachloroethylene (TCE), chlorobenzene (CB) and chloroform (CF) were selected as extraction solvents and acetone (Acet), acetonitrile (ACN), ethanol (EtOH) and methanol (MeOH) were selected as disperser solvents. Each combination of extraction solvent and disperser solvent was previously tested in order to observe if a separate phase would deposit at the bottom of the tube. For these preliminary tests, dichloromethane (DCM) was also included as an extraction solvent, but the formation of emulsion was not observed with any of the disperser solvents tested, so it was excluded from further experiments.

Table 7 - Factors and respective values for the screening design.

Factors	Values	
	Low (-1)	High (+1)
V_E - Volume of the extraction solvent (µL)	60	100
V_D - Volume of the disperser solvent (µL)	500	1000
V_S - Sample volume (mL)	5	13
t_E - Extraction time (min)	0	10
% NaCl (m/m)	0	10
S_E - Extraction solvent	TCC TCE	CB CF
S_D - Disperser solvent	Acet ACN	EtOH MeOH

The experimental screening design consisted of a total of sixteen experiences (Appendix 2). The recovery of each musk component analysed was selected as a response, so the design had a total of twelve responses. All responses were adjusted to a model with a R^2 superior than 0.932. The main effects were determined by the probability (*F*-probability) calculated for each factor. The probability values for each response are represented in Figure 5.

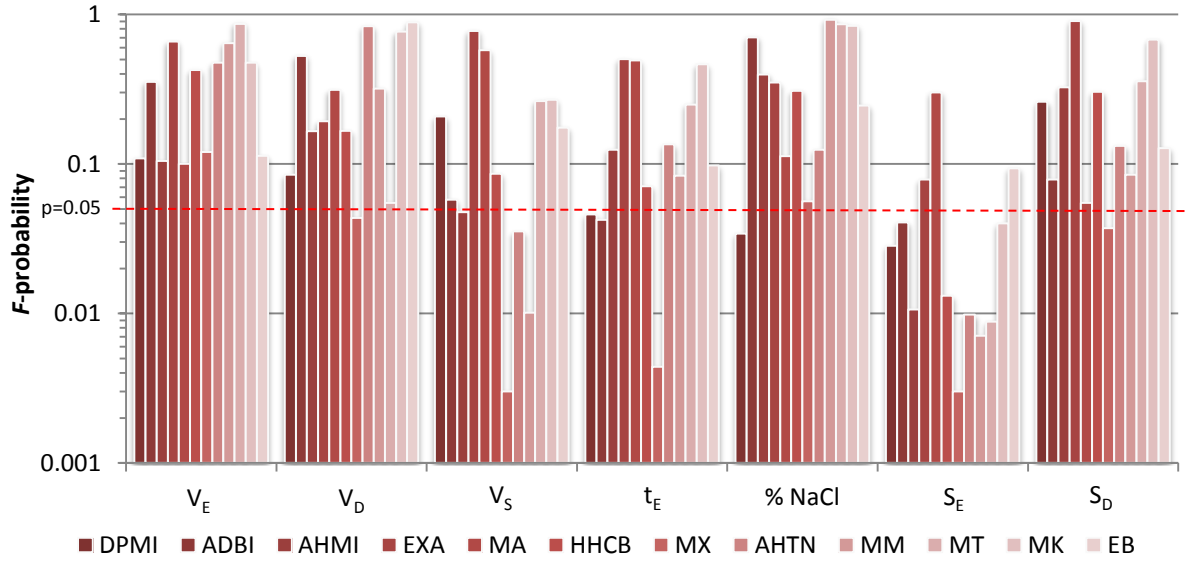

Figure 5 - *F*-probability obtained with screening design.

A *F*-probability ≤0.05 represents a significant effect on the response, efficiency, whereas 0.05 < *F*-probability ≤ 0.10 indicates a relative effect on the extraction. As can be seen, the volume of extraction solvent is the only factor that doesn't affect significantly or relatively any of the responses. The type and volume of disperser solvent only have a strong effect on the recovery of MX, but they also have a relative effect on a few other responses. The percentage of NaCl has a significant effect on the recovery of DPMI, and a relative effect on the recovery of MX. The extraction time and sample volume have a significant effect on three and four responses, respectively and a relative effect on some other responses. The type of extraction solvent presents the lowest *F*-probability values, evidently being the factor with stronger effect on most responses. It shows a significant effect on most responses except for three, two of which show a relative effect, being the recovery of MA the only response unaffected by this factor.

Among the factors identified, two are discrete variables (type of extraction and disperser solvents) and must be defined prior to the optimisation using CCD. Since the volume of the extraction solvent is not a significant factor for neither response, it should not be included as a factor for the optimisation and must be defined as well. In order to define these variables, desirability function was used (described in Appendix 1). The

desirability function was maximized to achieve a target recovery of 100%, with an acceptance range of 80 to 120%.

The optimal desirability was obtained for chloroform and ACN as extraction and disperser solvents, respectively, and around 80 µL of extraction solvent. A possible explanation for the better results with CF might be related to the dipole moment. CF is slightly less polar than CB (1.15 D and 1.54 D, respectively) (LSU Macromolecular Studies Group, 2013), which allows a better interaction between solvent molecules and slightly lipophilic compounds, such as synthetic musks. On the other hand, TCE and TCC have no dipole moment, which might not be as favourable, since synthetic musks are not completely polar compounds. CF also has the lowest water interfacial tension among the four solvents (CF: 0.0328 N/m; CB: 0.0374 N/m; TCE: 0.0444 N/m; TCC: 0.0450 N/m (National Oceanic and Atmospheric Administration, 1999)), allowing a higher efficiency in emulsion formation (Regueiro et al., 2008).

These three factors were defined, while the other four factors were further evaluated in the optimization step.

4.2 Central Composite Design

For the optimization of the method according to the chosen factors, central composite design (CCD) was applied (Table 8). A total of thirty experimental runs were done, including six assays that were performed in the centre of the cubic domain. The conditions set in each experiment are listed in Appendix 3, as well as the responses (recovery values) based on the experimental runs. Runs 16 and 19 were excluded from the design due to the lack of sedimentation of enough volume to be collected and analysed.

Table 8 - Experimental range and levels of process variables for the CCD.

Factors	Coded levels (x_i)				
	-1.483 (a)	-1	0	1	+1.483 (A)
X_1 - Sample volume (mL)	4.5	6.0	9.0	12.0	13.5
X_2 - Volume of the disperser solvent (µL)	400	500	700	900	1000
X_3 - Extraction time (min)	0	2	6	10	12
X_4 - *% NaCl (%m/m)*	0.0	2.0	6.0	10.0	12.0

Using the response surface methodology a mathematical relationship between dependent and independent variables was determined. The experimental data were fitted to a second-order polynomial equation and the coefficients of the quadratic model were calculated by a least-square regression analysis. The comparison between the model prediction and the experimental response is given in parities plots, which are presented in Appendix 4. Table 9 shows the second-order equations (significant variables in bold) and the model suitability using the ANOVA test.

Nitromusks present lower R^2 values, from 0.731 to 0.844, while polycyclic and macrocyclic musks present values above 0.889. The large R^2 values indicate a good relationship between the experimental data and the fitted model, indicating that the polycyclic and macrocyclic musks models are better adjusted than the nitro musks models.

Table 9 - Second-order polynomial equation and model suitability parameters for the response functions.

	R^2	*F*-ratio	Prob > F	LOF Prob > F
DPMI	$y = \mathbf{107.51} + \mathbf{2.45}x_1 - 0.73x_2 + 0.87x_3 - \mathbf{3.32}x_4 + \mathbf{5.51}x_1x_2 - \mathbf{5.32}x_1x_3 - \mathbf{2.82}x_2x_3 - \mathbf{3.62}x_1x_4 - \mathbf{3.39}x_2x_4 + \mathbf{7.01}x_3x_4 - 0.80{x_1}^2 - 1.59{x_2}^2 - 1.12{x_3}^2 + 1.55{x_4}^2$			
	0.906	8.99	0.0002	0.8801
ADBI	$y = \mathbf{100.95} - \mathbf{3.28}x_1 - 0.94x_2 + 1.52x_3 + \mathbf{6.60}x_4 + \mathbf{2.91}x_1x_2 - 0.68x_1x_3 - \mathbf{3.69}x_2x_3 + 1.49x_1x_4 - \mathbf{3.36}x_2x_4 + \mathbf{2.53}x_3x_4 - \mathbf{2.42}{x_1}^2 - 0.46{x_2}^2 + \mathbf{3.22}{x_3}^2 - 0.32{x_4}^2$			
	0.923	11.08	<0.0001	0.9808
AHMI	$y = \mathbf{103.10} - \mathbf{2.32}x_1 - 1.05x_2 + 0.72x_3 + \mathbf{5.02}x_4 + 1.38x_1x_2 + 0.04x_1x_3 - \mathbf{3.22}x_2x_3 + \mathbf{2.25}x_1x_4 - 1.27x_2x_4 + \mathbf{2.08}x_3x_4 - \mathbf{3.37}{x_1}^2 - 1.00{x_2}^2 + \mathbf{2.25}{x_3}^2 + 2.41{x_4}^2$			
	0.899	8.25	0.0003	0.2460
EXA	$y = \mathbf{103.92} - 2.30x_1 + 0.61x_2 + \mathbf{4.50}x_3 + \mathbf{8.83}x_4 + \mathbf{3.74}x_1x_2 - 0.98x_1x_3 - 2.34x_2x_3 + \mathbf{3.75}x_1x_4 - \mathbf{5.09}x_2x_4 + 0.75x_3x_4 + \mathbf{3.61}{x_1}^2 + \mathbf{3.57}{x_2}^2 + \mathbf{8.74}{x_3}^2 - \mathbf{12.69}{x_4}^2$			
	0.890	7.49	0.0004	0.2005
MA	$y = \mathbf{115.77} + \mathbf{8.71}x_1 + 2.92x_2 + 2.77x_3 + \mathbf{7.55}x_4 + \mathbf{5.70}x_1x_2 + 4.59x_1x_3 + 1.47x_2x_3 + 1.80x_1x_4 - 0.70x_2x_4 - 4.13x_3x_4 - 3.96{x_1}^2 - 4.77{x_2}^2 + 1.05{x_3}^26 + 6.34{x_4}^2$			
	0.815	4.08	0.0078	0.0336
HHCB	$y = \mathbf{96.77} - 0.09x_1 + 0.62x_2 - 0.29x_3 + \mathbf{1.97}x_4 - \mathbf{1.38}x_1x_2 - 0.28x_1x_3 - \mathbf{3.40}x_2x_3 - \mathbf{1.22}x_1x_4 - \mathbf{1.35}x_2x_4 + \mathbf{1.28}x_3x_4 - \mathbf{2.38}{x_1}^2 - 1.16{x_2}^2 + \mathbf{1.67}{x_3}^2 + \mathbf{3.31}{x_4}^2$			
	0.913	9.74	0.0001	0.2003
MX	$y = \mathbf{105.10} + \mathbf{6.18}x_1 - 3.07x_2 - 2.29x_3 + 0.74x_4 + 1.72x_1x_2 + 0.78x_1x_3 + 3.11x_2x_3 + 0.95x_1x_4 + 0.69x_2x_4 - 3.69x_3x_4 - 0.64{x_1}^2 - 0.44{x_2}^2 - 4.73{x_3}^2 + 4.34{x_4}^2$			
	0.731	2.52	0.0521	0.0672
AHTN	$y = \mathbf{102.44} - 3.54x_1 + 1.04x_2 + \mathbf{4.36}x_3 + \mathbf{15.86}x_4 + 1.27x_1x_2 - 4.35x_1x_3 - 3.90x_2x_3 + \mathbf{4.66}x_1x_4 - 0.28x_2x_4 + 3.97x_3x_4 - 2.30{x_1}^2 + \mathbf{6.70}{x_2}^2 + \mathbf{9.45}{x_3}^2 - \mathbf{8.86}{x_4}^2$			
	0.889	7.47	0.0004	0.2925
MM	$y = \mathbf{103.98} + \mathbf{6.87}x_1 - \mathbf{3.21}x_2 - 1.46x_3 + 0.55x_4 + 1.92x_1x_2 + 0.64x_1x_3 + 1.20x_2x_3 + 2.39x_1x_4 + 1.92x_2x_4 - \mathbf{5.21}x_3x_4 + 2.94{x_1}^2 - 1.62{x_2}^2 - 0.91{x_3}^2 - 0.90{x_4}^2$			
	0.844	5.02	0.0031	0.0804
MT	$y = \mathbf{110.18} + \mathbf{3.26}x_1 - 0.98x_2 + 0.23x_3 + 1.03x_4 + 0.07x_1x_2 + 2.01x_1x_3 + \mathbf{4.08}x_2x_3 + 1.46x_1x_4 + 0.78x_2x_4 - 1.18x_3x_4 - 1.15{x_1}^2 - 3.16{x_2}^2 - 1.77{x_3}^2 + \mathbf{5.52}{x_4}^2$			
	0.750	2.79	0.0365	0.3178
MK	$y = 12.85 - 4.93x_1 + 9.27x_2 - 12.20x_3 - \mathbf{22.10}x_4 + 1.03x_1x_2 - 1.47x_1x_3 + 0.20x_2x_3 - \mathbf{21.58}x_1x_4 + 12.93x_2x_4 - 10.63x_3x_4 + \mathbf{30.13}{x_1}^2 + \mathbf{26.80}{x_2}^2 + 24.30{x_3}^2 - 10.41{x_4}^2$			
	0.787	3.43	0.0164	-
EB	$y = \mathbf{20.96} + 3.53x_1 + 0.60x_2 + 3.25x_3 + 3.06x_4 - 0.93x_1x_2 + 4.72x_1x_3 - 2.45x_2x_3 - 2.14x_1x_4 - 4.69x_2x_4 - 1.89x_3x_4 + \mathbf{18.30}{x_1}^2 + \mathbf{29.77}{x_2}^2 + \mathbf{31.41}{x_3}^2 + 9.72{x_4}^2$			
	0.927	11.84	<0.0001	0.0001

All models show an *F*-probability < 0.05, except for MX (*F*-probability = 0.0521), implying that variations that occur in the responses should be associated with the model, rather than with the experimental error. The lack of fit (LOF) was not significant (p > 0.05) for most models, excluding the models for MA and EB, meaning that these two models are not as well fitted as the rest of the models.

The significant variables and interactions were identified by the Student's *t*-test (Figure 6 and Figure 7). If the Prob > |t| is less than 0.05, a variable is considered very significant and if it is between 0.05 and 0.10, it is considered relatively significant (95% confidence level). As can be observed, all variables and interactions have a significant effect on at least of one of the responses. When it comes to the main effects, the sample volume (X_1) and the percentage of NaCl (X_4) are the variables that significantly affect a larger number of responses, while the volume of disperser solvent (X_2) only significantly affects the recovery of MM. As for the quadratic effects, the variables that significantly affect a larger number of responses are the sample volume (X_1^2), the extraction time (X_3^2) and the percentage of NaCl (X_4^2). All interactions affect at least four responses in a significant way, except for the interaction between the sample volume and the extraction time (X_1X_3), which is only significant for the recovery of DPMI. It is also noticeable that nitro musks are generally affected by less variables and interactions than the other synthetic musks classes.

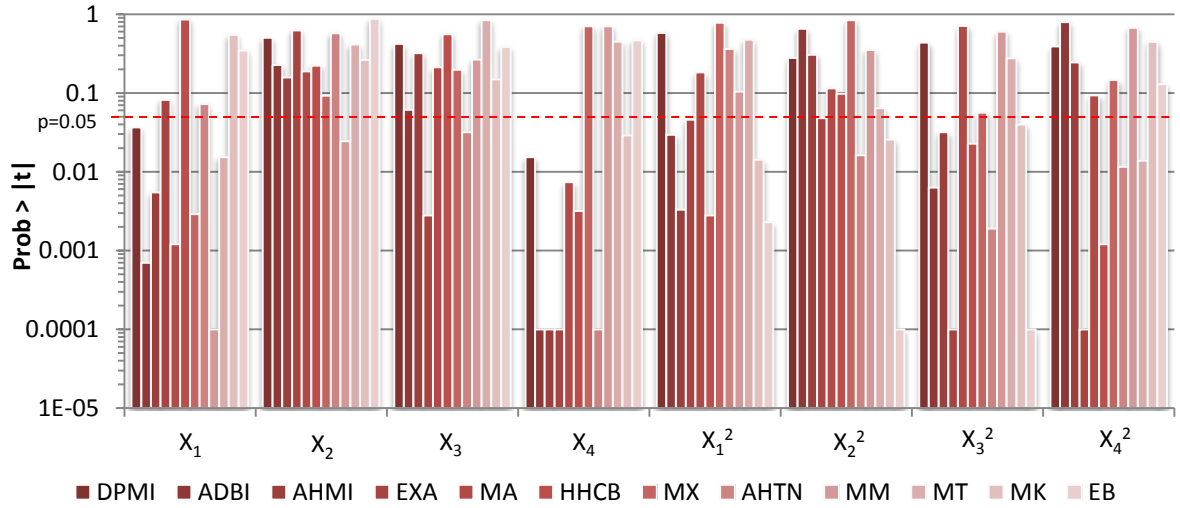

Figure 6 - Results from the Student's *t*-test for the main and quadratic effects.

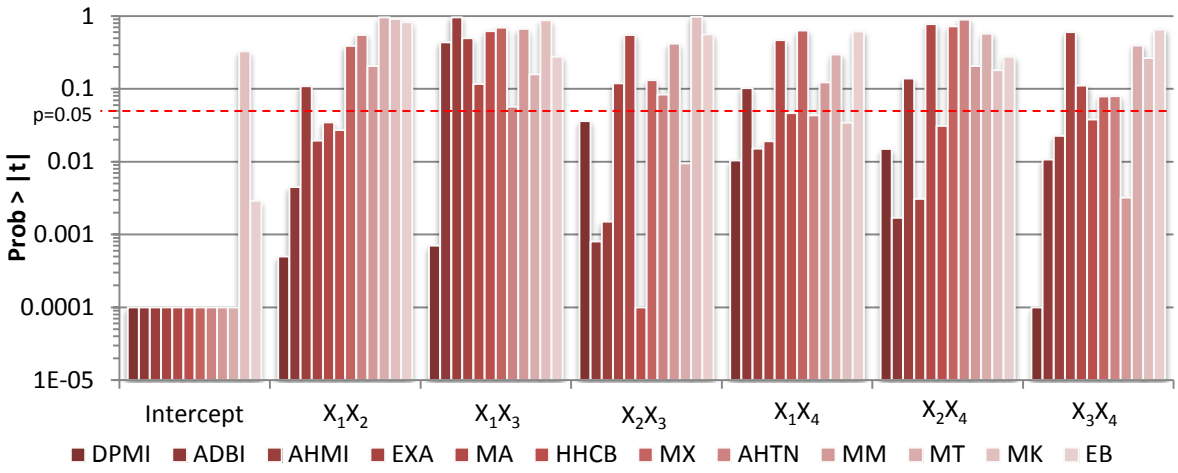

Figure 7 - Results from the Student's *t*-test for the intercept and the interactions.

The software allows the visualization of three-dimensional response surface and two-dimensional contour plots of the predicted response. As an example, the three-dimensional response surface plot for tonalide (AHTN) is represented in Figure 8, considering the two most significant variables (X_3 and X_4 in this case) and shows the response surface obtained by plotting the recovery vs. the extraction time and the percentage of NaCl , while the other two variables are fixed at their optimal (discussed further ahead). The interception with the surface plan % Rec = 100% is also shown in the plot, since it is the objective value. The respective contour plot is represented in Figure 9. The response surface plots for the rest of the compounds are in Appendix 5.

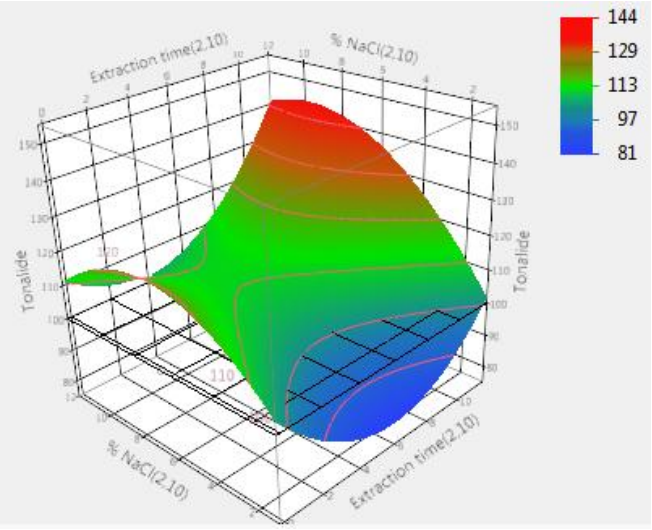

Figure 8 - Response surface plot, recovery vs. the extraction time and the percentage of NaCl, for AHTN (1 µg·L^{-1} of AHTN, 80 µL of CF, 880 µL of ACN, 6 mL of sample volume).

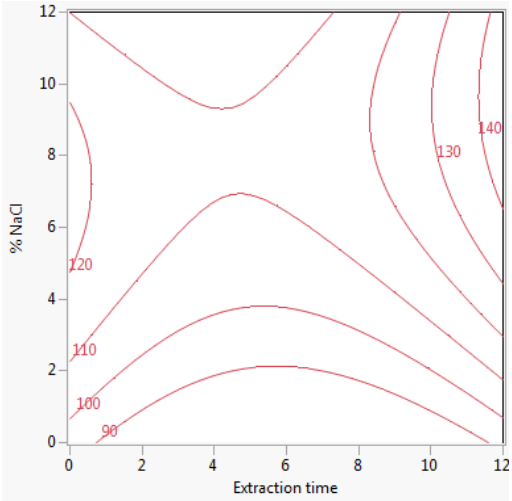

Figure 9 - Contour plot for AHTN (1 µg·L^{-1} of AHTN, 80 µL of CF, 880 µL of ACN, 6 mL of sample volume).

This kind of graphics allows a better understanding of how the variables influence the response. When working with a small number of responses, these graphics could be enough to determine the optimal conditions. However, since in this work there are twelve responses that should be optimized all at the same time, the desirability function was once again used, to predict the optimal conditions. The desirability function was maximized to achieve a target recovery of 100%, with an acceptance range of 80 to 120%. The optimal conditions obtained are listed in Table 10.

Table 10 - Optimal conditions obtained with the desirability function.

Sample volume (X_1; mL)	Volume of disperser solvent (X_2; µL)	Extraction time (X_3; min)	% NaCl (X_4)
6.0	881	2	3.5

The high volume of disperser solvent can be attributed to the fact that a larger amount of disperser solvent allows a more homogenous cloudy solution, permitting the extractant to be more efficiently dispersed in the aqueous solution. It was observed that the longer the sample was under ultrasonic treatment, the lower the volume of chloroform sedimented. This indicated that the ultrasounds are promoting the solubilisation of CF in water, which is not favourable to the extraction, so a low extraction time is expected. Since one of the principles of DLLME is that the solutes migrate to the extraction solvent almost instantly, it reinforces the suggestion that a low extraction time is optimal. It was expected that the addition of some salt would have a positive effect on the extraction, due to the salting out effect.

The recovery values predicted by the models at the optimal point, and the respective confidence intervals are listed in Table 11.

Table 11 - Recovery values at the optimal point (80 µL of CF, 880 µL of ACN, 2 minutes of extraction time, 3,5% of NaCl).

Compound	% Rec	Confidence Interval	
		Lower limit	Upper limit
DPMI	99%	93%	106%
ADBI	102%	98%	107%
AHMI	104%	100%	109%
EXA	110%	103%	118%
MA	94%	81%	108%
HHCB	101%	98%	104%
MX	88%	78%	99%
AHTN	105%	94%	117%
MM	91%	83%	99%
MT	100%	93%	107%
MK	94%	44%	143%
EB	97%	75%	120%

The prediction profiler at the optimal conditions, where the desirability function is represented, is displayed in Appendix 6.

4.3 Method validation

Under the selected conditions, the proposed method was evaluated in terms of linear range, correlation coefficient, limit of detection (LOD) and quantification (LOQ), precision and accuracy. Linearity was tested by the injection of the sedimented volume of extracted aqueous standard samples containing all the synthetic musks analysed at concentration levels ranging from 0.005 to 1.50 $\mu g \cdot L^{-1}$. The limits of detection and quantification were calculated based on the signal noise ratio (S/N) of individual peaks, assuming a ratio 3:1 to LODs and 10:1 for the LOQs. Precision was evaluated by a repeatability of extracted aqueous standards at three different concentration levels (0.25, 1.00 and 1.5 $\mu g \cdot L^{-1}$). The results are presented in Table 12.

Table 12 - Linearity results, detection and quantification limits and precision (% RSD) for each musk compound studied.

Compound	Linearity range ($\mu g \cdot L^{-1}$)	R^2	LOD ($ng \cdot L^{-1}$)	LOQ ($ng \cdot L^{-1}$)	% RSD (n=3)		
					0.25 $\mu g \cdot L^{-1}$	1.00 $\mu g \cdot L^{-1}$	1.50 $\mu g \cdot L^{-1}$
DPMI	0.05-1.50	0.9963	50	167	3.2	8.8	6.3
ADBI	0.005-1.50	0.9976	2	6	6.5	3.3	3.0
AHMI	0.005-1.50	0.9987	2	6	2.3	1.3	4.5
EXA	0.005-1.50	0.9993	3	10	1.5	7.2	4.0
MA	0.25-1.50	0.9973	83	278	18.2	9.4	5.6
HHCB	0.005-1.50	0.9966	0.004	0.01	6.9	11.1	1.0
MX	0.05-1.50	0.9986	36	119	13.5	11.9	9.6
AHTN	0.01-1.50	0.9942	8	25	5.2	3.1	1.4
MM	0.05-1.50	0.9960	50	167	2.4	9.5	1.8
MT	0.01-1.50	0.9964	63	208	8.0	10.5	2.5
MK	0.01-1.50	0.9982	2	8	6.2	1.4	7.6
EB	0.10-1.50	0.9949	4	13	4.9	7.6	14.2

R^2 – determination coefficient; n - number of replicates; LOD – limit of detection; LOQ – limit of quantification; % RSD – relative standard deviation percentage

All compounds analysed showed a linear behaviour, but some compounds were not detected in the lower concentrations, therefore having higher bottom limits for the linear range of calibration curves. The calibration curves are presented in Appendix 7. Concentration was correlated with the response factor ($RF=A_{compound}/A_{surrogate}$), where musk xylene-$d_{15}$ was used as the surrogate standard for nitro musks and tonalide-d_3 was used as the surrogate standard for polycyclic and macrocyclic musks. All calibration curves have relative standard deviation of the slope (s_a/a) bellow 5% and a correlation coefficient (R) superior to 0.995. However not all calibration curves check the parameter that states that

the intercept should contain the origin ($b-s_b < 0 < b+s_b$), namely the calibration curves for EXA, HHCB, MX, MM, MK and EB.

The LODs of polycyclic and macrocyclic musks ranged between 2 and 8 $ng \cdot L^{-1}$ and the LOQs ranged between 6 and 25 $ng \cdot L^{-1}$, except for HHCB and DPMI. HHCB exhibited much lower LOD and LOQ values of 0.004 $ng \cdot L^{-1}$ and 0.01 $ng \cdot L^{-1}$, respectively. On the contrary, higher LOD and LOQ values of 50 $ng \cdot L^{-1}$ and 167 $ng \cdot L^{-1}$ were obtained for DPMI. Nitro musks presented LOD and LOQ values similar to DPMI, ranging from 36 to 83 $ng \cdot L^{-1}$ and 119 to 278 $ng \cdot L^{-1}$, respectively, except for MK, which displayed values of 2 $ng \cdot L^{-1}$ and 8 $ng \cdot L^{-1}$, respectively. Comparing to the values found in literature when DLLME was used, the LODs of nitro musks were in the same order of magnitude to those obtained by López-Nogueroles et al. (2011), who applied DLLME to nitro musks. Panagiotou et al. (2009) and Yang and Ding (2012) used DLLME for the detection of polycyclic musks. The LODs obtained in this work were inferior to those obtained by the former, but superior to those obtained by latter, except for HHCB. The LOD and LOQ of HHCB were much lower than those obtained by any other extraction method found in literature. The relative standard deviation (RSD) values ranged from 1.0 to 18.2%, showing a satisfactory precision of the extraction methodology for all musks compounds analysed.

The precision on different water matrices including tap, river and sea water and wastewaters (influent and effluent), was also evaluated. No NaCl was added to sea water, since the average sea water already contains 3.5% of salt. Relative standard deviation (% RSD) values are presented in Table 13.

Table 13 - Precision (% RSD) in water samples at different spiked levels

	% RSD (n=3)									
	Tap water		Sea water		River water		Influent		Effluent	
Compound	0.25 $\mu g \cdot L^{-1}$	1.00 $\mu g \cdot L^{-1}$	0.25 $\mu g \cdot L^{-1}$	1.00 $\mu g \cdot L^{-1}$	0.25 $\mu g \cdot L^{-1}$	1.00 $\mu g \cdot L^{-1}$	0.25 $\mu g \cdot L^{-1}$	1.00 $\mu g \cdot L^{-1}$	0.25 $\mu g \cdot L^{-1}$	1.00 $\mu g \cdot L^{-1}$
DPMI	1.9	3.5	9.9	4.4	6.1	2.8	8.0	1.2	3.8	2.0
ADBI	6.4	5.8	3.8	4.8	7.3	4.3	4.8	3.6	5.1	1.0
AHMI	1.2	5.2	1.1	6.5	14.0	2.3	3.9	1.9	2.9	1.4
EXA	7.3	4.2	3.0	12.4	0.9	3.9	3.0	2.2	8.8	5.4
MA	15.2	12.7	4.3	8.0	27.3	7.8	20.1	1.7	9.3	8.1
HHCB	2.2	14.5	27.4	5.1	15.4	3.1	0.3	3.4	10.7	3.4
MX	18.5	10.6	7.3	3.0	4.5	1.9	33.9	5.1	6.2	7.7
AHTN	12.0	3.3	11.3	4.3	7.3	3.3	2.9	6.6	3.4	1.6
MM	16.3	24.7	6.2	6.9	13.4	5.7	11.9	2.0	6.4	0.7
MT	8.5	25.4	1.8	8.2	11.1	5.9	7.8	4.1	9.7	6.4
MK	25.9	6.9	23.5	12.5	9.2	3.7	7.3	14.7	13.5	2.1
EB	16.3	15.7	11.8	12.7	14.7	8.9	6.9	4.5	9.0	4.1

Polycyclic and macrocyclic musks present RSD values below 16.3%, showing a satisfactory precision regardless of the water matrix, with only one exception (27.3%).

Nitro musks present most values below 15. The highest RSD value was obtained with MX in influent water at a spiked level of 0.25 $\mu g \cdot L^{-1}$ (33.9%). It was expected that high spiked levels would lead to lower precision values, and in general, that was observed, though not in a significant way. Tap water was the matrix where more values above 15% were observed. The presence of gaseous chloride could be at fault, since it might promote the degradation of some of the compounds.

The accuracy in different types of aqueous matrices was calculated by recovery tests, using spiked samples. Recovery values are presented in Table 14.

Table 14 - Recoveries of synthetic musks in water samples at different spiked levels.

	% Rec									
	Tap water		Sea water		River water		Influent		Effluent	
Compound	0.25 $\mu g \cdot L^{-1}$	1.00 $\mu g \cdot L^{-1}$	0.25 $\mu g \cdot L^{-1}$	1.00 $\mu g \cdot L^{-1}$	0.25 $\mu g \cdot L^{-1}$	1.00 $\mu g \cdot L^{-1}$	0.25 $\mu g \cdot L^{-1}$	1.00 $\mu g \cdot L^{-1}$	0.25 $\mu g \cdot L^{-1}$	1.00 $\mu g \cdot L^{-1}$
DPMI	106%	80%	101%	79%	103%	79%	102%	101%	97%	95%
ADBI	96%	94%	84%	89%	97%	89%	103%	104%	90%	101%
AHMI	83%	87%	84%	94%	88%	91%	106%	96%	92%	99%
EXA	99%	98%	71%	98%	93%	80%	90%	103%	97%	71%
MA	91%	78%	92%	88%	92%	86%	79%	95%	107%	98%
HHCB	75%	97%	107%	96%	101%	105%	100%	97%	102%	100%
MX	82%	97%	98%	108%	92%	111%	99%	112%	114%	113%
AHTN	106%	91%	92%	101%	96%	83%	99%	71%	96%	84%
MM	102%	93%	105%	97%	86%	107%	105%	105%	115%	110%
MT	80%	89%	85%	94%	89%	103%	94%	108%	106%	114%
MK	95%	82%	93%	100%	98%	115%	88%	99%	100%	110%
EB	97%	98%	102%	85%	90%	100%	118%	112%	77%	43%

The recoveries were in the range of 71-118%, except for for the recovery of EB in effluent water at a spiked level of 1.00 $\mu g \cdot L^{-1}$ (43%). An average value of 95% was reached. No significant effect of the type of water matrix on the accuracy of the method was observed, except for lower recovery levels of EB in effluent water.

4.4 Real samples analysis

The concentrations of synthetic musks existing in the various water matrices were determined. The values are presented in Table 15.

With the exception of MK in effluent water, no other nitro musk was found in any water matrices. These results are expected, since MA, MM and MT were banned from the European Union and the use of MK and MX were restricted. As expected, tap water presented the lowest amount of synthetic musks with EB being the only musk quantified (228 $ng \cdot L^{-1}$), though HHCB and EXA were detected, but below the quantification limit. Sea and river water presented a total concentration of synthetic musks of 643 and 1401 $ng \cdot L^{-1}$,

respectively. About half of the amount of musks in sea water was HHCB and the other half was EB. In river water, about 60% of the musks detected were HHCB, followed by AHTN (33%), EXA (7%) and AHMI at a very low concentration. Comparing with values found in literature, the concentrations of synthetic musks found in river water were among the range reported in other studies. The concentration found in sea water was around ten times greater than the one found on the study that reported the highest concentration of musks in sea water, 64 $ng{\cdot}L^{-1}$ (Silva and Nogueira, 2010). As expected, much higher concentrations were found in wastewaters. A total concentration of 14369 and 5735 $ng{\cdot}L^{-1}$ were detected in influent and effluent water, respectively. In both cases, the musk found in higher concentration was HHCB, with around 80% of the total concentration in both cases. Once again this result is in accordance with the literature, where HHCB was clearly the synthetic musks detected in higher concentration. In influent water EXA, AHTN and DPMI were also found in considerably high concentrations. The concentrations of HHCB, AHTN and DPMI dropped to around half in effluent water, while EXA was completely removed. Trace concentrations of ADBI and AHMI were found in effluent water, and MK was detected at a concentration of 87 $ng{\cdot}L^{-1}$.

Table 15 - Concentrations of synthetic musks in different water matrices.

	C ($ng{\cdot}L^{-1}$)				
Compound	**Tap water**	**Sea water**	**River water**	**Influent**	**Effluent**
DPMI	ND	BQ	BQ	402	279
ADBI	ND	ND	ND	ND	8
AHMI	ND	ND	12	ND	22
EXA	BQ	ND	100	1391	ND
MA	ND	ND	ND	ND	ND
HHCB	BQ	336	828	11428	4816
MX	ND	ND	ND	ND	ND
AHTN	ND	ND	462	1147	524
MM	ND	ND	ND	ND	ND
MT	ND	ND	ND	ND	ND
MK	ND	ND	ND	ND	87
EB	228	307	ND	ND	ND

ND – not detected; BQ – bellow quantification limit

Examples of chromatograms obtained for extracted standard and for real water matrix, with and without spike, are presented in Appendix 8. The peaks of all synthetic musks were clearly separated (though the separation between some of them is only clear when zoomed in). Extracted standard and spiked effluent water present a peak for every synthetic musk, as expected. Since not all musks were detected in non-spiked real water, the chromatogram of effluent water without spike doesn't show the peak of some musk compounds (nitro and macrocyclic musks, except for MK), and the peaks of the rest of the musks are decreased, when compared to the spiked sample, as expected.

5 Conclusions

In this study, a UA-DLLME extraction method coupled to GC-MS to detected and quantify twelve synthetic musks was successfully developed. The optimization of the method was done using design of experiments. The influence of seven factors (volume of the extraction solvent, volume of the disperser solvent, sample volume, extraction time, ionic strength, extraction solvent and disperser solvent) was studied. The optimal conditions achieved were 80 μL of chloroform (as extraction solvent), 880 μL of acetonitrile (as disperser solvent), 6 mL of sample volume, 3.5% (m/m) of NaCl and 2 minutes of extraction time (defined as the time the sample underwent ultrasonic treatment).

Linearity was studied in the range from 0.005 to 1.50 $\mu g \cdot L^{-1}$, and all compounds analysed showed a linear behaviour, though some compounds were not detected in the lower concentrations.

The LODs of polycyclic and macrocyclic musks and MX ranged between 2 and 8 $ng \cdot L^{-1}$ and the LOQs ranged between 6 and 25 $ng \cdot L^{-1}$, except for HHCB and DPMI. HHCB exhibited very low LOD and LOQ values (0.004 $ng \cdot L^{-1}$ and 0.01 $ng \cdot L^{-1}$, respectively), being much lower than any values reported in the literature for the detection of synthetic musks in water samples. Nitro musks and DPMI presented LOD and LOQ ranging from 36 to 83 $ng \cdot L^{-1}$ and 119 to 278 $ng \cdot L^{-1}$, respectively.

The relative standard deviation (RSD) values of aqueous standard samples ranged from 1.0 to 18.2%, showing a satisfactory precision of the extraction methodology for all musks compounds analysed. In real water samples, RSD values ranged from 0.3 to 33.9%, but the majority of the values were below 15%.

Five types of real water samples (tap, sea, river water, effluent and influent wastewater) were analysed, and the recoveries obtained were in the range of 71-122%, except for one value (43%), with an average value of 95%. Reasonable values of recovery were obtained. No significant effect of the type of water matrix on the accuracy of the method was observed.

A total concentration of synthetic musks of 228, 643, 1401, 5735 and 14369 $ng \cdot L^{-1}$ were detected in tap, sea, river water, effluent and influent wastewater, respectively. The most detected musk was HHCB, followed by AHTN, EXA, DPMI and EB. Besides MK in effluent water, no other nitro musk was detected in any water matrix.

DLLME was shown to be an adequate, simple and fast extraction method for the detection of three synthetic musk classes in aqueous samples. It consumes very low volumes of organic solvents and appears to be a good alternative extraction method, since it is simple, low-cost, effective, eco-friendly and fast.

6 Limitations and Future Work

Although good results were achieved and the main objectives of this work were met, there were some limitations, most of them associated with time.

The time of each analysis was long (around 45 minutes) and in order to try to reduce the time of the analysis, the testing of a more appropriate column could have been important. However since the GC equipment was shared with other researchers, a substitution of the column was not possible.

Besides the fact that the GC equipment was shared with other researchers, there was a period of time when the GC was not working due to technical problems, which led to the schedule of experimental work to be delayed and the possibility of analysing various real water samples (opposed to just one sample per type of matrix) was eliminated.

The testing of some extractions done in a few random conditions in order to verify if the recovery values predicted by the models proposed by the CCD are accurate were also meant to be carried, but once again due to the lack of time, these experiments were not done. Consequently it is advised as future work.

It is also expected, as future work, for the method developed in this work to be used for the monitoring of synthetic musks in various real water samples.

The results of this thesis will be presented as a poster at an international conference, CHEMPOR 2014 - 12th International Chemical and Biological Engineering Conference, 10 - 12 September 2014, Porto (Portugal). The abstract submitted is presented in Appendix 9.

7 References

Abramsson-Zetterberg, L. and Slanina, P., 2002. Macrocyclic musk compounds--an absence of genotoxicity in the Ames test and the in vivo Micronucleus assay. *Toxicology Letters,* 135(1-2), pp. 155-163.

Agilent Technologies, 2011. *Agilent Bond Elut Plexa and Polymeric SPE Selection Guide.* [Online] Available at: http://www.chem.agilent.com/Library/selectionguide/Public/5990-8589EN.pdf [Accessed 16 April 2014].

Antony, J., 2003. *Design of Experiments for Engineers and Scientists.* Burlington, MA: Butterworth-Heinemann.

Arbulu, M. et al., 2011. A retention time locked gas chromatography-mass spectrometry method based on stir-bar sorptive extraction and thermal desorption for automated determination of synthetic musk fragrances in natural and wastewaters. *Journal of Chromatography A,* 1218(20), pp. 3048-3055.

Baltussen, E., Sandra, P., David, F. and Cramers, C., 1999. Stir bar sorptive extraction (SBSE), a novel extraction technique for aqueous samples: Theory and principles. *Journal of Microcolumn Separations,* 11(10), pp. 737-747.

Bester, K., 2004. Retention characteristics and balance assessment for two polycyclic musk fragrances (HHCB and AHTN) in a typical German sewage treatment plant. *Chemosphere,* 57(8), pp. 863-870.

Bester, K., 2009. Analysis of musk fragrances in environmental samples. *Journal of Chromatography A,* 1216(3), pp. 470-480.

Bezerra, M. A. et al., 2008. Response surface methodology (RSM) as a tool for optimization in analytical chemistry. *Talanta,* 76(5), p. 965–977.

Bonna-Agela Technologies, 2011. *Cleanert PEP.* [Online] Available at: http://www.agela.com/pro_show.aspx?id=16 [Accessed 16 April 2014].

Bower, K. M., 2013. *Design of Experiments (DOE).* [Online] Available at: http://asq.org/learn-about-quality/data-collection-analysis-tools/overview/design-of-experiments.html [Accessed 25 Maio 2014].

Breitholtz, M., Wollenberger, L. and Dinan, L., 2003. Effects of four synthetic musks on the life cycle of the harpacticoid copepod Nitocra spinipes. *Aquatic Toxicology,* 63(2), pp. 103-118.

Chase, D. A. et al., 2012. Occurrence of synthetic musk fragrances in effluent and non-effluent impacted environments. *The Science of the Total Environment,* Volume 416, pp. 253-260.

Chen, D. et al., 2007. The concentrations and distribution of polycyclic musks in a typical cosmetic plant. *Chemosphere,* 66(2), pp. 252-258.

Christolear, D., 2013. *Design of Experiments (DOE) Tutorial*. [Online] Available at: http://asq.org/learn-about-quality/data-collection-analysis-tools/overview/design-of-experiments-tutorial.html [Accessed 26 Maio 2014].

Chung, W.-H., Tzing, S.-H., Ding, W.-H. and Ding, W.-H., 2013. Dispersive micro solid-phase extraction for the rapid analysis of synthetic polycyclic musks using thermal desorption gas chromatography-mass. *Journal of Chromatography A,* Volume 1307, pp. 34-40.

Daughton, C. G. and Ternes, T. A., 1999. Pharmaceuticals and personal care products in the environment: agents of subtle change?. *Environmental Health Perspectives,* 107(6), pp. 907-938.

David, F. and Sandra, P., 2007. Stir bar sorptive extraction for trace analysis. *Journal of Chromatography A,* 1152(1-2), pp. 54-69.

Dean, J. R., 2009. *Extraction Techniques in Analytical Sciences.* Chichester, UK: John Wiley and Sons, Ltd.

Deblonde, T., Cossu-Leguille, C. and Hartemann, P., 2011. Emerging pollutants in wastewater: a review of the literature. *International Journal of Hygiene and Environmental Health,* 214(6), pp. 442-448.

Eh, M., 2004. New alicyclic musks: the fourth generation of musk odorants. *Chemistry and Biodiversity,* 1(12), pp. 1975-1984.

Einsle, T. et al., 2006. Membrane-assisted liquid-liquid extraction coupled with gas chromatography-mass spectrometry for determination of selected polycyclic musk compounds and drugs in water samples. *Journal of Chromatography A,* 1124(1-2), pp. 196-204.

Eriksson, L. et al., 2008. *Design of Experiments: Principles and Applications.* 3rd Edition ed. Umeå, Sweden: MKS Umetrics AB.

Etxebarria, N. et al., 2012. Extraction Procedures for Organic Pollutants Determination in Water. In: E. Lichtfouse, J. Schwarzbauer and D. Robert, eds. *Environmental Chemistry for a Sustainable World Volume 2: Remediation of Air and Water Pollution.* s.l.:Springer, pp. 171-236.

Fountain, S. T., 2002. A Mass Spectrometry Primer. In: D. T. Rossi and M. Sinz, eds. *Mass Spectrometry in Drug Discovery*. New York, USA: Marcel Dekker, Inc., pp. 25-84.

Guo, G.-H.et al., 2013. Screening level ecological risk assessment for synthetic musks in surface water of Lake Taihu, China. *Stochastic Environmental Research and Risk Assessment,* 27(1), pp. 111-119.

Heberer, T., 2002. Occurrence, Fate, and Assessment of Polycyclic Musk Residues in the Aquatic Environment of Urban Areas — A Review. *Acta Hydrochimica et Hydrobiologica,* 30(56), pp. 227-243.

Herren, D. and Berset, J. D., 2000. Nitro musks, nitro musk amino metabolites and polycyclic musks in sewage sludges. Quantitative determination by HRGC-ion-trap-MS/MS and mass spectral characterization of the amino metabolites. *Chemosphere,* 40(5), pp. 565-574.

Horii, Y. et al., 2007. Occurrence and fate of polycyclic musks in wastewater treatment plants in Kentucky and Georgia, USA. *Chemosphere,* 68(11), pp. 2011-2020.

Hübschmann, H.-J., 2009. *Handbook of GC/MS: Fundamentals and Applications*. 2nd Edition ed. Weinheim, Germany: WILEY-VCH Verlag GmbH and Co. KGaA.

Hutter, H. P. et al., 2009. Synthetic musks in blood of healthy young adults: relationship to cosmetics use. *Science of the Total Environment,* 407(17), pp. 4821-4825.

Hu, Z., Shi, Y. and Cai, Y., 2011. Concentrations, distribution, and bioaccumulation of synthetic musks in the Haihe River of China. *Chemosphere,* 84(11), pp. 1630-1635.

Kallenborn, R. and Rimkus, G. G., 1999. Synthetic musks in environmental samples: indicator compounds with relevant properties for environmental monitoring. *Journal of Environmental Monitoring,* Volume 1, pp. 70N-74N.

Kang, C. S. et al., 2010. Polybrominated diphenyl ethers and synthetic musks in umbilical cord serum, maternal serum, and breast milk from Seoul, South Korea. *Chemosphere,* 80(2), pp. 116-122.

Kannan, K. et al., 2005. Polycyclic musk compounds in higher trophic level aquatic organisms and humans from the United States. *Chemosphere,* 61(5), pp. 693-700.

Kraft, P., 2004. 'Brain aided' musk design. *Chemistry and Biodiversity,* 1(12), pp. 1957-1974.

Lapworth, D. J., Baran, N., Stuart, M. E. and Ward, R. S., 2012. Emerging organic contaminants in groundwater: A review of sources, fate and occurrence. *Environmental Pollution,* Volume 163, pp. 287-303.

Lee, I.-S., Lee, S.-H. and Oh, J.-E., 2010. Occurrence and fate of synthetic musk compounds in water environment. *Water Research,* 44(1), pp. 214-222.

Liu, H. et al., 2010. Simultaneous determination of UV filters and polycyclic musks in aqueous samples by solid-phase microextraction and gas chromatography-mass spectrometry. *Journal of Chromatography A,* 1217(43), pp. 6747-6753.

López-Nogueroles, M., Chisvert, A., Salvador, A. and Carretero, A., 2011. Dispersive liquid-liquid microextraction followed by gas chromatography-mass spectrometry for the determination of nitro musks in surface water and wastewater samples. *Talanta,* 4(1990-1995), p. 85.

LSU Macromolecular Studies Group, 2013. *Dipole Moment*. [Online] Available at: http://macro.lsu.edu/Howto/solvents/dipole%20moment.htm [Accessed 27 June 2014].

March, R. E., 2000. Quadrupole ion trap mass spectrometry: a view at the turn of the century. *International Journal of Mass Spectrometry,* 200(1-3), pp. 285-312.

Martins, M. L. et al., 2012. Microextração Líquido-Líquido Dispersiva (DLLME): Fundamentos e aplicações. *Scientia Chromatographica,* 4(1), pp. 35-51.

Matamoros, V., Jover, E. and Bayona, J. M., 2009. Advances in the determination of degradation intermediates of personal care products in environmental matrixes: a review. *Analytical and Bioanalytical Chemistry,* 393(3), pp. 847-860.

McGinty, D., Letizia, C. and Api, A., 2011a. Fragrance material review on ω-6-hexadecenlactone. *Food and Chemical Toxicology,* 49(2), p. S207–S211.

McGinty, D., Letizia, C. and Api, A., 2011b. Fragrance material review on cycloheptadeca-9-en-1-one. *Food and Chemical Toxicology,* 49(2), p. S93–S97.

McGinty, D., Letizia, C. and Api, A., 2011c. Fragrance material review on ethylene brassylate. *Food and Chemical Toxicology,* 49(2), p. S174–S182.

McGinty, D., Letizia, C. and Api, A., 2011d. Fragrance material review on ω-pentadecalactone. *Food and Chemical Toxicology,* 49(2), p. S193–S201.

McGinty, D., Letizia, C. and Api, A., 2011e. Fragrance material review on E- and Z-oxacyclohexadec-12(+13)-en-2-one. *Food and Chemical Toxicology,* 49(2), p. S152–S157.

McGinty, D., Letizia, C. and Api, A., 2011f. Fragrance material review on 3-methyl-1-cyclopentadecanone. *Food and Chemical Toxicology,* 49(2), p. S120–S125.

McMaster, M. C., 2008. *GC/MS: A Practical User's Guide*. 2nd Edition ed. New Jersey, USA: John Wiley and Sons, Inc..

Milojević, M., 2013. *Fragrantica: Musk*. [Online] Available at: http://www.fragrantica.com/notes/Musk-4.html [Accessed 25 February 2014].

Moeder, M., Schrader, S., Winkler, U. and Rodil, R., 2010. At-line microextraction by packed sorbent-gas chromatography-mass spectrometry for the determination of UV filter and polycyclic musk compounds in water samples. *Journal of Chromatography A,* 1217(17), pp. 2925-1932.

Moldovan, Z., 2006. Occurrences of pharmaceutical and personal care products as micropollutants in rivers from Romania. *Chemosphere,* 64(11), pp. 1808-1817.

Mookherjee, B. D. and Wilson, R. A., 1982. The Chemistry and Fragrance of Natural Musk Compounds. In: E. T. Theimer, ed. *Fragrance Chemistry: Science of the Sense of Smell*. New York: Academic Press, Inc, pp. 434-494.

Müller, E., Berger, R., Blass, E. and Sluyts, D., 2000. Liquid–Liquid Extraction. In: *Ullmann's Encyclopedia of Industrial Chemistry*. Weinheim: Wiley-VCH Verlag GmbH and Co. KGaA, pp. 249-307.

Nakata, H. et al., 2007. Bioaccumulation, temporal trend, and geographical distribution of synthetic musks in the marine environment. *Environmental Science and Technology,* 41(7), pp. 2216-2222.

National Oceanic and Atmospheric Administration, 1999. *CAMEO Chemicals*. [Online] Available at: http://cameochemicals.noaa.gov/ [Accessed 27 June 2014].

Osemwengi, L. I. and Steinberg, S., 2001. On-site solid-phase extraction and laboratory analysis of ultra-trace synthetic musks in municipal sewage effluent using gas chromatography-mass spectrometry in the full-scan mode. *Journal of Chromatography A,* 932(1-2), pp. 107-118.

Panagiotou, A. N., Sakkas, V. A. and Albanis, T. A., 2009. Application of chemometric assisted dispersive liquid-liquid microextraction to the determination of personal care products in natural waters. *Analytica Chimica Acta,* 649(2), pp. 135-140.

Park, G.-J., 2007. Design of Experiments. In: *Analytic Methods for Design Practice*. s.l.:Springer-Verlag, pp. 309-392.

Pawliszyn, J., 2002. *Sampling and Sample Preparation for Field and Laboratory*. 1st Edition ed. Amsterdam: Elsevier Science B.V..

Peck, A. and Hornbuckle, K., 2006. Synthetic musk fragrances in urban and rural air of Iowa and the Great Lakes. *Atmospheric Environment,* 40(32), pp. 6101-6111.

Peck, A. M., 2006. Analytical methods for the determination of persistent ingredients of personal care products in environmental matrices. *Analytical and Bioanalytical Chemistry,* 386(4), pp. 907-939.

Peck, A. M. and Hornbuckle, K. C., 2004. Synthetic musk fragrances in Lake Michigan. *Environmental Science and Technology,* 38(2), pp. 367-372.

Pedersen, J. A., Soliman, M. and Suffet, I. H. M., 2005. Human pharmaceuticals, hormones, and personal care product ingredients in runoff from agricultural fields irrigated with treated wastewater. *Journal of Agricultural and Food Chemistry,* 53(5), pp. 1625-1632.

Peters, R. J. B., Beeltje, H. and van Delft, R. J., 2008. Xeno-estrogenic compounds in precipitation. *Journal of Environmental Monitoring,* 10(6), pp. 760-769.

Pietrogrande, M. C. and Basaglia, G., 2007. GC-MS analytical methods for the determination of personal-care products in water matrices. *Trends in Analytical Chemistry,* 26(11), pp. 1086-1094.

Posada-Ureta, O. et al., 2012. Membrane assisted solvent extraction coupled to large volume injection-gas chromatography-mass spectrometry for trace analysis of synthetic musks in environmental water samples. *Journal of Chromatography A,* Volume 1227, pp. 38-47.

Prosen, H. and Zupančič-Kralj, L., 1999. Solid-phase microextraction. *Trends in Analytical Chemistry,* 18(4), pp. 272-282.

Quednow, K. and Püttmann, W., 2008. Organophosphates and Synthetic Musk Fragrances in Freshwater Streams in Hessen/Germany. *CLEAN – Soil, Air, Water,* 36(1), pp. 70-77.

Raab, U. et al., 2008. Concentrations of polybrominated diphenyl ethers, organochlorine compounds and nitro musks in mother's milk from Germany (Bavaria). *Chemosphere,* 72(1), pp. 87-94.

Ramírez, N., Borrull, F. and Marcé, R. M., 2012. Simultaneous determination of parabens and synthetic musks in water by stir-bar sorptive extraction and thermal desorption-gas chromatography-mass spectrometry. *Journal of Separation Science,* 35(4), pp. 580-588.

Ramírez, N., Marcé, R. M. and Borrull, F., 2011. Development of a stir bar sorptive extraction and thermal desorption-gas chromatography-mass spectrometry method for determining synthetic musks in water samples. *Journal of Chromatography A,* 1218(1), pp. 156-161.

Ravi, S., Padmanabhan, D. and Mamdapu, V. R., 2001. Macrocyclic musk compounds: Synthetic approaches to key intermediates for exaltolide, exaltone and dilactones. *Journal of the Indian Institute of Science,* Volume 81, pp. 299-312.

Regueiro, J. et al., 2008. Ultrasound-assisted emulsification-microextraction of emergent contaminants and pesticides in environmental waters. *Journal of Chromatography A,* 1190(1-2), pp. 27-38.

Reiner, J. L., Berset, J. D. and Kannan, K., 2007b. Mass flow of polycyclic musks in two wastewater treatment plants. *Archives of Environmental Contamination and Toxicology,* 52(4), pp. 451-457.

Reiner, J. L. and Kannan, K., 2010. Polycyclic Musks in Water, Sediment, and Fishes from the Upper Hudson River, New York, USA. *Water, Air, and Soil Pollution,* 214(1-4), pp. 335-342.

Reiner, J. L., Wong, C. M., Arcaro, K. F. and Kannan, K., 2007a. Synthetic musk fragrances in human milk from the United States. *Environmental Science and Technology,* 41(11), pp. 3815-3820.

Ren, Y. et al., 2013. Occurrence and removal of selected polycyclic musks in two sewage treatment plants in Xi'an, China. *Frontiers of Environmental Science and Engineering,* 7(2), pp. 166-172.

Rezaee, M. et al., 2006. Determination of organic compounds in water using dispersive liquid-liquid microextraction. *Journal of Chromatography A,* 1116(1-2), pp. 1-9.

Rodríguez, J. A., Aguilar-Arteaga, K., Díez, C. and Barrado, E., 2013. Recent Advances in the Extraction of Triazines from Water Samples. In: A. J. Price, ed. *Herbicides - Advances in Research.* s.l.:InTech.

Roosens, L., Covaci, A. and Neels, H., 2007. Concentrations of synthetic musk compounds in personal care and sanitation products and human exposure profiles through dermal application. *Chemosphere,* 69(10), pp. 1540-1547.

Royal Society of Chemistry, 2014. *ChemSpider*. [Online] Available at: http://www.chemspider.com/ [Accessed 20 February 2014].

Rüdel, H., Böhmer, W. and Schröter-Kermani, C., 2006. Retrospective monitoring of synthetic musk compounds in aquatic biota from German rivers and coastal areas. *Journal of Environmental Monitoring,* 8(8), pp. 812-823.

Schiavone, A. et al., 2010. Polybrominated diphenyl ethers, polychlorinated naphthalenes and polycyclic musks in human fat from Italy: comparison to polychlorinated biphenyls and organochlorine pesticides. *Environmental Pollution,* 158(2), pp. 599-606.

Schmeiser, H. H., Gminski, R. and Mersch-Sundermann, V., 2001. Evaluation of health risks caused by musk ketone. *International Journal of Hygiene and Environmental Health,* 203(4), pp. 293-299.

Silva, A. R. M. and Nogueira, J. M. F., 2010. Stir-bar-sorptive extraction and liquid desorption combined with large-volume injection gas chromatography-mass spectrometry for ultra-trace analysis of musk compounds in environmental water matrices. *Analytical and Bioanalytical Chemistry,* 396(5), pp. 1853-1862.

Simpson, N. J., 2000. *Solid-Phase Extraction: Principles, Techniques, and Applications.* New York: Marcel Dekker, Inc.

Skoog, D. A., Holler, F. J. and Crouch, S. R., 2007. *Principles of Instrumental Analysis.* 6th Edition ed. Belmont, USA: Thomson Brooks/Cole.

Sommer, C., 2004. The role of musk and musk compounds in the fragrance industry. In: *The Handbook of Environmental Chemistry Vol.3, Part X.* Berlin: Springer-Verlag, pp. 1-6.

Sousa, R. et al., 2013. Optimisation and application of dispersive liquid–liquid microextraction for simultaneous determination of carbamates and organophosphorus pesticides. *Analytical Methods,* 5(11), pp. 2736-2745.

Stevens, J. L. et al., 2003. Pesticides, Synthetic Musks, and Polychlorinated n-Alkanes in U. K. Sewage Sludge: Survey Results and Implications. *Environmental Science and Technology,* 37(3), pp. 462-467.

Sumner, N. R., Guitart, C., Fuentes, G. and Readman, J. W., 2010. Inputs and distributions of synthetic musk fragrances in an estuarine and coastal environment; a case study. *Environmental Pollution,* 158(1), pp. 215-222.

Tanabe, S., 2005. Synthetic musks-arising new environmental menace?. *Marine Pollution Bulletin,* 50(10), pp. 1025-1026.

Thomaidis, N. S., Asimakopoulos, A. G. and Bletsou, A. A., 2012. Emerging contaminants: a tutorial mini-review. *Global NEST Journal,* 14(1), pp. 72-79.

Vera Candioti, L., De Zan, M. M., Cámara, M. S. and Goicoechea, H. C., 2014. Experimental design and multiple response optimization. Using the desirability function in analytical methods development. *Talanta,* Volume 124C, pp. 123-138.

Villa, S. et al., 2012. First evidences of the occurrence of polycyclic synthetic musk fragrances in surface water systems in Italy: spatial and temporal trends in the Molgora River (Lombardia Region, Northern Italy). *The Science of the Total Environment,* Volume 416, pp. 137-141.

Wang, Y.-C. and Ding, W.-H., 2009. Determination of synthetic polycyclic musks in water by microwave-assisted headspace solid-phase microextraction and gas chromatography-mass spectrometry. *Journal of Chromatography A,* 1216(40), pp. 6858-6863.

Waters Corporation, 1998. *OASIS HLB Sample Extraction Products.* [Online] Available at: http://www.younglin.com/brochure_pdf/waters/HLB.pdf [Accessed 16 April 2014].

Wille, K. et al., 2012. Coupled chromatographic and mass-spectrometric techniques for the analysis of emerging pollutants in the aquatic environment. *Trends in Analytical Chemistry,* Volume 35, pp. 87-108.

Wollenberger, L., Breitholtz, M., Ole Kusk, K. and Bengtsson, B. E., 2003. Inhibition of larval development of the marine copepod Acartia tonsa by four synthetic musk substances. *The Science of the Total Environment,* 305(1-3), pp. 53-64.

Wu, S.-F. and Ding, W.-H., 2010. Fast determination of synthetic polycyclic musks in sewage sludge and sediments by microwave-assisted headspace solid-phase microextraction and gas chromatography-mass spectrometry. *Journal of Chromatography A,* 1217(17), pp. 2776-2781.

Xie, Z. et al., 2007. Air-sea exchange fluxes of synthetic polycyclic musks in the North Sea and the Arctic. *Environmental Science and Technology,* 41(16), pp. 5654-5659.

Yamagishi, T., Miyazaki, T., Horii, S. and Kaneko, S., 1981. Identification of musk xylene and musk ketone in freshwater fish collected from the Tama River, Tokyo. *Bulletin of Environmental Contamination and Toxicology,* 26(1), pp. 656-662.

Yang, C.-Y. and Ding, W.-H., 2012. Determination of synthetic polycyclic musks in aqueous samples by ultrasound-assisted dispersive liquid-liquid microextraction and gas chromatography-mass spectrometrometry. *Analytical and Bioanalytical Chemistry,* 402(4), pp. 1723-1730.

Yang, J.-J. and Metcalfe, C. D., 2006. Fate of synthetic musks in a domestic wastewater treatment plant and in an agricultural field amended with biosolids. *The Science of the Total Environment,* 363(1-3), pp. 149-165.

Yang, Q., Meng, X., Xia, L. and Feng, Z., 2003. Conservation status and causes of decline of musk deer (Moschus spp.) in China. *Biological Conservation,* Volume 109, p. 333–342.

Zeng, X. et al., 2007. Preliminary study on the occurrence and distribution of polycyclic musks in a wastewater treatment plant in Guandong, China. *Chemosphere,* 69(8), pp. 1305-1311.

Zgoła-Grześkowiak, A. and Grześkowiak, T., 2011. Dispersive liquid-liquid microextraction. *Trends in Analytical Chemistry,* 30(9), pp. 1392-1399.

Zhang, X. et al., 2008. Synthetic musks in the aquatic environment and personal care products in Shanghai, China. *Chemosphere,* 72(10), pp. 1553-1558.

Appendix 1 Design of Experiments

Design of experiments (DOE) is a powerful tool that can be used in a variety of experimental situations. DOE allows for multiple input factors to be manipulated determining their effect on a desired output (response) (Christolear, 2013). DOE deals with planning, conducting, analyzing and interpreting controlled tests to evaluate the factors that control the value of a parameter or group of parameters (Bower, 2013; Antony, 2003).

A strategically planned and executed experiment may provide a great deal of information about the effect of one or more factors on a response variable. One of the most common approaches is One-Variable-At-a-Time (OVAT), which involved the variation of one variable (factor) at a time, while holding the remaining factors constant. This approach is, however, inefficient and time-consuming when compared with changing various factor levels simultaneously, and may wield false optimum condition for the process (Bower, 2013; Antony, 2003). In order to minimize the consumption of resources and time, it is quite important to perform a minimum number of experiments and to obtain maximum information (Park, 2007). DOE is used to ensure that the selected experiments produce the maximum amount of relevant information (Eriksson et al., 2008). Additionally, by manipulating multiple inputs at the same time, DOE can identify important interactions that may be missed when experimenting with one factor at a time (Christolear, 2013).

Screening is used at the beginning of the experimental procedure and it is intended to explore many factors and determine the most important ones affecting a response (Eriksson et al., 2008). This kind of approach is an efficient way to reducing the number of factors that should be studied in the next step – response surface methodology (RSM). Most of the designs involve only 2 levels of each factor. The factors may be quantitative or categorical (discrete).

After the significant factors are selected, optimization designs follow. They allow modelling a second order response surface, estimating the coefficients by fitting the experimental data to the response functions, predicting the response of the fitted model and checking the adequacy of the model (Sousa et al., 2013). When the response surface methodology is applied, a mathematical relationship between dependent and independent variables is established. Usually, a second-order polynomial equation is applied, *i.e.*:

$$Y = b_0 + \sum_{i=1}^{k} b_i x_i + \sum_{i=1}^{k} b_{ii} {x_i}^2 + \sum_{j>i}^{k} \sum_{i=1}^{k} b_{ij} x_i x_j \qquad (1)$$

where Y refers to the process response, x_i to the codified independent variable, b_0 is the interception term, b_i is the influence of the variable i in the response, b_{ii} is the parameter that determines the shape of the curve and b_{ij} corresponds to the effect of the interaction among variable i and j.

The natural variables (X_i) must be converted into dimensionless codified values (x_i):

$$x_i = \frac{(X_i - X_0)}{\Delta X} \tag{2}$$

where X_0 denotes the value of variable i in the centre of the domain (x_i = 0) and ΔX refers to the difference of that variable between x_i = +1 and x_i = 0.

One of the well-known designs is central composite design (CCD), which is the one used in this work. It is described as follows: two-level (-1 and +1) factorial design points, axial or "star" points and centre points with all factors set to 0. All factors in axial points are set to 0, except one factor with the value ±a (Vera Candioti et al., 2014).

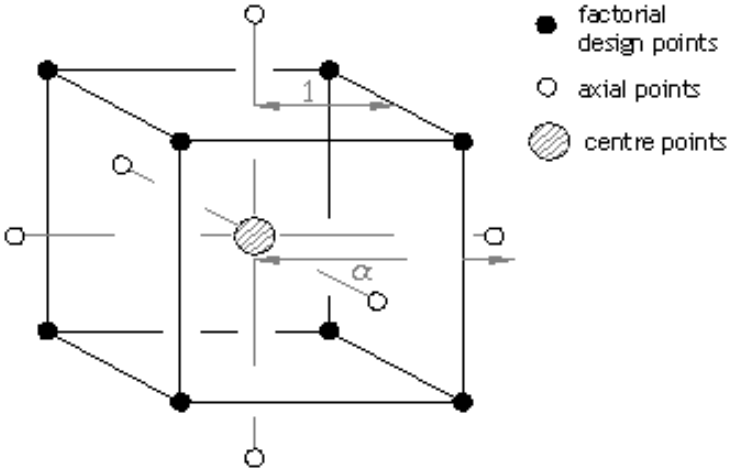

Figure A 1 - Schematic of a central composite design for three factors.

The statistical analysis uses an ANOVA (analysis of variance) test, which evaluates the model fitting adequacy. It is a collection of statistical models used to analyze the differences between group means and their associated procedures, such as "variation" among and between groups. The appropriate hypotheses for model evaluation are

$$H_0: b_i = b_{ij} = b_k = 0 \tag{3}$$

$$H_1: b_k \neq 0 \text{ for at least one } k. \tag{4}$$

Rejection of H_0 implies that at least one of the variables x_i, x_j, ..., x_k contributes significantly to the model. To determinate the statistical significance of the model, the Fisher's *F*-test is used. If the statistic F_0 exceeds $F_{\alpha,k,n-k-1}$ (similarly if F-probability is less than 0.05 for 95% confidence level) the H_0 is rejected and there is at least one variable that contributes significantly to the model, and the response variation can be attributed to

the model, not to random errors. In order to determine the parameters and/or interactions with statistical meaning it is usual to use the Student's t-test. So, if t-probability is smaller than 0.05, the parameter or interaction is considered to be significant.

The desirability function was developed as a solution to optimize multiple responses. This function is based on the idea that the quality of a product or process that has many features is completely unacceptable if one of them is outside of a "desirable" limit. Its aim is to find operating conditions that ensure compliance with the criteria of all the involved responses and, at the same time, to provide the best value of compromise in the desirable joint response (Bezerra et al., 2008). This is achieved by converting the multiple responses into a single one, combining the individual responses into a composite function followed by its optimization. The desirability function allows the analyst to find the experimental conditions (factor levels) to reach, simultaneously, the optimal value for all the evaluated variables, including the researcher's priorities during the optimization procedure.

Appendix 2 Results from the screening design

The experimental screening design consisted of a total of sixteen experiences. The conditions for each experiment are shown in Table A 1. The recovery values obtained during the experiments, in which the screening design was based is shown in Table A 2.

Table A 1 – Conditions set for each experiment for the screening design.

Run	V_E (uL)	V_D (uL)	V_S (mL)	t_E (min)	% NaCl (m/m)	S_E	S_D
1	100	1000	5	10	0	CF	EtOH
2	100	500	13	0	10	CB	EtOH
3	60	1000	13	0	0	TCE	Acet
4	100	500	13	10	10	TCE	EtOH
5	100	1000	5	10	10	CB	ACN
6	100	500	13	0	0	CB	MeOH
7	60	1000	13	0	10	CF	ACN
8	100	1000	5	0	10	TCC	EtOH
9	60	500	5	0	0	CB	Acet
10	60	1000	13	10	10	TCE	MeOH
11	60	500	5	10	0	TCC	Acet
12	60	1000	13	10	0	CF	MeOH
13	60	500	5	0	10	TCC	ACN
14	100	1000	5	0	0	TCC	MeOH
15	100	500	13	10	0	TCE	ACN
16	60	500	5	10	10	CF	Acet

Table A 2 - Recovery values obtained during the experimental runs for the screening design.

Run	DPMI	ADBI	AHMI	EXA	MA	HHCB	MX	AHTN	MM	MT	MK	EB
1	118%	96%	94%	117%	103%	115%	69%	74%	61%	91%	88%	121%
2	59%	90%	85%	88%	106%	70%	70%	70%	71%	75%	346%	98%
3	144%	76%	89%	47%	104%	77%	52%	65%	45%	62%	118%	166%
4	101%	87%	92%	61%	98%	85%	46%	88%	43%	53%	135%	201%
5	60%	95%	85%	113%	101%	73%	74%	47%	65%	90%	406%	107%
6	87%	88%	80%	87%	113%	81%	71%	52%	69%	79%	526%	146%
7	76%	96%	96%	104%	119%	104%	93%	84%	94%	101%	109%	97%
8	102%	90%	100%	145%	133%	156%	54%	89%	77%	81%	82%	238%
9	63%	73%	68%	61%	106%	69%	65%	41%	60%	82%	278%	125%
10	168%	79%	85%	49%	141%	74%	49%	69%	38%	59%	128%	190%
11	148%	91%	103%	119%	113%	198%	92%	95%	92%	82%	117%	116%
12*	-	-	-	-	-	-	-	-	-	-	-	-
13	95%	93%	96%	126%	128%	113%	60%	79%	78%	73%	68%	146%
14	131%	87%	102%	122%	130%	177%	53%	82%	64%	72%	110%	368%
15	130%	90%	90%	27%	89%	77%	57%	63%	48%	56%	98%	127%
16	75%	86%	92%	98%	114%	99%	71%	82%	69%	92%	89%	130%

* Run 12 was excluded from the design because there was no sedimented phase.

A model was estimated for each response and Table A 3 shows the coefficient of determination and the analysis of variance for all models.

Table A 3 - Coefficient of determination (R^2) and analysis of variance for the screening design.

	R^2	F ratio	Prob > F
DPMI	0.976	10.96	0.0366
ADBI	0.968	8.33	0.0536
AHMI	0.973	9.81	0.0428
EXA	0.964	7.30	0.0642
MA	0.965	7.45	0.0624
HHCB	0.977	11.44	0.0345
MX	0.988	22.86	0.0128
AHTN	0.977	11.49	0.0343
MM	0.984	17.28	0.0192
MT	0.981	13.96	0.0261
MK	0.954	5.67	0.0899
EB	0.932	3.75	0.1519

Appendix 3 CCD experimental results

Table A 4 shows the pattern and conditions set in the experiments for CCD. The recovery values obtained for the twelve synthetic musks analysed during the experiments are shown in Table A 5.

Table A 4 - Conditions set for in each experiment for the CCD.

Run	Pattern	X_1 (mL)	X_2 (µL)	X_3 (min)	X_4 (%)
1	0000	9.0	700	6	6.0
2	+++−	12.0	900	10	2.0
3	++−−	12.0	900	2	2.0
4	+−+−	12.0	500	10	2.0
5	a000	4.5	700	6	6.0
6	0000	9.0	700	6	6.0
7	−+−−	6.0	900	2	2.0
8	−−−−	6.0	500	2	2.0
9	−+++	6.0	900	10	10.0
10	A000	13.5	700	6	6.0
11	+−−+	12.0	500	2	10.0
12	−−+−	6.0	500	10	2.0
13	+−++	12.0	500	10	10.0
14	0A00	9.0	1000	6	6.0
15	++++	12.0	900	10	10.0
16	000a	9.0	700	6	0.0
17	000A	9.0	700	6	12.0
18	++−+	12.0	900	2	10.0
19	+−−−	12.0	500	2	2.0
20	0000	9.0	700	6	6.0
21	−+−+	6.0	900	2	10.0
22	0000	9.0	700	6	6.0
23	−++−	6.0	900	10	2
24	−−−+	6.0	500	2	10
25	00a0	9.0	700	0	6
26	0000	9.0	700	6	6
27	−−++	6.0	500	10	10
28	0a00	9.0	400	6	6
29	0000	9.0	700	6	6
30	00A0	9.0	700	12	6

Table A 5 - Recovery values obtained during the experimental runs for the CCD.

Run	DPMI	ADBI	AHMI	EXA	MA	HHCB	MX	AHTN	MM	MT	MK	EB
1	112%	102%	101%	101%	111%	96%	105%	95%	104%	112%	0%	10%
2	105%	88%	87%	98%	141%	91%	110%	74%	108%	118%	120%	131%
3	141%	100%	100%	103%	108%	104%	107%	92%	104%	102%	134%	103%
4	98%	88%	94%	92%	110%	99%	109%	85%	113%	111%	104%	112%
5	101%	101%	100%	118%	94%	93%	101%	107%	106%	108%	113%	64%
6	103%	97%	99%	100%	116%	96%	105%	94%	105%	109%	0%	14%
7	100%	101%	102%	100%	101%	102%	82%	95%	81%	102%	82%	103%
8	103%	98%	103%	99%	103%	90%	109%	93%	107%	114%	95%	96%
9	102%	99%	100%	103%	99%	97%	88%	124%	83%	108%	98%	99%
10	109%	92%	94%	106%	123%	93%	107%	97%	117%	110%	88%	85%
11	94%	102%	101%	114%	130%	98%	116%	108%	117%	116%	0%	101%
12	108%	101%	104%	104%	98%	93%	92%	102%	102%	99%	81%	101%
13	106%	112%	115%	122%	114%	103%	108%	128%	109%	113%	0%	131%
14	102%	102%	103%	117%	102%	97%	93%	125%	93%	97%	77%	103%
15	106%	106%	106%	122%	146%	95%	107%	126%	107%	117%	0%	99%
16	-	-	-	-	-	-	-	-	-	-	-	-
17	105%	111%	116%	90%	144%	109%	116%	116%	105%	126%	0%	73%
18	99%	102%	105%	113%	137%	98%	119%	126%	122%	116%	105%	99%
19	-	-	-	-	-	-	-	-	-	-	-	-
20	107%	102%	105%	105%	122%	99%	103%	103%	102%	112%	0%	15%
21	87%	103%	105%	104%	119%	105%	99%	110%	100%	103%	115%	113%
22	114%	99%	104%	108%	114%	97%	105%	96%	99%	105%	0%	16%
23	100%	97%	99%	113%	99%	94%	102%	108%	100%	109%	87%	105%
24	98%	106%	105%	112%	112%	95%	111%	104%	106%	112%	96%	106%
25	103%	107%	108%	116%	106%	101%	93%	125%	101%	104%	82%	105%
26	100%	99%	101%	100%	109%	95%	112%	111%	108%	114%	0%	10%
27	129%	129%	118%	136%	114%	107%	86%	142%	85%	96%	0%	110%
28	104%	99%	101%	107%	112%	93%	116%	119%	110%	111%	109%	96%
29	111%	104%	105%	107%	117%	94%	99%	99%	102%	104%	0%	13%
30	105%	111%	110%	131%	133%	102%	97%	131%	106%	111%	93%	101%

* Runs 16 and 19 were excluded from the design because there was no sedimented phase.

Appendix 4 CCD parity plots

Parity plots represent the actual (experimental) vs. the predicted (by the model) values of the responses (recoveries). The parity plots of all responses are represented from Figure A 2 to Figure A 13.

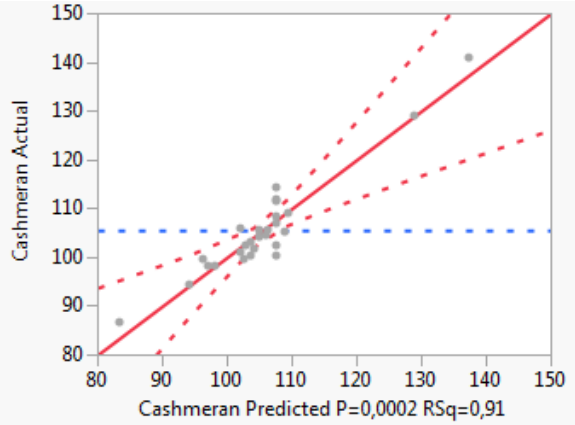

Figure A 2 – Parity plot of DPMI.

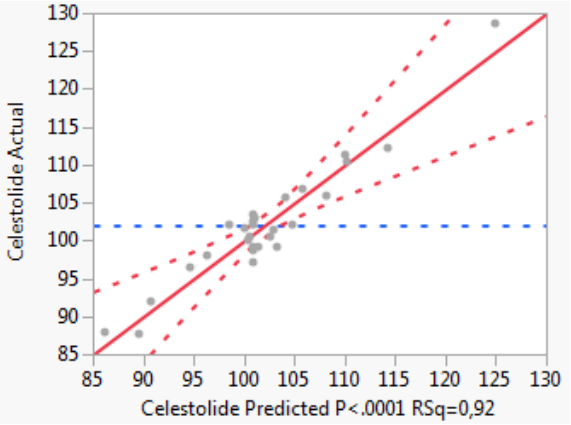

Figure A 3 - Parity plot of ADBI.

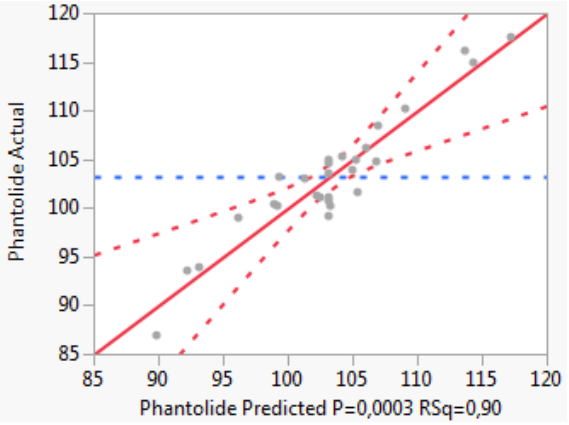

Figure A 4 - Actual by predicted plot of AHMI.

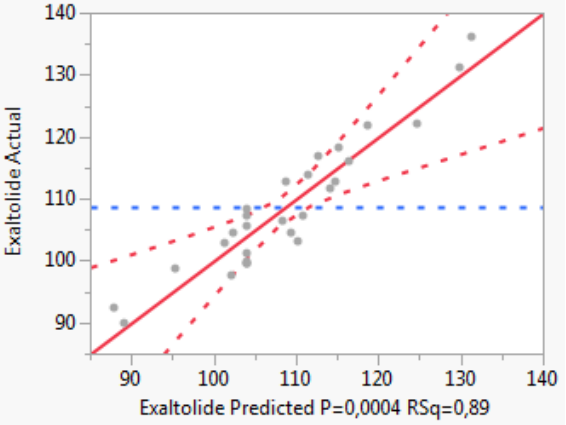

Figure A 5 - Actual by predicted plot of EXA.

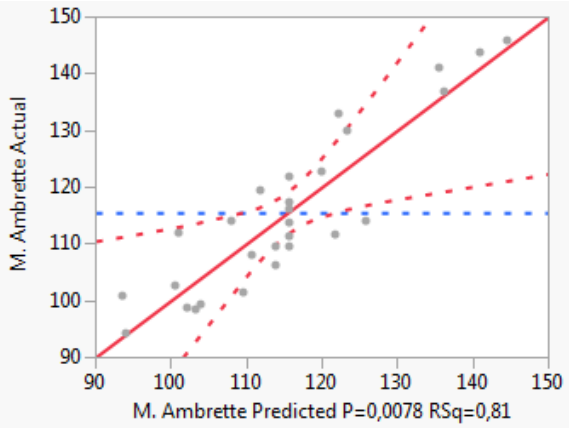

Figure A 6 - Parity plot of MA.

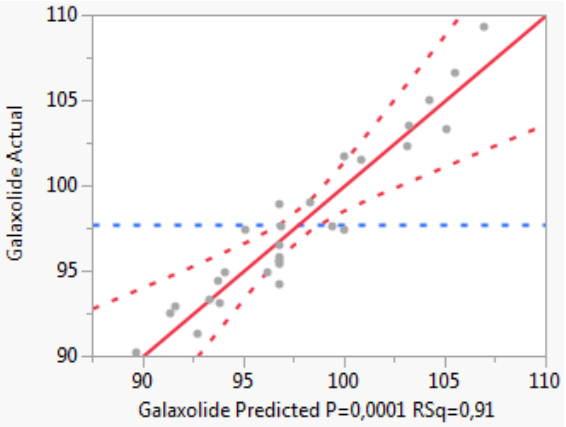

Figure A 7 - Parity plot of HHCB.

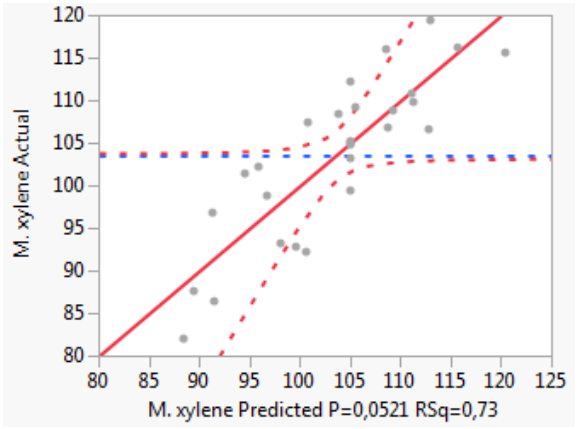

Figure A 8 - Parity plot of MX.

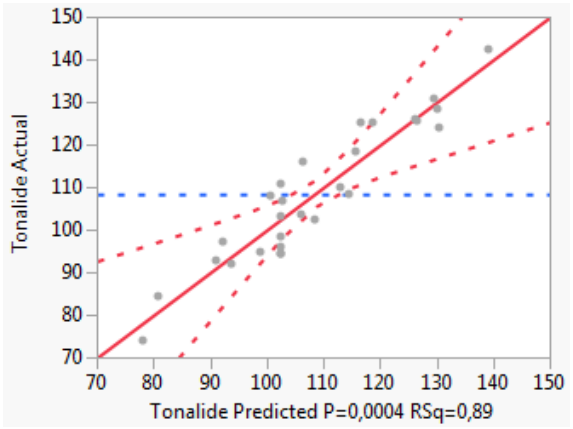

Figure A 9 - Parity plot of AHTN.

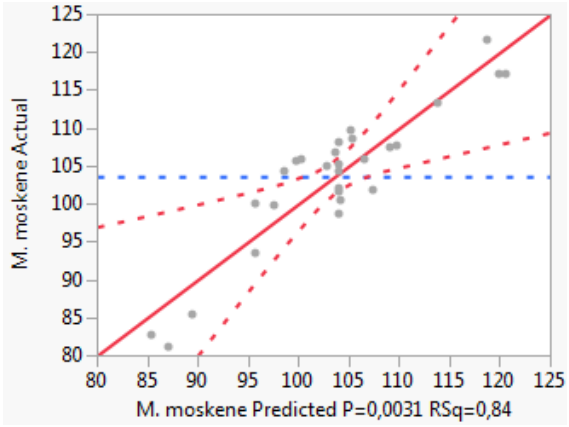

Figure A 10 - Parity plot of MM.

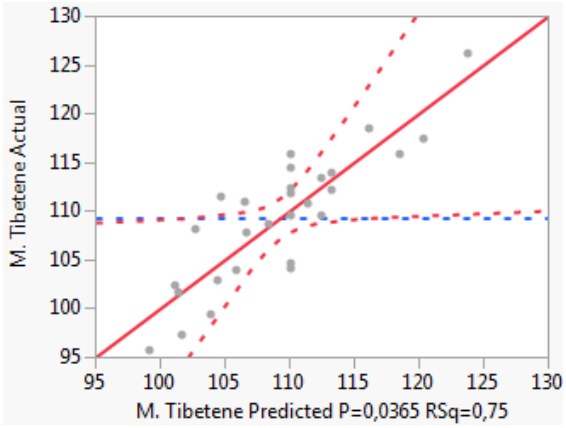

Figure A 11 - Parity plot of MT.

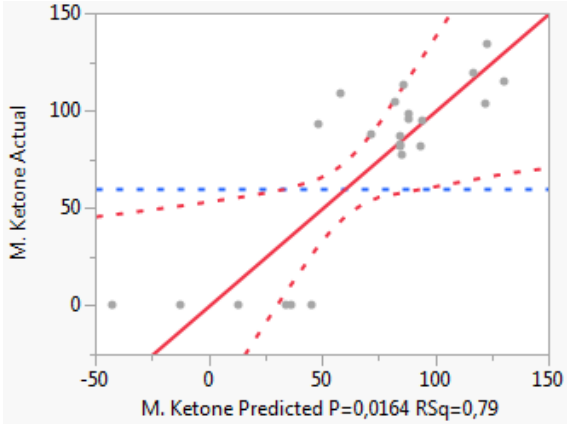

Figure A 12 - Parity plot of MK.

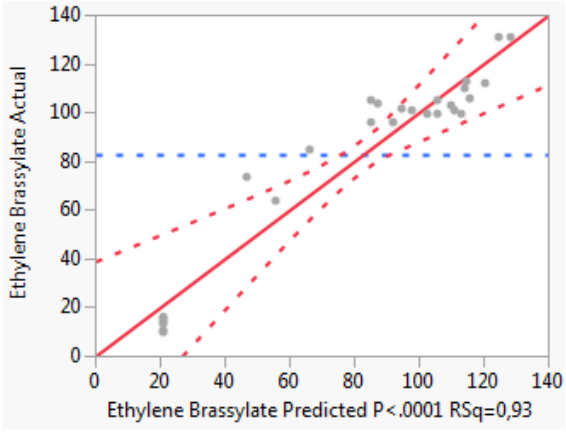

Figure A 13 - Parity plot of EB.

Appendix 5 CCD response surface plots

The three-dimensional response surface plot for the synthetic musks analysed are represented from Figure A 14 to Figure A 24. They show the response surface obtained by plotting the recovery vs. two most significant variables for each case, while the other two variables are fixed at their optimal points. The interception with the surface plan % Rec = 100% is also shown in the plot, since it is the objective value.

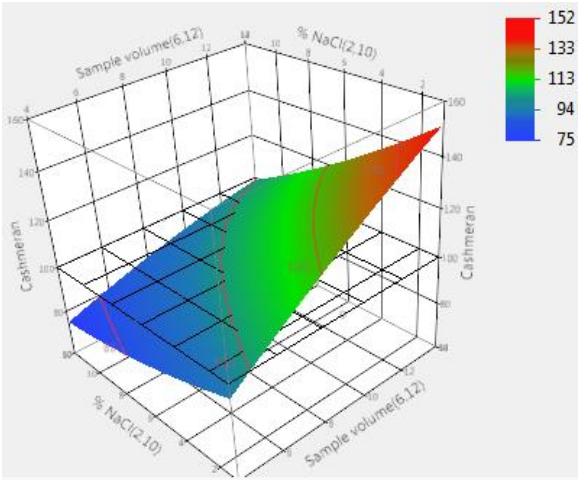

Figure A 14 - Response surface plot, recovery vs. percentage of NaCl and sample volume, for DPMI (1 µg·L^{-1} of AHTN, 80 µL of CF, 880 µL of ACN, 2 minutes of extraction time).

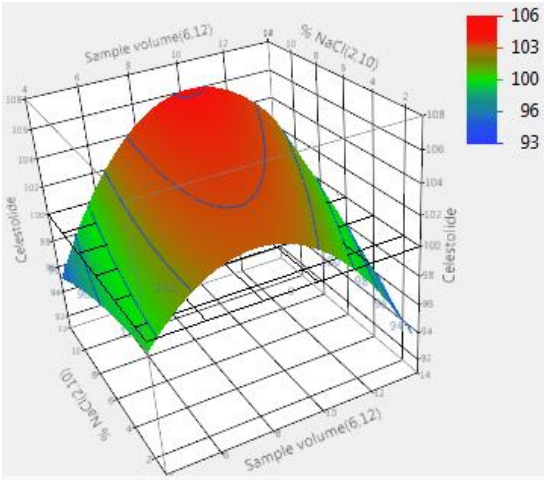

Figure A 15 - Response surface plot, recovery vs. percentage of NaCl and sample volume, for ADBI (1 µg·L^{-1} of AHTN, 80 µL of CF, 880 µL of ACN, 2 minutes of extraction time).

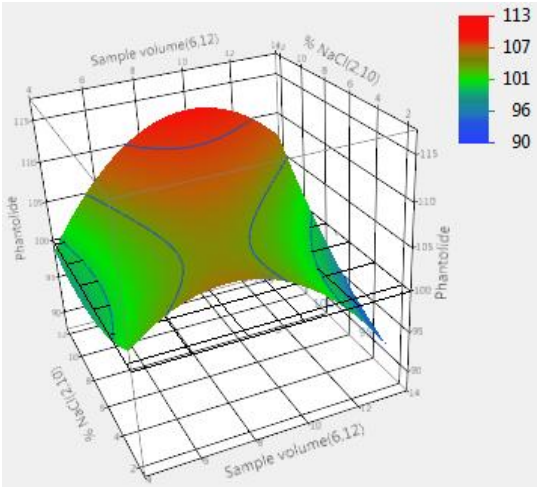

Figure A 16 - Response surface plot, recovery vs. percentage of NaCl and sample volume, for AHMI (1 µg·L^{-1} of AHTN, 80 µL of CF, 880 µL of ACN, 2 minutes of extraction time).

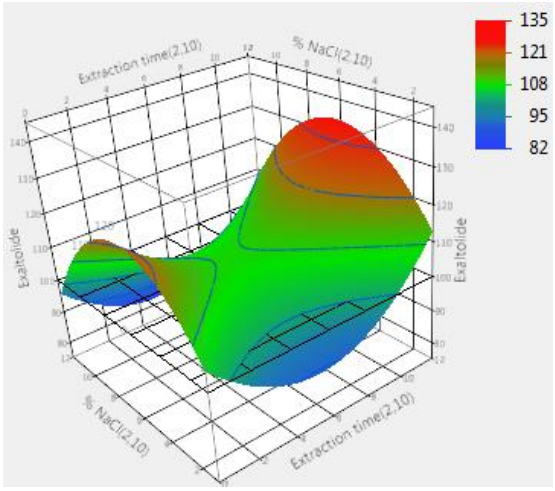

Figure A 17 - Response surface plot, recovery vs. percentage of NaCl and extraction time, for EXA (1 µg·L^{-1} of AHTN, 80 µL of CF, 880 µL of ACN, 6 mL of volume sample).

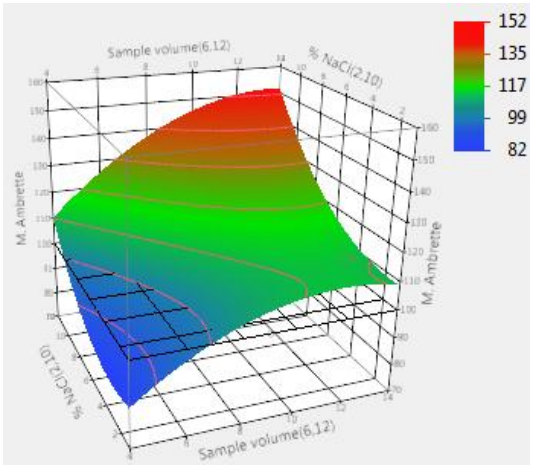

Figure A 18 - Response surface plot, recovery vs. percentage of NaCl and sample volume, for MA (1 µg·L^{-1} of AHTN, 80 µL of CF, 880 µL of ACN, 2 minutes of extraction time).

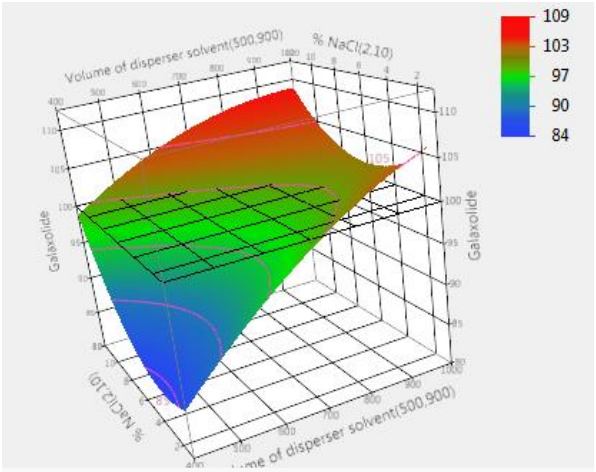

Figure A 19 - Response surface plot, recovery vs. percentage of NaCl and volume of ACN, for HHCB (1 µg·L^{-1} of AHTN, 80 µL of CF, 6 mL of volume sample, 2 minutes of extraction time).

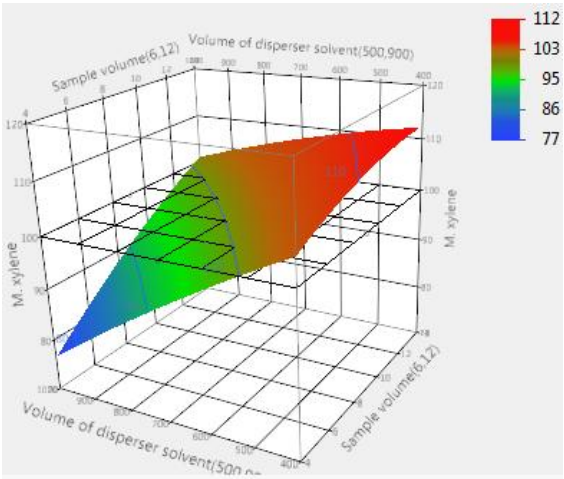

Figure A 20 - Response surface plot, recovery vs. volume of ACN and sample volume, for MX (1 µg·L^{-1} of AHTN, 80 µL of CF, 3.5% of NaCl, 2 minutes of extraction time).

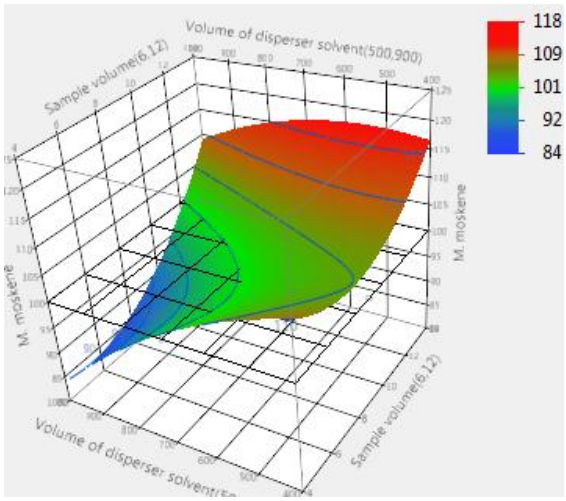

Figure A 21 - Response surface plot, recovery vs. volume of ACN and sample volume, for MM (1 µg·L^{-1} of AHTN, 80 µL of CF, 3.5% of NaCl, 2 minutes of extraction time).

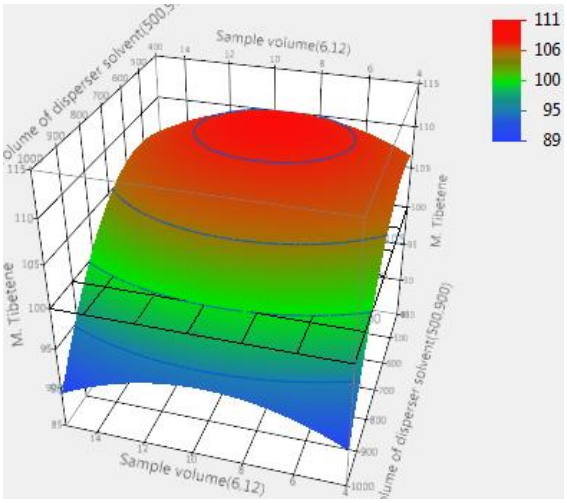

Figure A 22 - Response surface plot, recovery vs. volume of ACN and sample volume, for MT (1 µg·L^{-1} of AHTN, 80 µL of CF, 3.5% of NaCl, 2 minutes of extraction time).

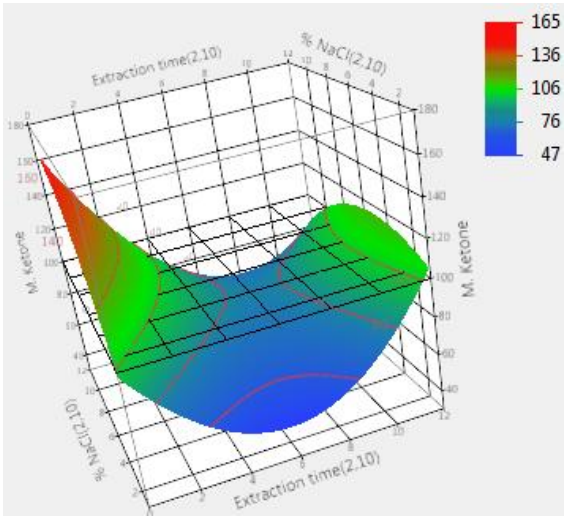

Figure A 23 - Response surface plot, recovery vs. percentage of NaCl and extraction time, for MK (1 µg·L^{-1} of AHTN, 80 µL of CF, 880 µL of ACN, 6 mL of volume sample).

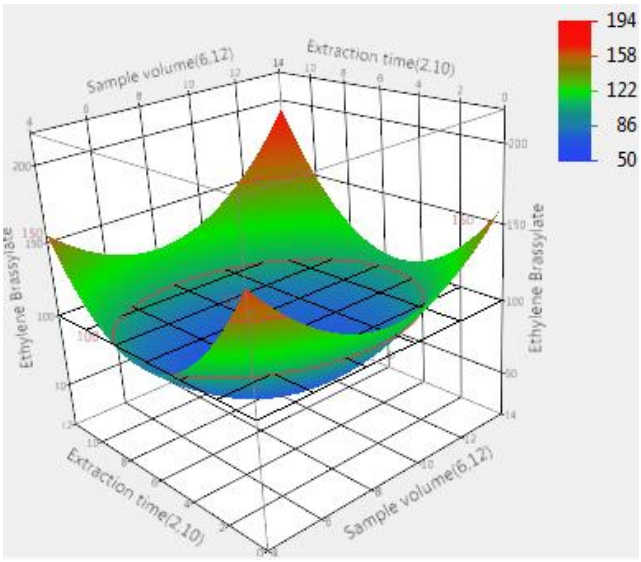

Figure A 24 - Response surface plot, recovery vs. extraction time and sample volume, for EB (1 µg·L^{-1} of AHTN, 80 µL of CF, 880 µL of ACN, 3.5% of NaCl)

Appendix 6 CCD prediction profiler

The prediction profiler shows a graphic for how each response varies with each factor, while maintain the other factors fixed. It also shows the desirability function set for each response, and its variation with each factor. Figure A 25 shows the prediction profiler after the maximization of the desirability function, representing the optimal point.

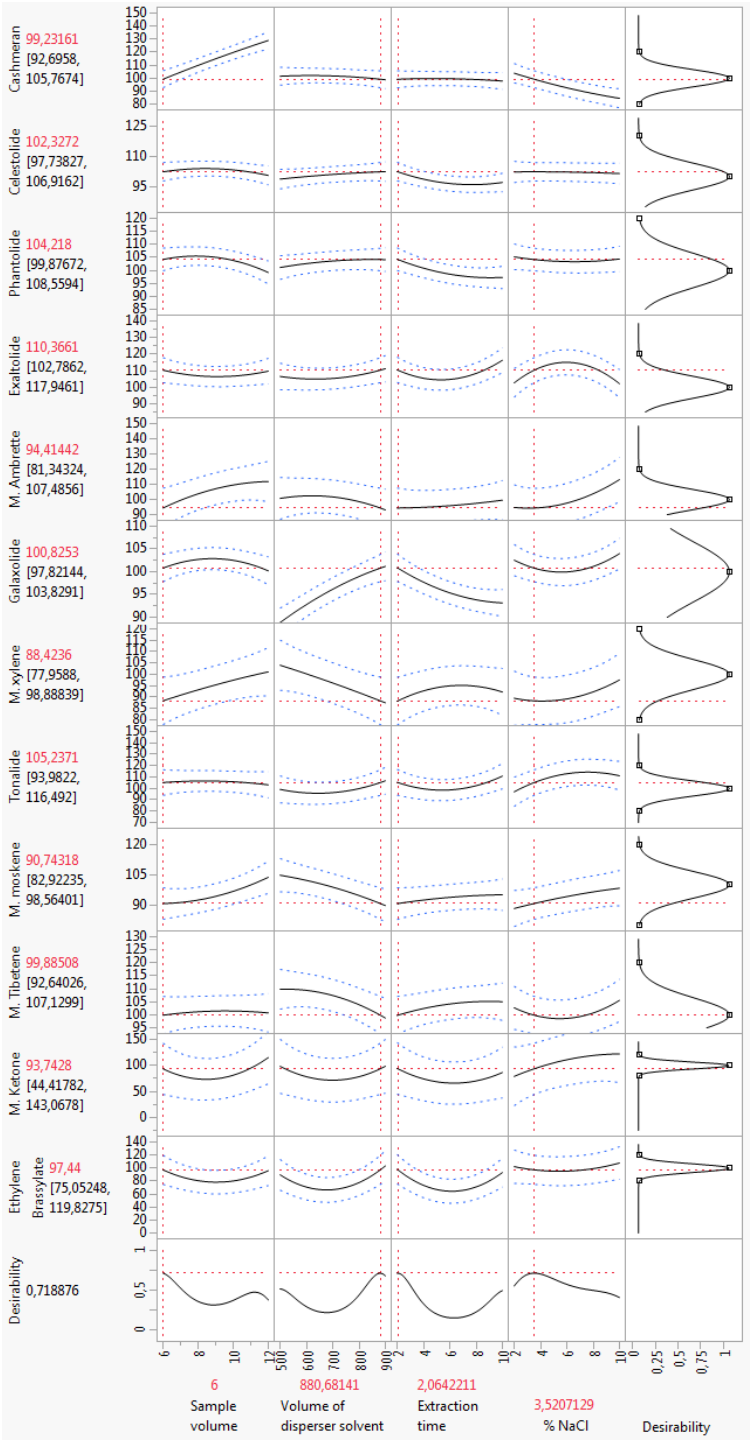

Figure A 25 - Prediction profiler after the maximization of the desirability function, showing the variation of each response with each factor, while the other factors are fixed at the optimal point.

Appendix 7 Calibration curves

The average response factors (RF) obtained for each synthetic musk at different concentrations, used for the calibration curves are shown in Table A 6. The calibration curves for each compound are represented from Figure A 26 to Figure A 37. The calibration curves equations and their respective validation parameters are shown in Table A 7.

Table A 6 - Response factors (RF) obtained for the calibration curves.

C (µg/L)	RF											
	DPMI	ADBI	AHMI	EXA	MA	HHCB	MX	AHTN	MM	MT	MK	EB
1.50	1.753	3.366	2.749	1.238	3.043	1.490	2.084	1.562	3.194	3.991	3.602	0.083
1.25	1.449	2.883	2.328	1.073	2.513	1.257	1.644	1.275	2.512	3.319	3.083	0.072
1.00	1.190	2.400	1.890	0.857	1.982	1.030	1.339	1.037	2.019	2.799	2.524	0.053
0.75	0.955	1.856	1.457	0.672	1.417	0.816	1.025	0.872	1.637	2.045	1.966	0.044
0.50	0.647	1.197	0.978	0.471	0.976	0.575	0.642	0.600	0.893	1.141	1.369	0.026
0.25	0.282	0.579	0.447	0.253	0.550	0.261	0.296	0.228	0.469	0.705	0.699	0.008
0.10	0.114	0.185	0.125	0.137	ND	0.214	0.068	0.118	0.146	0.179	0.368	0.002
0.05	0.019	0.110	0.073	0.103	ND	0.085	0.037	0.039	0.085	0.074	0.173	ND
0.01	ND	0.017	0.016	0.061	ND	0.061	ND	0.015	ND	0.061	0.067	ND
0.005	ND	0.010	0.006	0.048	ND	0.037	ND	ND	ND	ND	ND	ND

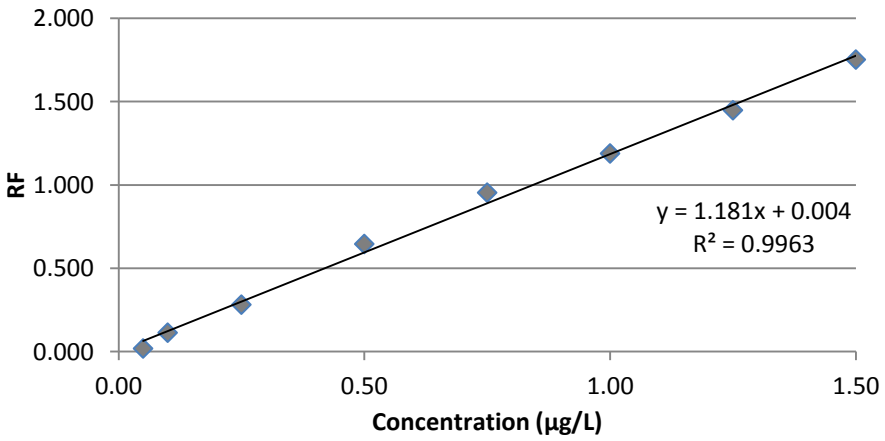

Figure A 26 – Graphic representation of the calibration curve of cashmeran (DPMI) by GC-MS, using surrogate standard.

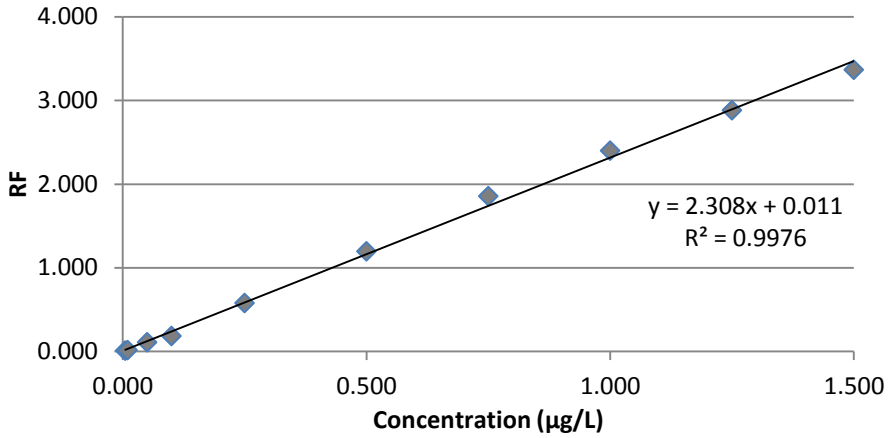

Figure A 27 - Graphic representation of the calibration curve of celestolide (ADBI) by GC-MS, using surrogate standard.

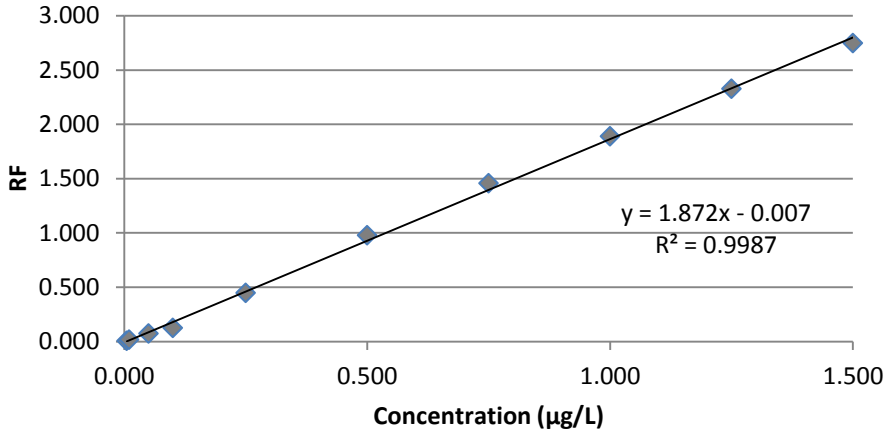

Figure A 28 - Graphic representation of the calibration curve of phantolide (AHMI) by GC-MS, using surrogate standard.

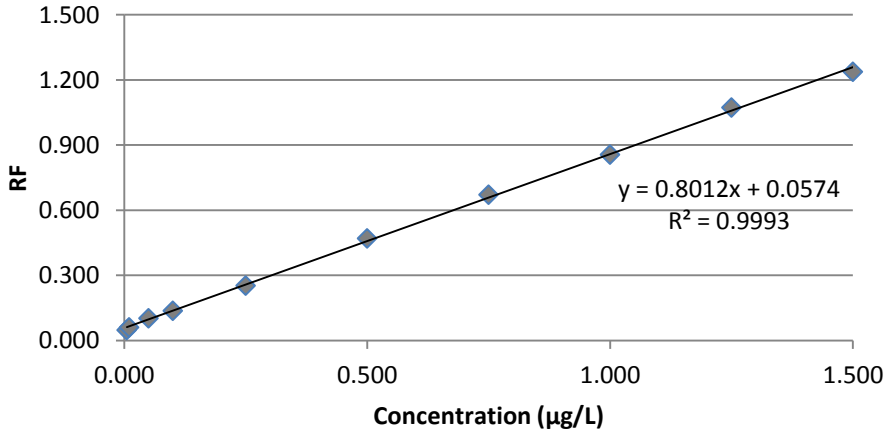

Figure A 29 - Graphic representation of the calibration curve of exaltolide (EXA) by GC-MS, using surrogate standard.

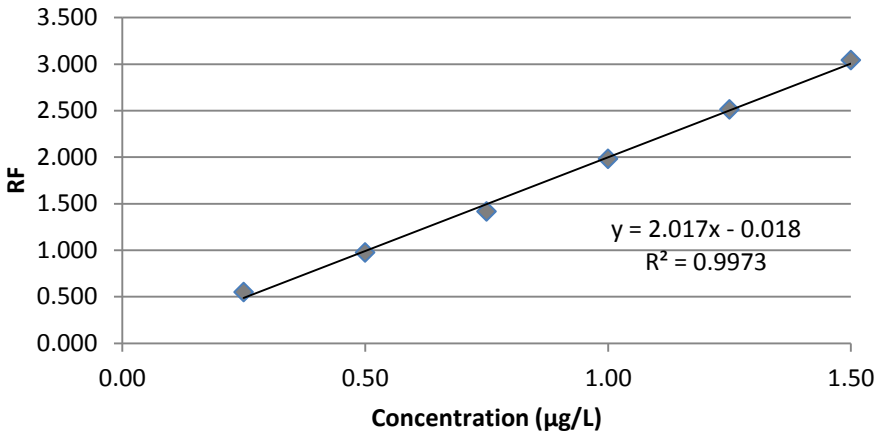

Figure A 30 - Graphic representation of the calibration curve of musk ambrette (MA) by GC-MS, using surrogate standard.

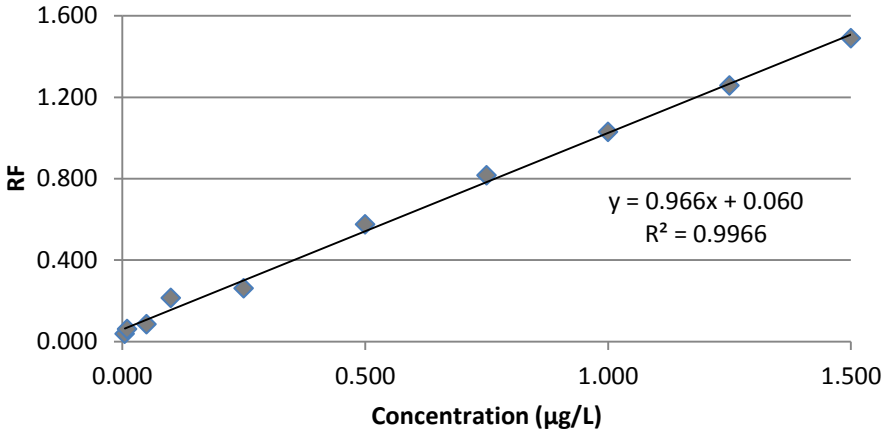

Figure A 31 - Graphic representation of the calibration curve of galaxolide (HHCB) by GC-MS, using surrogate standard.

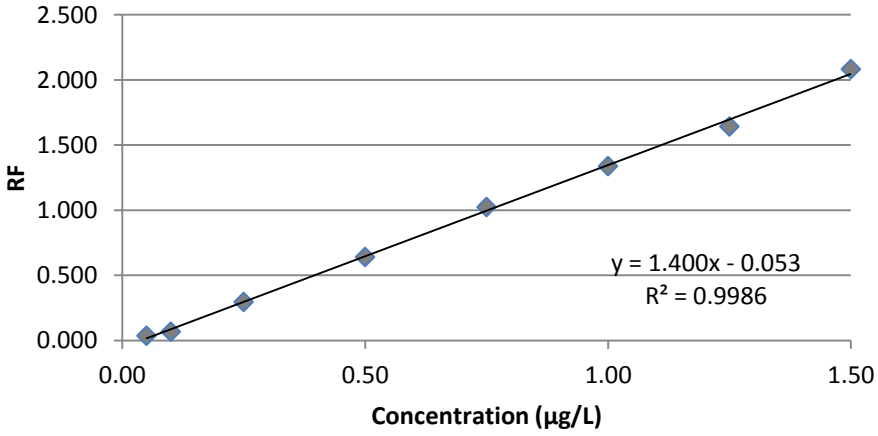

Figure A 32 - Graphic representation of the calibration curve of musk xylene (MX) by GC-MS, using surrogate standard.

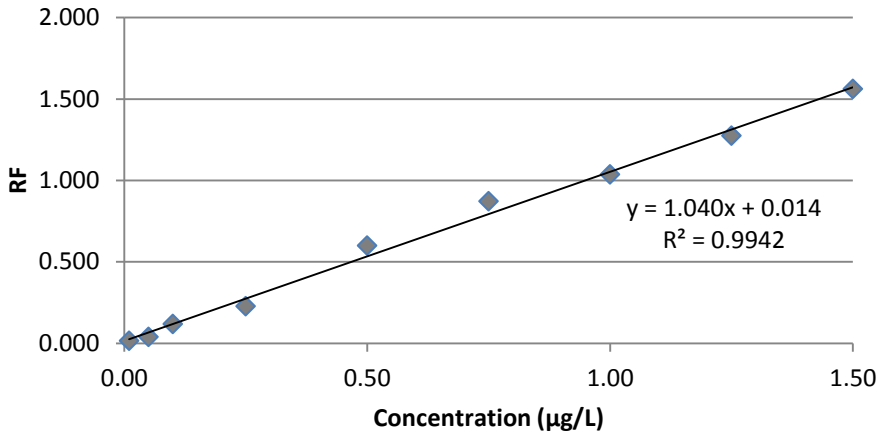

Figure A 33 - Graphic representation of the calibration curve of tonalide (AHTN) by GC-MS, using surrogate standard.

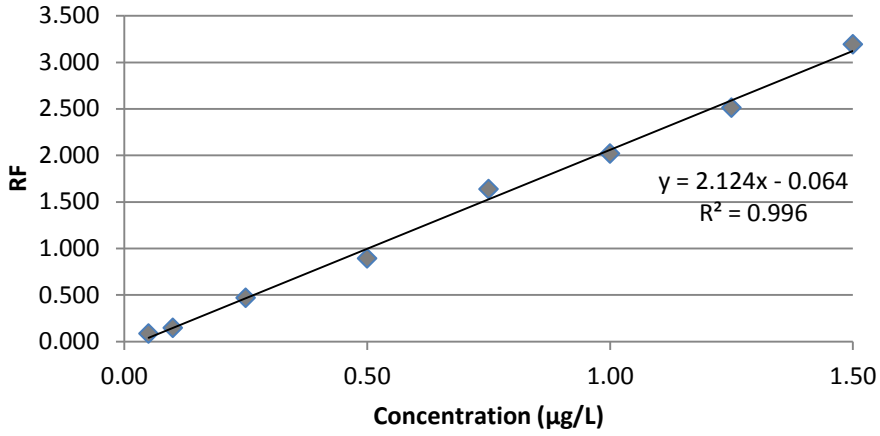

Figure A 34 - Graphic representation of the calibration curve of musk moskene (MM) by GC-MS, using surrogate standard.

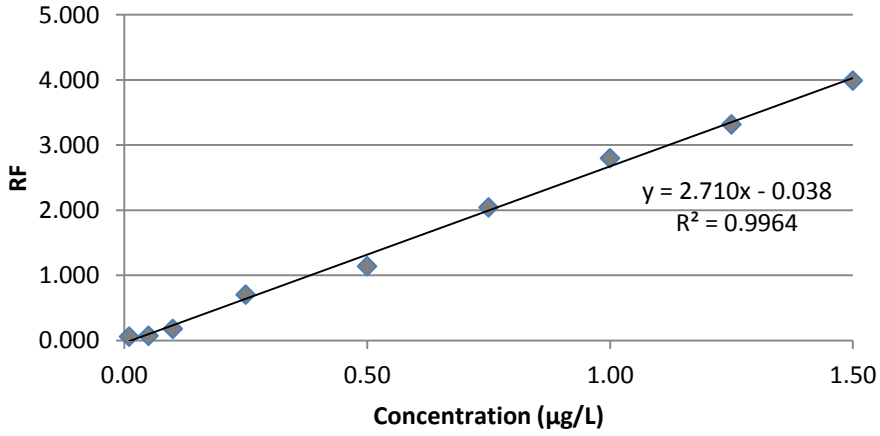

Figure A 35 - Graphic representation of the calibration curve of musk tibetene (MT) by GC-MS, using surrogate standard.

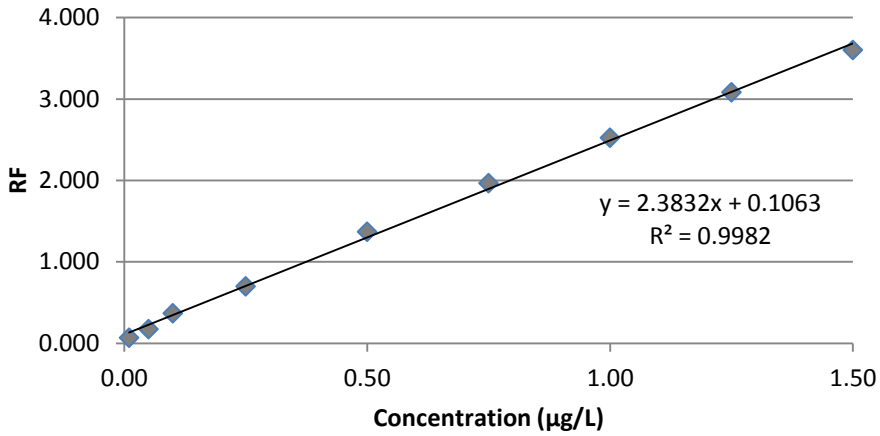

Figure A 36 - Graphic representation of the calibration curve of musk ketone (MK) by GC-MS, using surrogate standard.

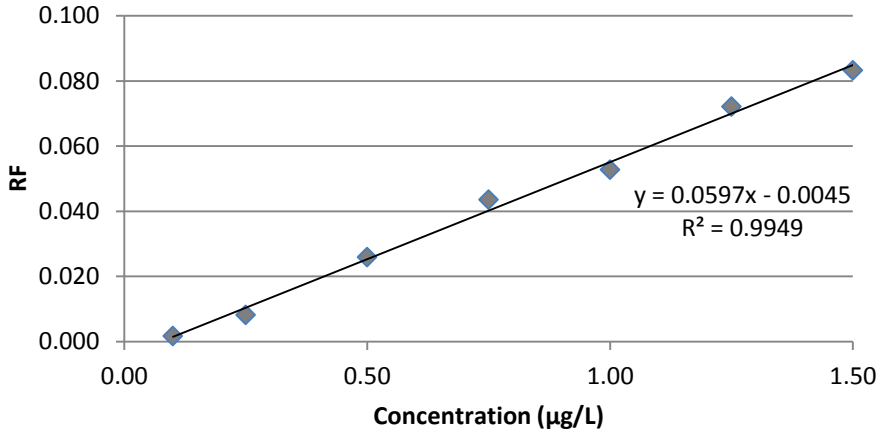

Figure A 37 - Graphic representation of the calibration curve of ethylene brassylate (EB) by GC-MS, using surrogate standard.

Table A 7- Calibration curves equations and their respective validation parameters.

	Calibration curve equation $y = (a \pm s_a)\, x + (b \pm s_b)$	R (> 0.995)	s_a/a (< 5%)	$\frac{b-s_b}{b+s_b}$	$(b-s_b < 0 < b+s_b)$
DPMI	$RF = (1.18 \pm 0.03) \times C + (0.00 \pm 0.02)$	0.998 ✓	2.5% ✓	$\frac{-0.02}{0.02}$	✓
ADBI	$RF = (2.31 \pm 0.04) \times C + (0.01 \pm 0.03)$	0.999 ✓	1.8% ✓	$\frac{-0.02}{0.04}$	✓
AHMI	$RF = (1.87 \pm 0.02) \times C + (-0.01 \pm 0.02)$	0.999 ✓	1.3% ✓	$\frac{-0.02}{0.01}$	✓
EXA	$RF = (1.801 \pm 0.007) \times C + (0.057 \pm 0.006)$	1.000 ✓	0.9% ✓	$\frac{0.052}{0.063}$	✗
MA	$RF = (2.02 \pm 0.05) \times C + (-0.02 \pm 0.05)$	0.999 ✓	2.6% ✓	$\frac{-0.07}{0.03}$	✓
HHCB	$RF = (0.97 \pm 0.02) \times C + (0.06 \pm 0.02)$	0.998 ✓	2.1% ✓	$\frac{0.04}{0.07}$	✗
MX	$RF = (1.40 \pm 0.02) \times C + (-0.05 \pm 0.02)$	0.999 ✓	1.6% ✓	$\frac{-0.07}{-0.03}$	✓
AHTN	$RF = (1.04 \pm 0.03) \times C + (0.01 \pm 0.02)$	0.997 ✓	2.9% ✓	$\frac{-0.01}{0.04}$	✓
MM	$RF = (2.12 \pm 0.06) \times C + (-0.06 \pm 0.05)$	0.998 ✓	2.6% ✓	$\frac{-0.11}{-0.02}$	✗
MT	$RF = (2.71 \pm 0.06) \times C + (-0.04 \pm 0.05)$	0.998 ✓	2.3% ✓	$\frac{-0.09}{0.01}$	✓
MK	$RF = (2.38 \pm 0.04) \times C + (-0.11 \pm 0.03)$	0.999 ✓	1.6% ✓	$\frac{0.08}{0.14}$	✗
EB	$RF = (0.060 \pm 0.002) \times C + (-0.005 \pm 0.002)$	0.997 ✓	3.2% ✓	$\frac{-0.006}{-0.003}$	✗

R – correlation coefficient; a – slope; s_a - standard deviation of the slope; s_a/a – relative standard deviation of the slope; b – intercept; s_b - standard deviation of the intercept

Appendix 8 Chromatograms

Figure A 38 shows an example of a chromatogram obtained for an extracted standard (1.00 $\mu g \cdot L^{-1}$). Figure A 39 and Figure A 40 show examples of chromatograms obtained for real water matrix (effluent wastewater), with (1.00 $\mu g \cdot L^{-1}$) and without spike, respectively.

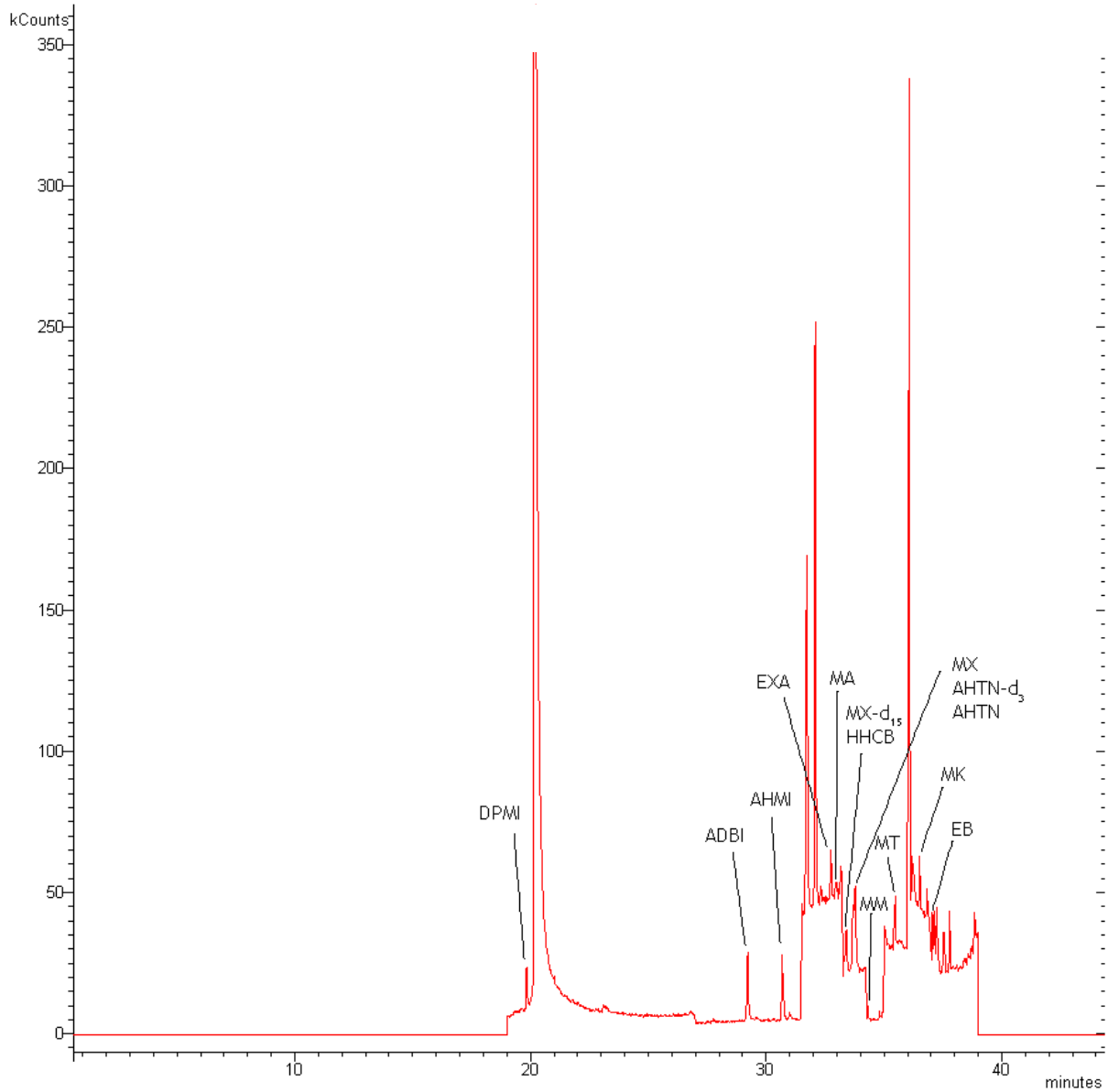

Figure A 38 – Chromatogram of extracted 1.00 $\mu g \cdot L^{-1}$ standard.

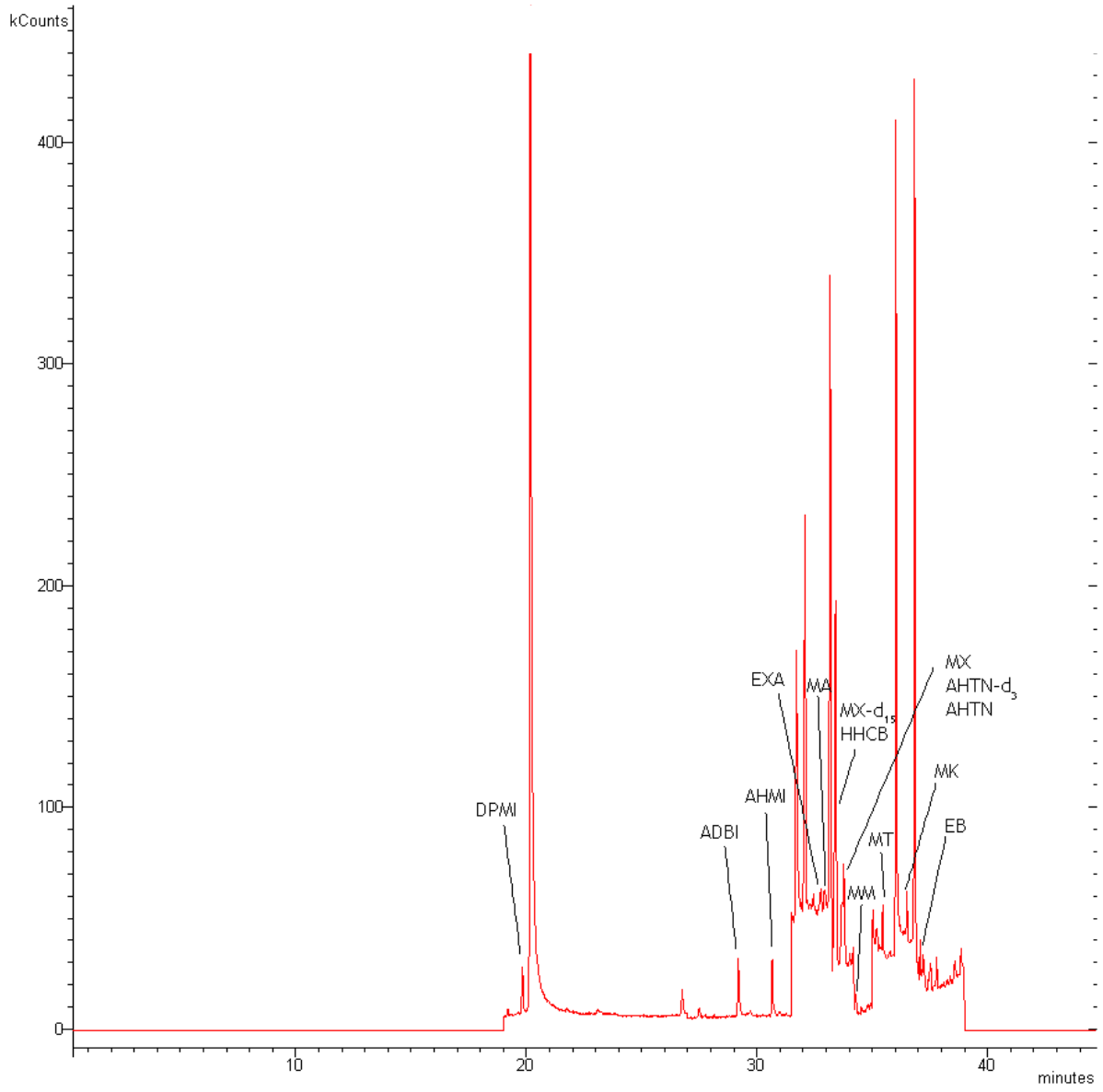

Figure A 39 - Chromatogram of wastewater effluent. spiked at 1.00 µg·L^{-1}.

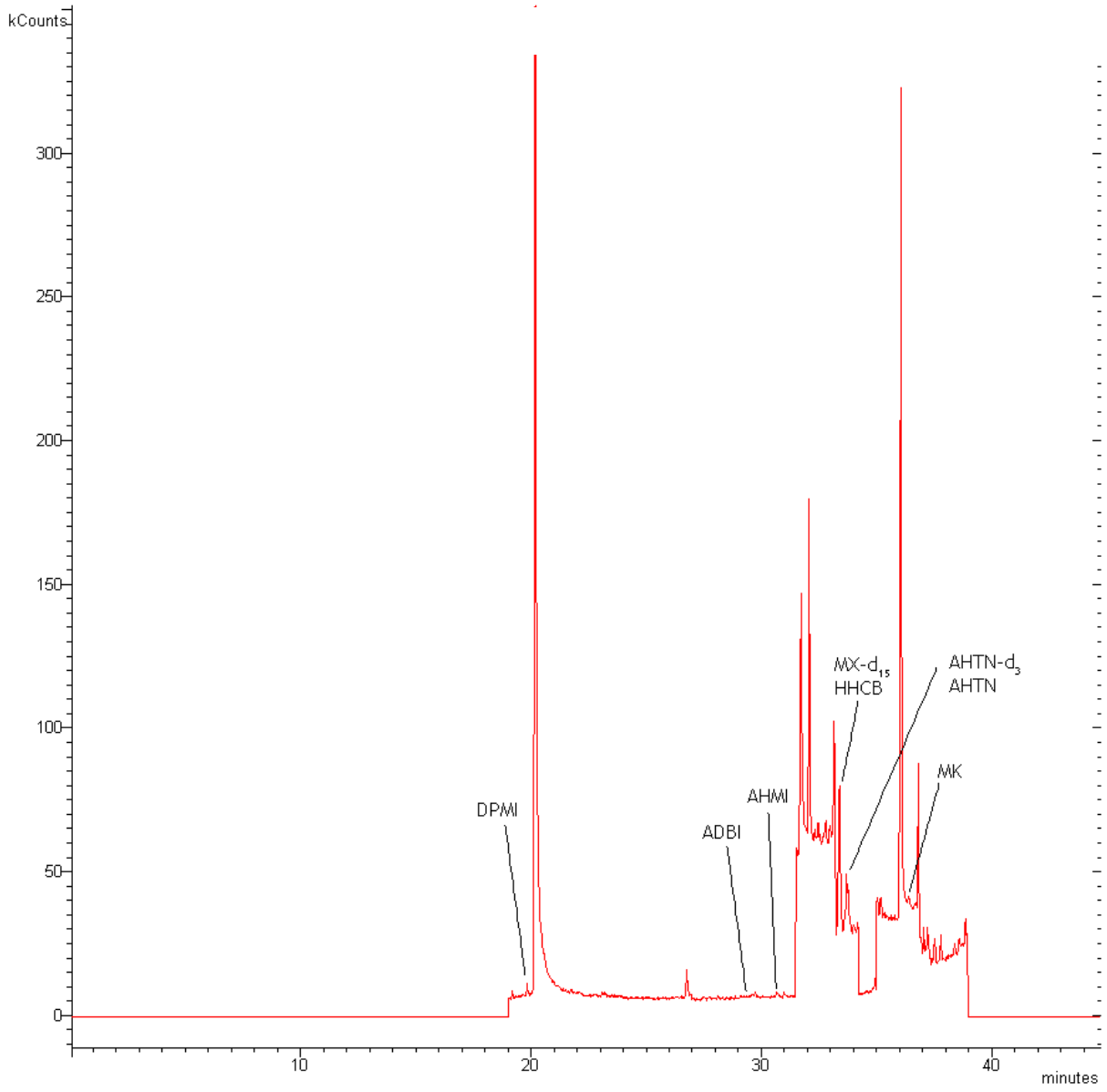

Figure A 40 - Chromatogram of wastewater effluent, without spike.

Appendix 9 Abstract submitted to conference

CHEMPOR 2014 - 12th International Chemical and Biological Engineering Conference, 10 - 12 September 2014, Porto (Portugal)

Ultrasound-Assisted Dispersive Liquid-Liquid Microextraction for the Determination of Synthetic Musk Fragrances in Water Matrices

POSTER (#7)
Journal: JCB

V. Homem[1,], A.A. Alves[1], A. Alves[1], L. Santos[1]. (1) LEPABE – Laboratory for Process Engineering, Environment, Biotechnology and Energy, Faculty of Engineering, University of Porto, Rua Dr. Roberto Frias, 4200-465 Porto, Portugal; *vhomem@fe.up.pt.*

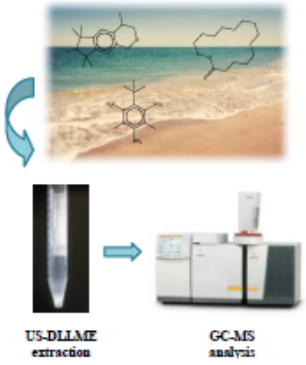

A simple, fast and sensitive analytical method based on ultrasound-assisted dispersive liquid-liquid microextraction (US-DLLME) followed by gas chromatography–mass spectrometry (GC–MS) was developed and optimized for the determination of twelve synthetic musk fragrances in water samples. Several DLLME parameters, such as type and volume of extraction and dispersive solvents, sample volume, extraction time and ionic strength were studied using a screening design. The obtained significant factors were optimized by using a central composite design (CCD). Under optimized conditions, the analytical methodology was validated and its applicability was tested in several aqueous matrices (river, sea water, wastewater and drinking water).

Introduction

Synthetic musk fragrances are organic compounds used in a wide variety of cosmetics and personal care products (makeup, perfumes, body lotions, deodorants, soaps, shampoo, etc) and household products (detergents, fabric softeners and air fresheners) [1]. These compounds are usually divided into four main chemical groups: nitro, polycyclic, macrocyclic and alicyclic musks [2]. The nitromusk group includes alkylated dinitro- and trinitrobenzenes, as musk ambrette (MA), ketone (MK), moskene (MM), tibetene (MT) and xylene (MX) [3]. Due to their toxicological and bioaccumulative properties, the use of these synthetic musks declined significantly in the past years. Currently, the use of MA, MK and MM in cosmetic products was prohibited in the European Union, while that of MX and MK was restricted [4]. The polycyclic musk fragrances, other important group, were introduced in the 50s. They are chemically acetylated and highly methylated pyran, tetralin and indane compounds [5] and the most representatives are cashmeran (DPMI), celestolide (ADBI), galaxolide (HHCB), phantolide (AHMI) and tonalide (AHTN). Macrocyclic musks were more recently introduced in the market and are large ringed ketones and lactones (10 to 15 carbons), chemically similar to animal and plant musk odorants [5] (e.g. exaltolide (EXA), ethylene brassylate(EB)). Finally, the alicyclic musks are the latest generation of synthetic musk fragrances and are known as cycloakyl ester or linear musks [2] (e.g. cyclomusk, helvetolide).

Due to the widespread and extremely high incidence of use of personal care products, these compounds are continuously introduced into the environment mainly through sewer systems [2, 6]. In fact, since these compounds are bio-accumulative, have a lipophilic and persistent nature and are only partially biodegradable, most conventional wastewater treatment plants (WWTPs) are not able to completely remove them, leading to natural waterways contamination.

In the past decades, it was believed that musks were inert and had no toxic effects to humans and environment [7]. However, recent reports suggest that they can cause toxic effects, be carcinogenic (namely the nitromusks) and cause estrogen imbalance in aquatic animals [8]. Due to the lack of information, there are no certainties about the impact of these contaminants. Therefore, it is extremely important to carry out monitoring studies to examine the concentrations of synthetic musks in the environmental, namely in water matrices.

For this purpose a new microextraction method based on ultrasound-assisted dispersive liquid–liquid microextraction (DLLME) was developed and optimized using a design of experiments (DoE) approach.

Materials and Methods

Solid standards of synthetic polycyclic musks DPMI, ADBI, AHMI, HHCB and AHTN were obtained from LGC Standards (Barcelona, Spain) with 99% purity, except for HHCB, which contains approximately 25% of diethyl phthalate. MT and MM were also purchased as 10 mg/L solution in cyclohexane from LGC Standards. MA and MK were purchased as solid standards from Dr. Ehrenstorfer (Augsburg, Germany) with 99

1

and 98% purity, respectively. MX (100 mg/L solution in ACN), EXA (≥98% purity) and EB (≥95% purity) were obtained from Sigma-Aldrich (St. Louis, MO, USA). AHTN-d_3 and MX-d_{15}, used as surrogate standards, were purchased as 100 mg/L solution in iso-octane and in acetone, respectively, from Dr. Ehrenstorfer (Augsburg, Germany). Analytical reagent grade chloroform, chlorobenzene, carbon tetrachloride and tetrachloroethylene were tested as extraction solvents, while ethanol, methanol, acetone and acetonitrile were tested as disperser solvents. All solvents were purchased from Sigma-Aldrich (St. Louis, MO, USA).

For the optimized US-DLLME procedure, the water sample was transferred to a polyethylene centrifuge tube and AHTN-d_3 and MX-d_{15} were added (surrogates). Then, the mixture of the dispersive and extraction solvent was rapidly injected into the sample solution using a syringe and the mixture was sonicated. The resultant cloudy solution was centrifuged for 10 min at 4000 rpm and the sedimented phase were collected and transferred into a 100 µL insert placed inside a 1.5 mL vial, which was injected in the GC-MS for analysis.

Chromatographic analyses were performed by a Varian Ion Trap GC-MS system (Walnut Creek, CA, USA), using an electron impact ionization mode. The separation was carried out using a CP-Sil 8 CB capillary column (50 m × 0.25 mm i.d., 0.12 µm) from Agilent Technologies (Palo Alto, CA, USA). For these analyses, the GC oven was programmed from 60 °C (hold for 1 min) to 150 °C at 6 °C/min (hold for 10 min), to 225 °C at 6 °C/min and, to 300 °C at 20 °C/min; (total analysis time = 45 min). For quantitative analysis of target compounds, selected ion storage (SIS) mode was applied.

Due to the widespread use of synthetic musk fragrances, special precautions were taken in order to prevent contamination. During this study, analysts avoided the use of personal care products containing fragrance compounds and procedural blanks were analyzed with every extraction batch.

Results and discussion

In this study, an US-DLLME methodology combined with GC-MS analysis was applied to determine simultaneously twelve synthetic musk fragrances (five nitromusks, five polycyclic and two macrocyclic) in water samples. In this kind of extraction, several variables may affect the recoveries. Therefore, a two step experimental design was performed to obtain the optimal extraction conditions - screening design followed by a central composite design (a surface response design).

In the screening design seven factors were selected: (1) type of extraction solvent, (2) volume of extraction solvent, (3) type of dispersion solvent, (4) volume of dispersion solvent, (5) extraction time, (6) sample volume and (7) ionic strength. A fraction factorial design was chosen to verify the influence of these factors on the extraction, using the recoveries as the response. The main effects were determined by the probability (F-probability) calculated for each factor.

A central composite design was applied to those selected factors, in order to optimize the extraction procedure. Using this response surface methodology a mathematical relationship between dependent and independent variables was established. The experimental data were reasonably fitted to a second-order polynomial equation and the coefficients of the quadratic model were calculated by a least-square regression analysis. Finally, the significant variables and interactions were identified by the Student's t-test. Three-dimensional response surface and two-dimensional contour plots of the predicted responses were also obtained using the JMP software. Analysing these results, the best conditions for the simultaneous extraction of twelve musk compounds were established.

In order to evaluate the developed US-DLLME-GC-MS methodology different quality parameters were evaluated (limits of detection and quantification, linearity, precision, accuracy and global uncertainty). In order to evaluate the applicability of the proposed method, synthetic musks were determined in different aqueous matrices - river, sea water, wastewater and drinking water. The results showed that HHCB was the most frequently detected musk.

Conclusions

In this study, an ultrasound-assisted dispersive liquid-liquid microextraction procedure combined with GC-MS analysis was successfully applied to the analysis of twelve musk compounds in different aqueous samples. This method presents good repeatability, reproducibility and high extraction efficiency that allow the detection of synthetic musks in the ng/L range. Furthermore, this technique is simple and fast compared to other extraction techniques and, for that reason, may be easily applied for routine analysis.

Acknowledgements
The authors wish to thank to Fundação para a Ciência e a Tecnologia (FCT-Portugal) for the post-doctoral SFRH/BPD/76974/2011.

References
[1] M.A. Mottaleb, L.I. Osemwengie, M.R. Islam, G.W. Sovocool, *Aquatic Toxicology*, 106-107 (2012) 164.
[2] M. Arbulu, M.C. Sampedro, N. Unceta, A. Gomez-Caballero, M.A. Goicolea, R.J. Barrio, *Journal of Chromatography A*, 1218 (2011) 3048.
[3] J.-D. Berset, *Analytical Chemistry,* 72 (2000) 2124.
[4] European Parliament, Official Journal of the European Union, L342 (2009) 59.
[5] N.R. Sumner, C. Guitart, G. Fuentes, J.W. Readman, *Environmental Pollution*, 158 (2010) 215.
[6] Z. Hu, Y. Shi, Y. Cai, *Chemosphere*, 84 (2011) 1630.
[7] T. Heberer, *Acta Hydrochimica et Hydrobiologica*, 30 (2003) 227.
[8] Y. Lu, T. Yuan, W. Wang, K. Kannan, *Environmental Pollution*, 159 (2011) 3522.